As-mineral-humic substance interactions – Influence of natural organic matter on sorption and mobility of As

Dissertation

zur Erlangung des Grades eines Doktors der Naturwissenschaften

der Geowissenschaftlichen Fakultät
der Eberhard Karls Universität Tübingen

vorgelegt von
Prasesh Sharma
Kathmandu, Nepal

2010

Tag der mündlichen Prüfung: Sept 24. 2010

Dekan: Prof. Dr. Peter Grathwohl

1. Berichterstatter: Prof. Dr. Andreas Kappler

2. Berichterstatter: Dr. Andreas Voegelin

TABLE OF CONTENTS

1

Introduction

As contamination and distribution. Arsenic is a toxic element of significant global environmental concern due to its contamination of ground waters and soils (Smedley and Kinniburgh, 2002). In most As contaminated areas such as in South and South East Asia, As occurs naturally from geogenic sources, sorbed onto a variety of mineralogical hosts like hydrated ferric oxides and phylosillicates (clay) and sulphides (Nickson et al., 2000; Smedley and Kinniburgh, 2002). Dissolution of As bearing minerals (e.g. via oxidation of arsenical sulphides or via reductive dissolution of As containing Fe-oxides) and desorption of As from (hydro)oxides have been proposed to be the main mechanisms of As release into ground and surface waters (Smedley and Kinniburgh, 2002; Wang and Mulligan, 2007). However, As can also originate from human activities such as metallurgy, for decoration and pigmentation, and in pyrotechnics and warfare (Nriagu, 2002). In Bangladesh alone, about 85 million people are facing a serious threat because of poisonous levels of As in their drinking water, several times higher than the WHO recommended safety limit of 10 μg/L (Smedley and Kinniburgh, 2002). Apart from South and South-East Asia other regions which have large scale As contamination are parts of Argentina, Chile, Mexico, Thailand, China, Taiwan, US and also Eastern Europe (Vaughan, 2006).

As speciation. Arsenic is present in both inorganic and organic forms in natural waters, whereas the latter one represents the minor fraction. Under oxidizing conditions, inorganic As is usually present as arsenate [As(V)] and under reducing conditions as arsenite [As(III)] (Fig. 1). The geochemical behavior of As, its toxicity, and its uptake by plants is strongly controlled by its chemical speciation (Smedley and Kinniburgh, 2002; Dixit and Hering, 2003). In aqueous pH-neutral solutions, arsenite exists as uncharged species with pK_a values of 9.2, 12.1 and 13.4 whereas arsenate has pK_a values of 2.2, 6.9, and 11.5 and exists mostly as charged $H_2AsO_4^-$ and $HAsO_4^{2-}$ (Warwick et al., 2005). The speciation and mobility of As in the environment is primarily controlled by adsorption onto metal oxides, clay minerals surfaces but also by the presence of competing agents such as phosphate, silicate and humic substances (or natural organic matter (NOM)) (Redman et al., 2002; Dixit and Hering, 2003; Ko et al., 2004; Bauer and Blodau, 2006; Ritter et al., 2006).

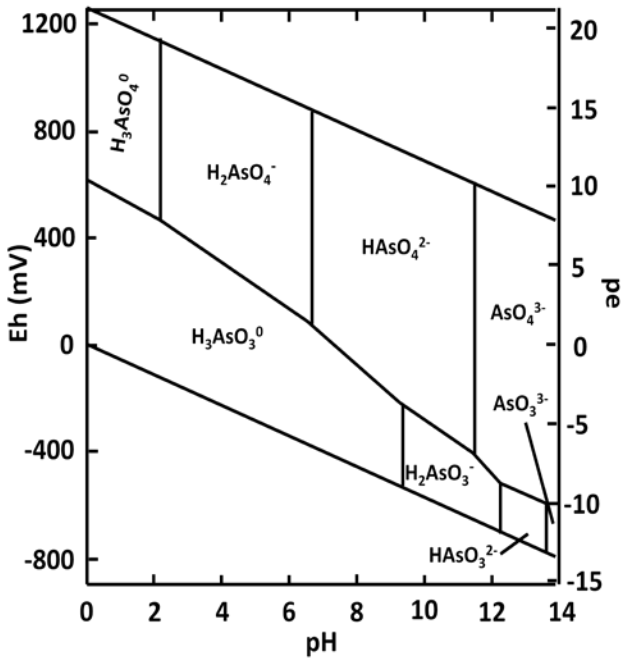

Fig. 1(left). An *Eh-pH* diagram of aqueous, aerobic As-solution at 25°C and 1 bar of pressure (Smedley and Kinniburgh, 2002).

Humic Substances (HS)/Natural organic matter (NOM). HS (or NOM) are mixtures of polydisperse, heterogeneous polyelectrolytes formed by degradation of plant and microbial biopolymers (Stevenson, 1994; Kelleher and Simpson, 2006; Simpson et al., 2007a). They are negatively charged molecules at neutral pH due to the presence of carboxylic and phenolic groups on aromatic residues and aliphatic chains. The solubility and conformation of HS/NOM in aqueous media are determined by pH, ionic strength, and the interaction of the deprotonated functional groups (carboxyl and hydroxyl) with metals and polyvalent cations (Stevenson, 1994; Hay and Myneni, 2007; Bauer et al., 2009(submitted)). NOM is ubiquitous in both aquatic and terrestrial environments; however, the source of the NOM (eg. terrestrial, aquatic or riverine) determines its structure and chemical behavior (Fimmen et al., 2007). The concentration of NOM in groundwater (aquifers) and surface water (rivers and lakes) ranges from around 0.1 mg C/l to several hundred mg C/l (Stevenson, 1994).

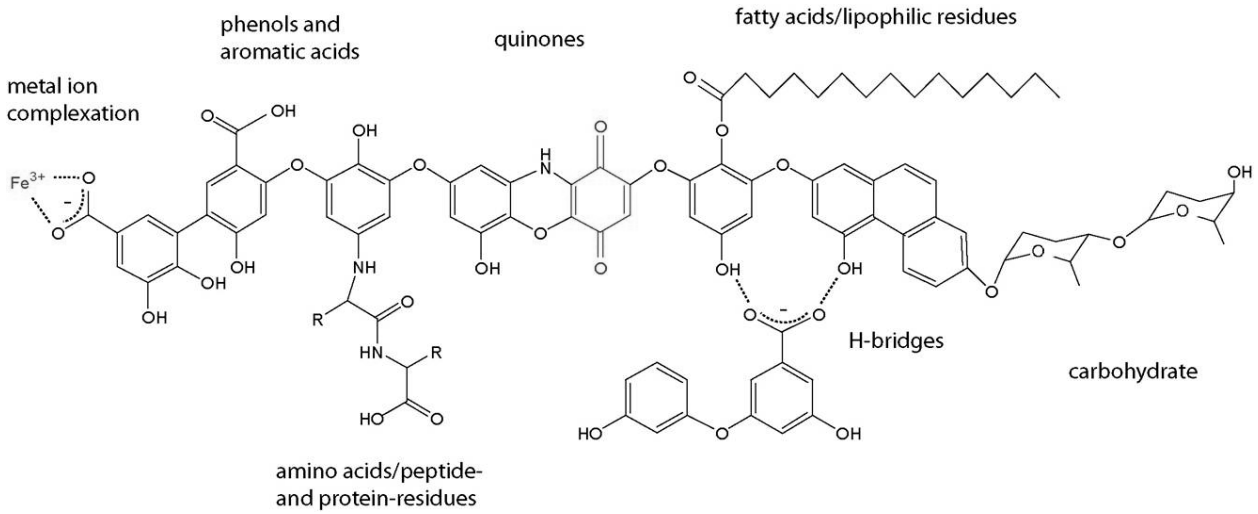

a) Humic Acid (modified from Stevenson, 1994)

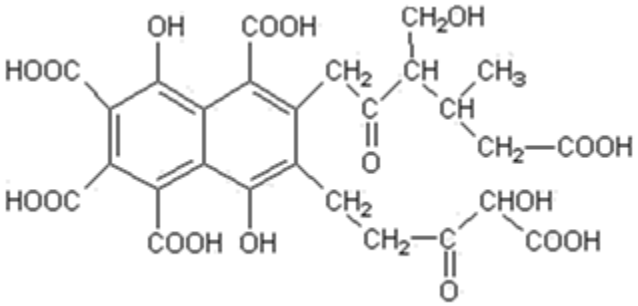

(b) Fulvic acid (Buffle, 1977)

Fig. 2. Model structure of (a) humic and (b) fulvic acids illustrating their main building blocks.

Fulvic acids (FA), humic acids (HA) (Fig. 2a and 2b) and humins, are three operationally defined fractions of NOM. FA is soluble in the entire pH range whereas HA is only soluble at high pH and precipitates at acidic pH. Humins are insoluble at all pH values and were described to be chemically less reactive compared to FA and HA. FA also posseses a higher amount of carboxylic and phenolic groups compared to HA, which consists of a more aromatic structure (Stevenson, 1994). Most importantly, the molecular weight of FA is significantly smaller than that of HA. The smaller size of FA means there is less steric hindrance upon interaction with minerals and can therefore interact with As bound to sorption sites that otherwise is less accessible to HA (Weng et al., 2009). Both FA and HA bind strongly to metal oxides and clay minerals (Stevenson, 1994; Gu et al., 1994). Humic substances or NOM are actively involved in almost all biogeochemical process that occur in soils including complexation, redox reactions and (im)mobilization of As.

As-NOM-Fe minerals interactions. NOM interacts with As in several ways (Fig. 3). Both redox states of As sorb strongly to mineral surfaces and particularly to iron oxides although the

bonding mechanism of As(III) and As(V) might vary depending on the crystalinity of the iron mineral and other geochemical conditions such as pH (Fig. 3-mechanism ‘a’). At neutral pH, As(III) binds to a greater extent than As(V) to minerals such as ferrihydrite, a commonly found iron mineral in the environment (Raven et al., 1998; Dixit and Hering, 2003; Herbel and Fendorf, 2006). However, As(III) is also more mobile and thus can be desorbed more easily than As(V). In presence of competing agents such as phosphate and NOM, the sorption of both redox states of As to Fe oxides and clay minerals have been found to decrease (Goldberg and Manning, 1996; Goldberg, 2002) (Fig. 3-mechanism ‘b’). NOM competes with As for sorption sites at mineral surfaces potentially increasing As mobility but also favor desorption of As from Fe(III) minerals (Warwick et al., 2005; Redman et al., 2002; Bauer and Blodau, 2009). It was shown that humic and fulvic acid in the presence of NOM and Fe(III) mineral suspensions (i.e. hematite (Ko et al., 2007; Redman et al., 2002), goethite (Grafe et al., 2001; Weng et al., 2009), ferrihydrite (Simeoni et al. 2003) increase desorption of As(V) and As(III) in batch experiments. Although less extensively studied in flow-through systems, NOM also affects transport and desorption processes of both As redox states from mineral surfaces (Grafe et al., 2001; Grafe et al., 2002). Other competing compounds such as phosphate, because of its analogous structure to arsenate (Goldberg, 2002; Dixit and Hering, 2003), and silica, because it effectively binds to Fe minerals (Waltham and Eick, 2005; Luxton et al., 2006), can also interfere in As-Fe minerals interactions. Phosphate, in particular, has been found to be more effective than silica in mobilizing As (Goldberg, 2002; Dixit and Hering, 2003; Stollenwerk et al., 2005).

Arsenic binds to NOM in presence of a cation bridge such as Fe, Al and Mn to form binary As-NOM and ternary As-metal-NOM colloids and complexes as proposed before by several authors (Ritter et al., 2005; Buschmann et al., 2006; Bauer and Blodau, 2009). In particular, binding of

As to NOM via an iron metal bridge has been suggested to be a common complexation mechanism between As and NOM (Ritter et al., 2005; Wang and Mulligan, 2007). NOM can trigger the first step of the formation of these complexes by sorbing to Fe-oxy(hydr)oxides and then leaching Fe from the oxide surface during interaction of NOM with Fe(III) minerals(Fig. 3-mechanism ‘c’). During this process Fe-NOM complexes and FH-NOM colloids are formed (Liang et al., 1992). These dissolved complexes and colloids can interact with free As to form ternary As-Fe-NOM complexes and colloids (Blodau and Bauer, 2009) (Fig. 3-mechanism ‘d’).

NOM is as well a key player in soil and environmental redox chemistry. Redox active functional groups in NOM such as quinones (see fig. 2a for quinone group) can subsequently form reactive semiquinone radicals. These radicals can transfer electrons from the mineral to As or vice-versa thereby changing the speciation of As and NOM both (Jiang et al., 2009) (Fig. 3-mechanism ‘e’). Microbially mediated As-Fe mineral-NOM interactions could also take place and alter the sorption behavior of As onto Fe minerals as well as the geochemistry of the minerals itself although this has not been previously demonstrated before in the same system (Fig. 3-mechanism ‘f’). In addition, the presence of NOM can also enhance microbial/chemical reduction thereby either releasing As that was bound to the Fe-oxy(hydr)oxides or by changing the redox state of As during the reduction process.

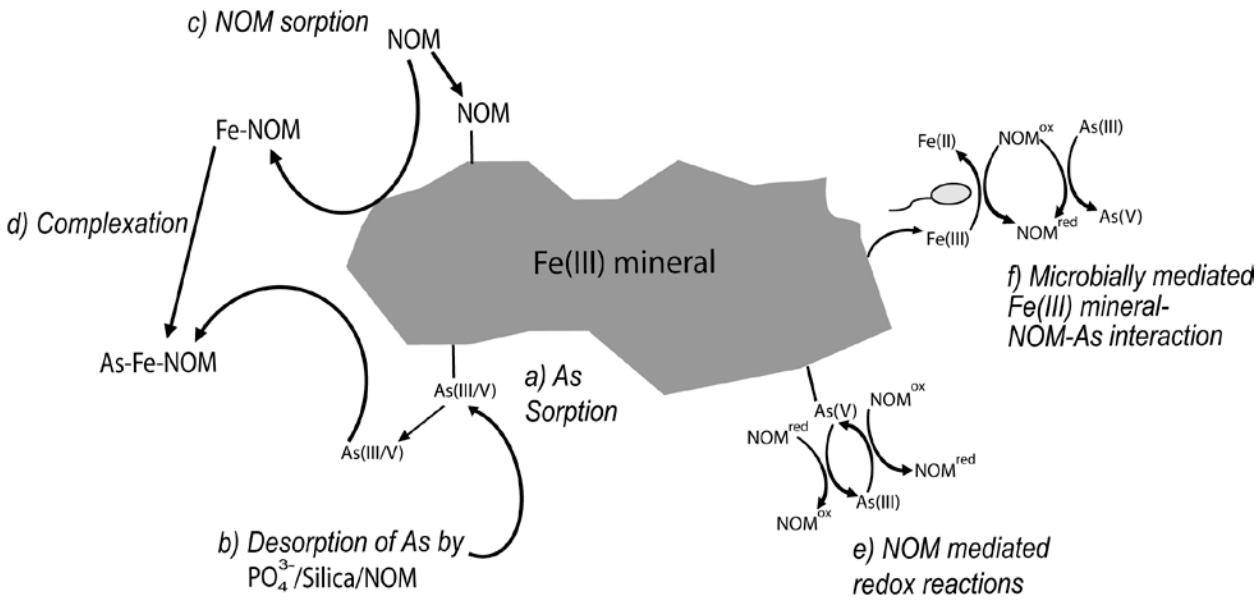

Fig. 3. Interaction of As, Fe mineral and NOM: a) Sorption of As(III)/As(V) to Fe(III) mineral, b) Desorption and release of As from mineral surfaces by competing agents of As such as phosphate, silica or NOM, c) Sorption of NOM to Fe(III) mineral surface, d) Leaching of Fe ions by NOM from Fe mineral surface, subsequent formation of Fe-NOM colloids/complexes and further interactions with As to form As-Fe-NOM colloids/complexes, e) Reversible redox reactions of NOM with surface bound As and f) Reduction of Fe(III) minerals by microbes in presence of NOM and consequent oxidation of As(III) by reduced NOM.

As-NOM-clay mineral interactions. Clay minerals are another commonly found mineral group in the environment. Clay minerals are hydrous aluminum phylosilicates, built of tetrahedral (Si) and octahedral (Al) sheets and formed from weathering products of silicate rocks (Sposito, 1989). Kaolinite, a 1:1 layer type and illite, a 2:1 layer type clay are two commonly found clay minerals in natural environments. In many As contaminated areas, such as in Bangladeshi aquifers, a significant amount of clay minerals is present due to high weathering activity of

silicate rocks (Hossain, 2006). NOM, on the other hand is present from underlying peat deposits or being transported into the aquifers from surface waters due to intense irrigation leading to large groundwater withdrawal (Burgess et al., 2010). In natural waters colloidal or particulate clays are abundantly found in permanently or conditionally charged states, which may trigger interactions with NOM (Goldberg, 2002). Arsenic adsorption has also been found to be positively correlated with clay content of soils in As-contaminated aquifers (Elkhatib et al., 1984; Lin and Puls, 2004). Experiments to quantify As adsorption onto clay minerals such as kaolinite, montmorillionite, and illite have been studied in the laboratory as a function of pH and redox state (Goldberg, 2002). However, studies on As interaction to clay-NOM complexes has lacked attention compared to As-clay interactions. Dissolved NOM can compete with As for same sorption sites in clay minerals, as in Fe oxides, thereby mobililizing more As to the environment. However, organic coating on clays can also change the reactivity of the clay mineral surface and increase the number of binding sites for metal contaminants. This provides an effective mechanism for the removal of potentially toxic substances from the environment, including As (Saada et al., 2005; Gaskova et al., 2002). Although iron and clay mineral structures differ significantly, the sorption processes and interactions of As and NOM with clay minerals are similar (Fig. 4). Both species of As sorb onto clay minerals (Fig 4.-mechanism ‘a’) however, unlike in case of Fe minerals, As(V) has been found to sorb more to some clays such as kaolinite and illite compared to As(III) (Lin and Puls, 2004). In addition to NOM, the presence of high amounts of phosphate in the groundwater that originates from fertilizers and dissolved silicate weathering products also affects the sorption/desorption of As in clay minerals (Fig 4.-mechanism ‘b’). Both components are effective competing agents which force As to remain in solution or to desorb from mineral phases. NOM can sorb as effectively in clay minerals like in

Fe minerals (Fig 4.-mechanism ‘c’). Ternary complex formation could also be possible if NOM interaction with clay minerals triggers leaching of metal ions such as Ca^{2+}, Al^{3+}, Mg^{2+} and $Fe^{2/3+}$ present in the silicate layers which could be involved in formation of ternary complexes with As and NOM (Fig 4.-mechanism ‘d’). Similarly, microbially mediated processes can also take place at clay mineral surfaces in the presence of a redox active ion such as iron (Fig 4.-mechanisms ‘e and f’).

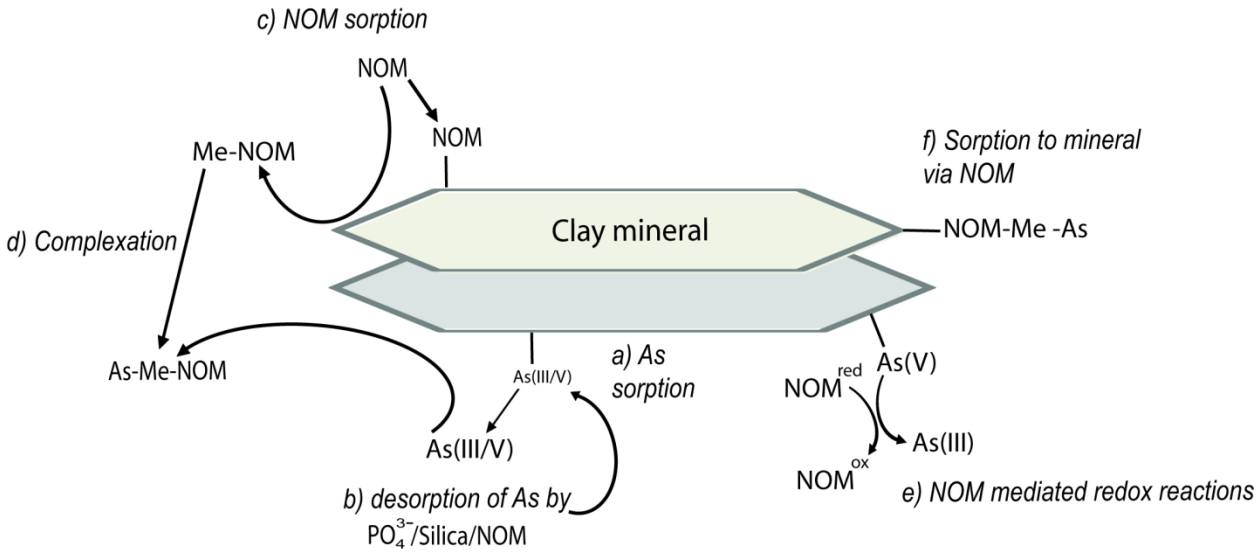

Fig. 4. Interaction of As-NOM-clay minerals: a) Sorption of As(III)/As(V) to clay minerals, b) Desorption and release of As from clay mineral surface by competing agents of As such as phosphate, silica or NOM, c) Sorption of NOM to clay mineral surface, d) Interaction of metal ions (Me) leached from clay mineral surface, formation of Me-NOM colloids/complexes, and interaction of Me-NOM colloids/complexes to form As-Me-NOM colloids/complexes, e) Redox reactions of NOM with surface bound As and f) Sorption of As to clay minerals via Me-NOM complexes.

Knowledge gaps. From previous studies, we know that biogeochemical interactions of As with minerals are significantly affected by the presence of HS/NOM in the environment. However,

there are still a significant number of open questions. This will help to explain sequestration and mobility of As in the presence of NOM. For example, the presence of ternary complexes of NOM, Fe and As has been proposed recently but their mechanisms of their formation in the environment as well as the structure of the complexes have not yet been identified. Despite a lot of interest in transport of As via Fe-oxides in presence of NOM, a comprehensive study of the influence of different concentrations of NOM on As transport is still to be conducted. Similarly, transport studies with regards to desorption of As from FH-coated sand in presence of NOM has not to this day been carried out. Most studies with NOM have also been performed with highly purified organic matter, such as humic and fulvic acids purchased from the International Humic Substances Society (IHSS). These studies, moreover, have not been carried out with soil organic matter (SOM) extracted under environmentally relevant conditions. Also, similar to batch systems as mentioned earlier, it is unclear in which form As is mobilized in the environment in transport systems i.e. either as free As or as dissolved or colloidal As-NOM and As-Fe-NOM or As-FH and As-FH-NOM colloids. Lastly, with respect to transport of As, effect of ionic strength transport of As through mixture of iron oxides in presence of NOM have not yet been conducted.

With regards to interaction of As with clay minerals, there have been only a handful studies on sorption of As to clay minerals in presence of humics. Moreover, the desorption of As by competing ions such as phosphate and silicate from clay-NOM complexes which could also occur in the environment have not been previously studied. The knowledge of formation, characterization and chemical behaviour of clay-NOM aggregates is also limited due to the complex interactions between the two components.

Objectives of the study. Based on the knowledge gaps previously mentioned, the specific goals of this study were as follows:

- to demonstrate and quantify the formation of As-Fe-NOM complexes and colloids upon reaction of dissolved Fe-NOM complexes/colloids with As to identify the Fe-NOM and As-Fe-NOM colloids/complexes (chapter 2)

- to quantify the transport of As through ferrihydrite-coated sand and determine desorption of As from ferrihydrite-coated in presence and absence of HA, FA and to show that SOM can be more effective than purified HA and GFA in transporting and desorbing As (chapter 3)

- to determine in which form As is mobilized in flow-through systems (as dissolved As, as dissolved/colloidal As-NOM or as dissolved ternary As-Fe-NOM complexes or As-FH colloids or As-NOM-FH colloids) (chapter 3)

- to determine whether humic acids affects desorption of As(V) from ferrihydrite-coated sand in flow-through systems at different ionic strength (chapter 4)

- to identify and quantify the reactive functional groups on the kaolinite and illite mineral surfaces responsible for humic acid and trace metal sorption (chapter 5)

- to determine the effect of HA on sorption of As to clay only (kaolinite and illite) systems in comparison to clay presorbed with HA (kaolinite-HA and illite-HA)(chapter 6)

- to quantify desorption of As from As pre-sorbed clay and clay-HA complexes by silicate and phosphate (chapter 6)

References

Amstaetter, K., Borch, T., Larese-Casanova, P., Kappler, A. Transformation of arsenic by Fe(II)-activated goethite (α-FeOOH). *Environmental Science & Technology*, **2010**, *44*, 102–108.

Bauer, M. B., Blodau, C. Mobilization of arsenic by dissolved organic matter from iron oxides, soils and sediments. *Environmental Science & Technology*, **2006**, *354*, 179-190.

Bauer, I., Amstaetter, K., Haderlein, S., Kappler, A. Influence of ionic strength on structure and redox activity of humic substances. **Submitted to** *Geochimica Et Cosmochimica Acta*, **2009**.

Buffle J. Les substances humiques et leurs interactions avec les ions mineraus. In Conference Proceedings de la Commission d'Hydrologie Appliquee de l'A.G.H.T.M. L'University d'Orsay, pp. 3–10. 1977.

Buschmann, J., Kappeler, A., Indauer, U., Kistler, D., Berg, M., Sigg, L. Arsenite and arsenate binding to dissolved humic acids: Influence of pH, type of humic acid, and Aluminum. *Environmental Science & Technology*, **2006**, *40*, 6015-6020.

Burgess, W.G., Hoque, M.A., Michael, H.A., Voss, C.J., Breit, G.N., Ahmed, K.M. Vulnerability of deep groundwater in the Bengal aquifer system to contamination by arsenic. *Nature Geoscience*, **2010**, *3*, 83-87.

Dixit, S., Hering, J. G., Comparison of Arsenic(V) and Arsenic(III) sorption onto iron oxide minerals:implications for arsenic mobility. *Environmental Science & Technology*, **2003**, *37*, 4182-4189.

Elkhatib, E.A., Bennett, O.L., Wright, R.J. Arsenic sorption and desorption in soils. *Science Society of American Journal*, **1984**, *48*, 1025-1030.

Fimmen, R. L., Cory, R. M., Chin, Y. P., Trouts, T. D., Mcknight, D. M. Probing the oxidation-reduction properties of terrestrially and microbially derived dissolved organic matter. *Geochimica Et Cosmochimica Acta*, **2007**, *71*, 3003-3015.

Gaskova, O.L., Bukaty, M.B. Sorption of different cations onto clay minerals: Modelling approach with ion exchange and surface complexation. *Physics and Chemistry of the Earth*, **2008**, *33*, 1050–1055.

Goldberg, S., Johnston, C. T. Mechanisms of arsenic adsorption on amorphous oxides evaluated using macroscopic measurements, vibrational spectroscopy and surface complexation modeling. *Journal of Colloid and Interface Science*, **2001**, *234*, 204–216.

Grafe, M., Eick, M.J., Grossl, P.R. Adsorption of arsenate(V) and arsenite(III) on goethite in the presence and absence of dissolved organic carbon. *Science Society of American Journal*, **2001**, *65*, 1680–1687.

Grafe, M., Eick, M., Gross, P.R., Saunders, A.M. Adsorption of arsenate and arsenite on ferrihydrite in the presence and absence of dissolved organic carbon. *Journal of Environmental Quality*, **2002**, *31*, 1115–1123.

Gu, B., Schmitt, J., Chen, Z., Liang, L., McCarthy, J. Adsorption and desorption of different organic matter fractions on iron oxide. *Geochimica Et Cosmochimica Acta*, **1994**, *59*, 219-229.

Hay, M. B.; Myneni, S. C. B. Structural environments of carboxyl groups in natural organic molecules from terrestrial systems. Part 1: Infrared spectroscopy. *Geochimica Et Cosmochimica Acta*, **2007**, *71*, 3518–3532.

Herbel, M., Fendorf, S. Biogeochemical processes controlling the speciation and transport of arsenic within iron coated sands. *Chemical Geology*, **2006**, *228*, 16–32.

Hossain, M. F. Arsenic contamination in Bangladesh – an overview. *Agriculture, Ecosystems and Environment*, **2006**, *113*, 1-16.

Jiang, J., Bauer, I., Paul, A., Kappler, A. Arsenic redox changes by microbially and chemically formed semiquinone radicals and hydroquinones in a humic substance model quinone. *Environmental Science & Technology*, **2009**, *43*, 3639-3645.

Iler, R.K. 1979. The chemistry of Silica. Wiley-Interscience, New York.

Ilwon, K., Ju-Yong, K., Kyoung-Woong, K. Arsenic speciation and sorption kinetics in the As–hematite–humic acid system. *Colloids and Surfaces A:Physicochemical and Engineering Aspects*, **2004**, *234*, 43-50.

Ilwon, K., Davis, A. P., Ju-Yong, K., Kyoung-Woong, K. Effect of contact order on the adsorption of inorganic arsenic species onto hematite in the presence of humic acid. *Journal of Hazardous Materials*, **2006**,*141*, 53-60.

Kelleher, B. P., Simpson, A. J. Humic substances in soils: Are they really chemically distinct? *Environmental Science & Technology*, **2006**, *40*, 4605-4611.

Liang, L., McCarthy, J. F., Jolley, L. W., McNabb, J. A., Mehlhorn, T. L. Iron dynamics: transformation of Fe(II)/Fe(III) during injection of natural organic matter in a sandy aquifer. *Geochimica Et Cosmochimica Acta*, **1992**, *57*, 1987-1999.

Lin, Z., Puls, R.W. Adsorption, desorption and oxidation of arsenic affected by clay minerals and aging process. *Environmental Geology*, **2000**, *39*, 753-759.

Luxton, T.P., Tadanier, C.J., Eick, M.J. Mobilization of arsenite by competitive interaction with silicic acid. *Soil Science Society of America Journal*, **2006**, *70*, 204-214.

Manning, B.A., Goldberg, S. Arsenic(III) and arsenic(V) adsorption on three California Soils. *Soil Chemistry*, **1997**, *162*, 886-895.

Meng, X., Bang, S., Korfiatis, G.P. Effects of silicate, sulfate, and carbonate on arsenic removal by ferric chloride. *Water Research*, **2000**, *34*, 1255-1261.

Nickson, R. T., Mcarthur, J. M., Ravenscroft, P., Burgess, W. G., Ahmed, K. M. Mechanism of arsenic release to groundwater, Bangladesh and West Bengal. *Applied Geochemistry*, **2000**, *15*, 403-413.

Nriagu, J.O. Arsenic poisoning though the ages. *In* W.T. Frankenberger (ed.) Environmental chemistry of arsenic. Marcel Dekker, Inc. New York, 2003

Raven, K.P., Jain, A., Loeppert, R.H., 1998. Arsenite and arsenate adsorption on ferrihydrite: Kinetics, equililibrium, and adsorption envelopes. *Environmental Science and Technology*, **1998**, *32*, 344-349.

Redman, A. D., Macalady, D. L., Ahmann, D. Natural organic matter affects arsenic speciation and sorption onto hematite. *Environmental Science & Technology*, **2002**, *36*, 2889-2896.

Ritter, K., Aiken, G. R., Ranville, J. F., Bauer, M., and Macalady, D. L. Evidence for the aquatic binding of arsenate by natural organic matter-suspended Fe(III). *Environmental Science & Technology*, **2006**, *40*, 5380-5387.

Saltikov, C.W. and Olson, B.H. Homology of E. coli R773 arsA, arsB, and arsC in arsenic resistant bacteria isolated from raw sewage and arsenic enriched creek waters. *Applied and Environmental Microbiology*, **2002**, *68*, 280-288. (abstract/paper).

Saada, A., Breeze, D., Crouze, C., Cornu, S., Baranger, P. Adsorption of arsenic(V) on kaolinite and on kaolinite-humic acid complexes – role of humic acid nitrogen groups. *Chemosphere*, **2003**, *51*, 757-763.

Simeoni, M. A., Batts, B. D., McRae, C. Effect of groundwater fulvic acid on the adsorption of arsenate by ferrihydrite and gibbsite. *Applied Geochemistry*, **2003**, *18*, 1507–1515.

Simpson, A. J., Simpson, M. J., Smith, E., and Kelleher, B. P. Microbially derived inputs to soil organic matter: Are current estimates too low ? *Environmental Science & Technology*, **2007a**, *41*, 8070-8076.

Stevenson, F.J. Humus Chemistry: Genesis, Composition, Reactions. Wiley: New York, 1994.

Smedley, P. L., Kinniburgh, D. G. A review of the source, behaviour and distribution of arsenic in natural waters. *Applied Geochemistry*, **2000**, *17*, 517-568.

Smith, E., Naidu, R., Alston, A.M. Chemistry of inorganic arsenic in soils. II. Effect of phosphorus, sodium, and calcium on arsenic absorption. *Journal of Environmental Quality*, **2002**, *31*, 557-563.

Sposito, G. 1994. The chemistry of soils. Oxford Univ. Press, New York.

Stollenwerk, K.G., Breit, G.N., Welch, A.H., Yount, J.C., Whitney, J.W., Foster, A.L., Uddin, M.N., Majumder, R.K., Ahmed, N. Arsenic attenuation by oxidized aquifer sediments in Bangladesh. *Science of the Total Environment*, **2007**, *379*, 133-150.

Swedlund, P.J., Webster, J.G. Adsorption and polymerization of silicic acid on ferrihydrite, and its effect on arsenic adsorption. *Water Research*, **1999**, *33*, 3413-3422.

Tipping, E., Higgins, D.C. The effect of adsorbed humic substances on the colloid stability of haematite particles. *Colloid and Surfaces*, **1982**, *5*, 85–92.

Ullah, S.M. Arsenic contamination of groundwater and irrigated soil of Bangladesh. In: International Conferences on As pollution of groundwater in Bangladesh: Causes, effects and remedies, Dhaka Community Hospital, Dhaka, Bangladesh, 8–12 February1998.

Vaughan, D.J. Arsenic, *Elements*, **2006**, *2*, 71-75.

Violante, P., Pigna, M. Competitive sorption of arsenate and phosphate on different clay minerals and soils. *Soil Science Society of America Journal*, **2002**, *66*, 1788–1796.

Waltham, C.A., Eick, M.J. Kinetics of arsenic adsorption on goethite in the presence of sorbed silicic acid. *Soil Science Society of America Journal*, **2002**, 70, 204-214

Wang, K., Xing, B. Structural and sorption characteristics of adsorbed humic acid on clay minerals. *Journal of Environmental Quality*, **2005**, *34*, 342-349.

Wang, S., Mulligan, C. N. Effect of natural organic matter on arsenic release from soils and sediments into groundwater. *Environmental Geochemistry and Health*, **2006**, *28*, 197-214.

Warwick, P., Inam, E., Evans, N., Arsenic's interaction with humic acid. *Environmental Chemistry*, **2005**, *2*, 119-124.

Weng, L., Riemsdijk, W.H.V., Hiemstra, T. Effects of fulvic and humic acids on arsenate adsorption to goethite: Experiments and modeling. *Environmental Science & Technology*, **2009**, *43*, 7198–7204.

2

Formation of binary and ternary colloids and dissolved complexes of Organic matter, Fe and As

Prasesh Sharma, Johannes Ofner, Andreas Kappler

Published in *Environmental Science and Technology*, **2010**, *44*, 4479-4485

Environ. Sci. Technol. **2010,** *44,* 4479–4485

Formation of Binary and Ternary Colloids and Dissolved Complexes of Organic Matter, Fe and As

PRASESH SHARMA,[†] JOHANNES OFNER,[‡] AND ANDREAS KAPPLER*,[†]

Geomicrobiology, Center for Applied Geosciences, University of Tuebingen, Germany, and Atmospheric Chemistry Research Laboratory, University of Bayreuth, Germany

Received December 2, 2008. Revised manuscript received March 28, 2010. Accepted April 15, 2010.

Natural organic matter can change As speciation via redox reactions and complexation influencing its mobility and toxicity. Here we show that binary and ternary colloids and dissolved complexes of As(V), Fe and organic matter (OM) form at environmentally relevant conditions and analyzed these colloids/complexes using ATR-FTIR- and Mössbauer-spectroscopy. Dissolved Fe−OM complexes and ferrihydrite-OM colloids were formed by reacting OM with ferrihydrite ($Fe(OH)_3$). Mössbauer-spectroscopy showed that 95% of the Fe in the Fe−OM fraction were present as ferrihydrite−OM colloids while the remaining 5% were in the dissolved fraction. In As(V) plus Fe−OM systems (containing both dissolved and colloidal Fe−OM), 3.5−8 μg As(V)/mg OC was bound to the Fe−OM complexes/colloids compared to <0.015 μg As(V)/mg OC in As-OM systems (without Fe). Upon filtration of As−Fe−OM complexes/colloids with a 3 kDa filter, ∼6% As was found in the dissolved fraction and ∼94% As in colloidal Fe−OM. This suggests that As(V) is associated with Fe−OM mainly via ferrihydrite-OM colloids but to a small extent also in dissolved Fe−OM complexes via Fe-bridging. Since As-contaminated soils and aquifers contain Fe(III) minerals and OM, colloids of As with OM-loaded ferrihydrite and complexes of As with dissolved Fe−OM have to be considered when studying As transport.

Introduction

Arsenic is a toxic element of significant global environmental concern due to its contamination of ground waters and soils (*1*). In Bangladesh alone, about 85 million people are facing a serious threat because of poisonous levels of arsenic in their drinking water, up to 1000 times the WHO recommended safety limit of 10 μg/L (*2, 3*).

Arsenic is present in inorganic and to a smaller extent in organic forms in natural waters. Under oxidizing conditions, inorganic As is usually present as arsenate [As(V)] and under reducing conditions as arsenite [As(III)]. The environmental behavior of arsenic, its toxicity, and the uptake by plants depend strongly upon its speciation (*2–4*). In aqueous pH-neutral solutions, arsenite exists as uncharged species with pK_a values of 9.2, 12.1, and 13.4, whereas arsenate has pK_a values of 2.2, 6.9, and 11.5 and exists as $H_2AsO_4^-$ and $HAsO_4^{2-}$ at circumneutral pH (*1*). The mobility of arsenic in the environment is primarily controlled by adsorption onto clay minerals and metal oxide surfaces but also by interactions with natural organic matter (NOM) (*4–9*).

Interactions of As with Fe (oxy) hydroxides, clay minerals, soils, and sediments have been widely studied (*6–10*). However, research on As−NOM interactions has been carried out only recently. Humic substances (or NOM) are formed during degradation of biopolymers, are polymeric and polydisperse, and are ubiquitous in nature. Humic substances interact not only with arsenic but also with other metal ions and minerals in soil via adsorption, complexation, and redox reactions (*5–7, 11–17*).

NOM competes with arsenic for sorption sites at mineral surfaces potentially increasing arsenic mobility (*1, 6–10, 18*). Additionally, it has been suggested that arsenic binds to NOM forming As−NOM complexes and that arsenic can undergo redox reactions with NOM changing its mobility and toxicity (*1, 12–14*). Due to their sizes that belong mostly to the colloidal size fraction (between 2 and 300 nm or even higher depending upon aggregation (*11*), most metal−humic complexes fall as well into the colloidal size range. Arsenic was found to bind less strongly to humic substances (by complexation) compared to binding with hydrous iron oxides (*1*). However, it is assumed that in particular in case of low iron oxide content in the environment, humic substances can have a significant effect on mobilization of arsenic (*1*).

The presence of ternary complexes of NOM, Fe ions, and As has been proposed recently (*6–8, 14–16*) and in particular binding of As to NOM via an iron metal bridge has been suggested (*8*). However, the structure(s) of these ternary complexes, the mechanisms of their formation as well as the role of such complexes in the behavior of As in the environment have not been identified yet.

The objectives of this study thus were (i) to demonstrate that the interaction of OM with Fe(III) oxides forms dissolved Fe−OM complexes and/or ferrihydrite−OM colloids similar to the potential formation of such aggregates in the environment (Figure 1), (ii) to demonstrate that the interaction of these Fe−OM complexes/colloids with dissolved As in groundwater leads to the formation of ternary As−Fe−OM complexes/colloids, and (iii) to determine to which extent these aggregates are dissolved and colloidal.

Materials and Methods

Reagents. Stock solutions of 1 mM arsenate (Na_2HAsO_4) and 1 M NaCl were prepared in deionized water. Pahokee peat humic acid (PHA) was purchased from the International Humic Substances Society. 0.1 mg/mL PHA solution was prepared by dissolving dry PHA in 5 mM NaCl, pH-adjustment to pH 7 (using 1 M NaOH), stirring for 1 h and filtration (0.45 μm, cellulose acetate, Millipore).

Synthesis of Ferrihydrite. Ferrihydrite (FH) was freshly synthesized before each experiment by hydrolyzing 0.2 M $FeNO_3 \cdot 9H_2O$ with 1 M KOH at circumneutral pH (7−7.5) (*19*). The precipitates were identified as 2-line FH by μ-XRD (Supporting Information (SI) Figure S1) with a surface area of 239.7 g/m^2 determined using single-point Brunau−Emmett−Teller (BET) N_2 adsorption isotherms (ASAP 2000, Micrometrics).

Synthesis of FH−OM Colloids and Dissolved Fe−OM Complexes. FH was added as a suspension (1 mM final concentration) to the PHA solution (0.1 mg/mL; 49.94 mg C/L) and shaken at 200 rpm on a horizontal shaker at room temperature in the dark (Figure 1). No pH change occurred after FH addition. After 72 h of incubation the suspension was filtered (0.45 μm, cellulose acetate, Millipore) to separate

* Corresponding author phone: +49-7071-2974992; fax: +49-7071-295059; e-mail: andreas.kappler@uni-tuebingen.de.
[†] University of Tuebingen.
[‡] University of Bayreuth.

10.1021/es100066s
Published on Web 04/30/2010

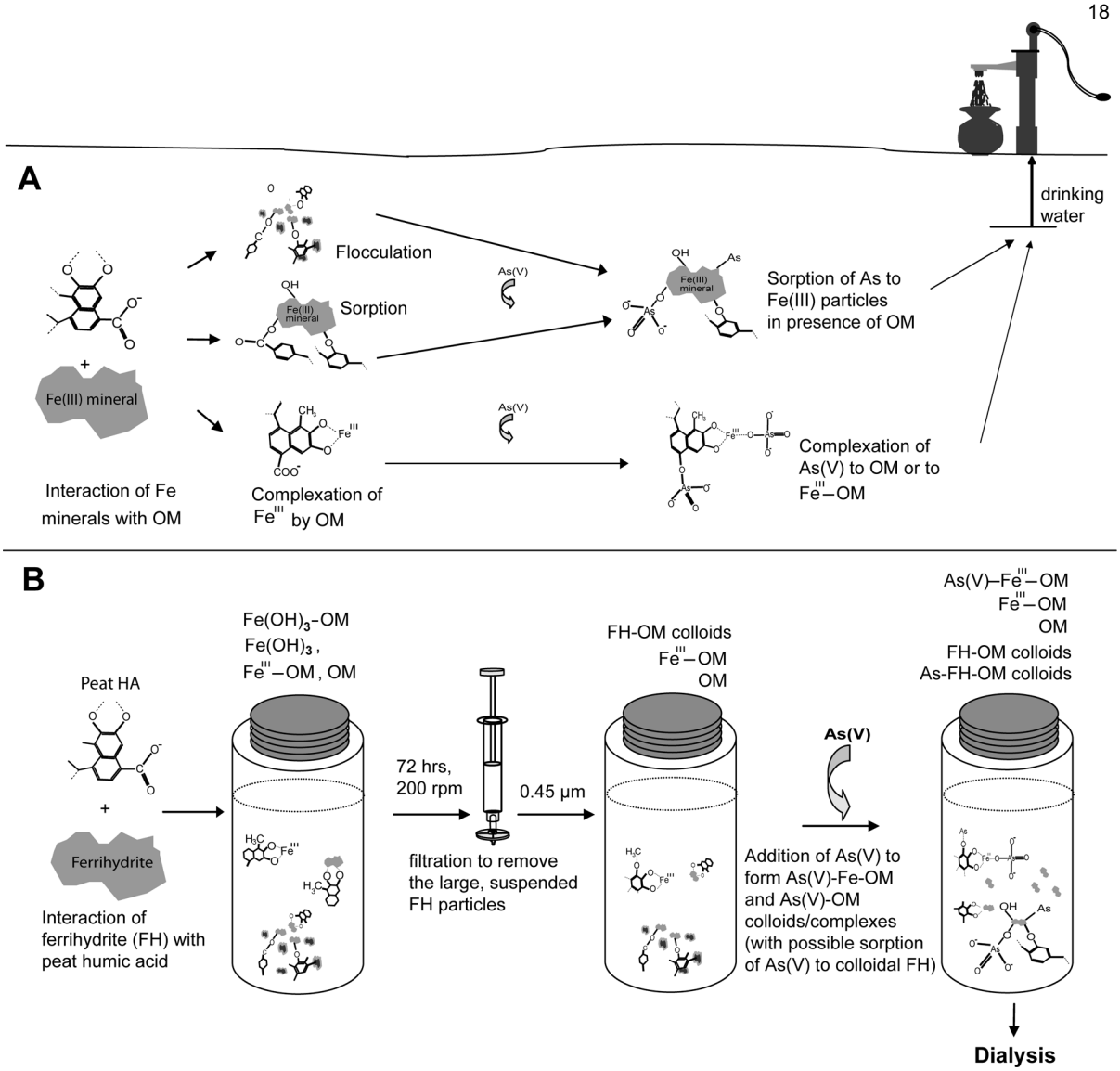

FIGURE 1. (A) Illustration of how As(V)−OM and As(V)−Fe−OM colloids/complexes potentially form in nature and ultimately reach drinking water. (B) Lab experiment simulating the environmental process described in (A): Sequential process of formation of Fe−OM colloids/complexes via interaction of humic acid with Fe(III) minerals and in the second step the formation of As(V)−Fe−OM colloids/complexes via interaction of the Fe−OM colloids/complexes with dissolved As(V).

dissolved Fe−OM complexes and ferrihydrite−OM colloids from remaining FH particles. Dissolved organic carbon (DOC) and humic-bound Fe were quantified in the filtrate (see below).

To determine whether the Fe−OM aggregates are colloidal and/or dissolved by Mössbauer spectroscopy, ^{57}Fe−OM aggregates were prepared. First, a $^{57}FeCl_2$ solution was prepared by dissolving ^{57}Fe(0) in 1 M HCl. 50 μL H_2O_2 (from a 35% H_2O_2 stock) was added to 1 mL of 0.53 M $^{57}FeCl_2$ solution to oxidize Fe(II) to Fe(III). Simultaneously, 0.81 g of nonlabeled $Fe(NO_3)_3$ was dissolved in 11.5 mL Millipore water and mixed with the oxidized $^{57}FeCl_2$ solution. Under rigid stirring, 1 M KOH was added dropwise until the pH was circumneutral. After 2 h, the FH-suspension was washed four times with deionized water and at the end brought to a volume of 5 mL yielding a 0.5 M ^{57}Fe−FH suspension. ^{57}Fe−OM complexes/colloids were synthesized by incubating ^{57}Fe−FH and PHA using the same protocol as used for nonlabeled FH. For Mössbauer spectroscopy, the samples were freeze-dried.

Synthesis of Colloids and Dissolved Complexes of As(V)−OM and As(V)−Fe−OM. To synthesize As(V)−Fe−OM colloids/complexes, 100 μM As(V) was added to the Fe−OM fraction. After As(V) addition, the pH was still 7. This mixture was incubated on a horizontal shaker (200 rpm) for 0−48 h in the dark. To synthesize As(V)−OM colloids/complexes, 100 μM As(V) was added to OM solutions and also incubated for 0−48 h. Since we used only As(V) in our experiments, throughout the paper we will use the terms As−OM and As−Fe−OM colloids/complexes.

Noncomplexed As was separated from As bound in As−OM and As−Fe−OM colloids/complexes using 1000 MWCO Regenerate Cellulose ester membrane dialysis bags (Roth, Germany). The dialysis bags were washed in deionized water (24 h) before usage to remove any leachable OC and then placed in 5 mM NaCl. Ten-mL aliquots of the As−Fe−OM and As−OM solutions were placed in the dialysis bag and the ends of the bag were closed with a PTFE clip. The As−Fe−OM and Fe−OM fractions were dialyzed for 5 days. Samples were taken from outside the dialysis bags every 24 h for As quantification. After sampling, the solution outside was replaced by fresh 5 mM NaCl solution. After 5 days, samples from inside the dialysis bags were analyzed for OM-bound Fe and OM-bound As. A 10-mL aliquot was taken separately from the As−Fe−OM fraction and subjected to centrifugal filtration with a nominal 3 kDa (~2 nm, see (*20*))

MWCO filter (Millipore) to separate dissolved As from As present in colloids (following (*16*)). The pH of the solution did not change during ultrafiltration. Arsenic sorption to dialysis bags was quantified by incubating bags with 100 μM As(V) followed by As quantification after 5 days. Each experiment was repeated twice and within each experiment three samples were analyzed per setup.

Analytical Methods. To quantify the amount of Fe in the Fe−OM and As−Fe−OM colloids/complexes, Fe was extracted by adding 500 μL of sample to 500 μL of 1 M HCl at 90 °C at 150 rpm in a thermomixer. After 30 min, the suspension (including precipitated humic substances) was centrifuged at 14 000 rpm for 15 min and the supernatant was analyzed for total Fe by the spectrophotometric ferrozine assay (*21*).

To quantify As, solution from inside and outside the dialysis bags as well as samples from the 3 kDa filtration were acidified by 1 M HNO_3, centrifuged for 3 min (14 000 rpm) and analyzed for total As by ICP-MS. DOC was quantified from filtered solutions (0.45 μm, cellulose acetate, Millipore) by a TOC analyzer. To analyze Fe−OM and As−Fe−OM colloids/complexes by ATR-FTIR spectroscopy, samples containing Fe−OM and As−Fe−OM colloids/complexes were concentrated 10-fold using a vacuum centrifugation concentrator (SpeedVac, Bachhofer, Reutlingen, Germany) at 35 °C and 1500 rpm. Concentrating the samples did not change the pH. (ATR-)FTIR spectra were recorded using a Bruker IFS 113v FTIR-instrument (for details see SI S1).

The ratio of the absorbance at 465 and 665 nm (E4/E6) was determined for the organic matter to evaluate the preferential sorption of certain OM fractions to FH. The absorbance was measured in a plate reader (FlashScan 550, Jena Analytik, Germany).

Mössbauer spectra for the freeze-dried ^{57}Fe−FH and ^{57}Fe−OM samples were collected with a constant acceleration drive system in transmission mode and with a ^{57}Co source at room temperature. Samples were mounted in a close-cycle exchange-gas cryostat (Janis, U.S.) that allowed cooling of the sample to 5 and 77 K. An alpha-Fe metal foil was used for calibration at room temperature. Spectra calibration and fitting was performed with Recoil software (University of Ottawa, Canada) using Voigt based spectral lines.

Results and Discussion

Sorption of OM to Fe Minerals and Formation of Fe−OM Colloids and Dissolved Complexes. In order to simulate the interaction of organic matter (OM) with Fe(III) (hydr)oxides in the environment, we incubated ferrihydrite (FH) with Pahokee Peat Humic Acid (PHA) (Figure 1). During incubation of FH with PHA, a significant fraction of OM sorbed to the FH surface. In addition, FH particles in the colloidal size range associated with OM and became separated from the FH aggregates forming Fe−OM colloids. Simultaneously, some Fe ions leached from the Fe(III) mineral lattice leading to complexation of Fe by the PHA. Due to the 0.45 μm filtration step used in our study, the "dissolved" fraction (passing the filter) contained dissolved complexes but also colloids. Therefore, in a second step we separated truly aqueous dissolved from colloidal fractions to determine their respective importance (see below).

Quantification of DOC in ferrihydrite−PHA mixtures after incubation for 72 h revealed sorption of approximately 32% of the added OM to FH as indicated by the decrease in DOC from 49.9 to 33.9 mg C/L (Figure 2 and SI Figure S2) yielding a surface-normalized sorption of ~0.7 mg C/m^2 FH (calculated with the BET surface area of 239.7 m^2/g). Compared to a previous study with ferrihydrite and OM extracted from a Typic Haplorthod soil (*22*) with a surface-normalized sorption of 1.1 mg/m^2, OM sorption in our experiments was slightly

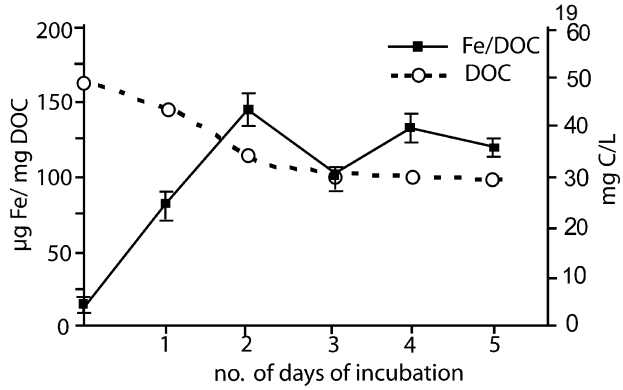

FIGURE 2. Complexation of Fe by Pahokee Peat Humic Acid (PHA) after incubation of the humic acids with poorly crystalline iron(III) hydroxide (ferrihydrite). DOC (defined by filtration through a 0.45 μm filter) and amount of total Fe bound to PHA are plotted against the number of days ferrihydrite and humic acids were incubated. The error bars indicate the standard deviation calculated from three independent samples each.

lower but in the same range. This difference could be due to the more acidic pH (pH 4.0) or the different humic material used in their experiments. UV absorption measurements of dissolved PHA before addition to FH showed slightly higher E4/E6 values compared to the remaining dissolved PHA after interaction with FH. Lower E4/E6 ratios typically represent a higher degree of aromaticity (*23*) suggesting that the nonsorbed PHA (including Fe−OM colloids/complexes) remaining after interaction of PHA with FH were slightly more aromatic than the original PHA (SI Table S3). This confirms a recent study in which a preferential sorption of some NOM fractions over others was suggested (*24*).

In addition to sorption to the Fe(III) mineral surface, humic compounds can leach and complex Fe ions from the Fe(III) mineral (*25, 26*). Additionally, nm- and μm-sized ferrihydrite particles can be coated by OM and separated from the remaining bulk ferrihydrite leading to flocculated colloidal ferrihydrite−OM aggregates (*25*). During the first days of incubation of PHA with FH, the DOC concentration decreased and in parallel the concentration of Fe associated with the PHA molecules (on a per DOC basis) increased (Figure 2). This suggests that the DOM covers the sorption sites at the FH mineral surface and at the same time Fe ions and/or Fe nanoparticles are leached and solubilized from the mineral phase by the DOM. After 3 days of incubation, DOC concentrations and Fe content reached a steady state suggesting that no more free sites at the FH particle surface were available for OM sorption (SI Figure S1). Based on these experiments, the incubation time for FH and PHA was set to 72 h followed by filtration to isolate Fe−OM colloids/complexes for synthesis of ternary As−Fe−OM colloids/complexes. Particle size measurements showed that the size range of the molecules in the original PHA solution was around 30 nm whereas for Fe−OM (and As−Fe−OM, see below) samples it was between 80 and 110 nm (SI Table S4) and thus in the colloidal size range.

The existence of Fe−OM colloids/complexes was demonstrated by ATR-FTIR spectroscopy (Figure 3). The two broad absorption bands at 1595 and 1390 cm^{-1} in the OM sample indicate asymmetric and symmetric vibrations for carboxyl (COO^-) groups (*27–29*). Complexation of COO^- groups with metals causes a frequency shift and changes in the shape of the stretching bands of COO^- (*30*). A frequency shift of the absorptions from 1595 to 1585 cm^{-1} and 1390 to 1340 cm^{-1} was indeed observed in the Fe−OM samples probably caused by the formation of Fe−OM colloids/complexes and suggesting binding of Fe to the OM via COO^- (*28*). The broad peaks in the Fe−OM spectrum at around

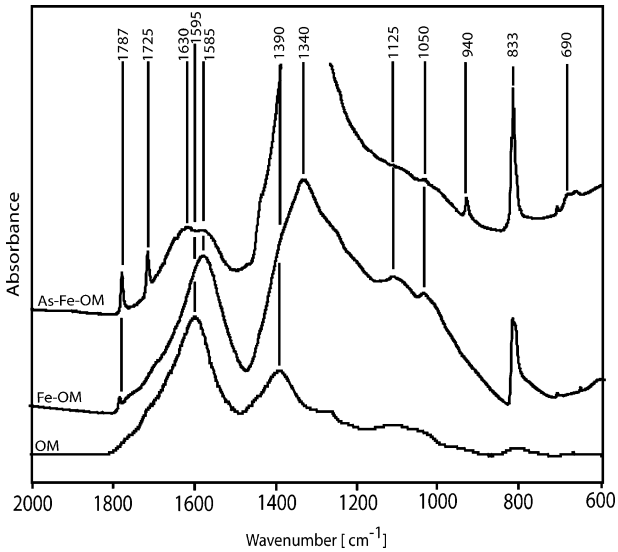

FIGURE 3. ATR-FTIR spectra comparing OM with Fe−OM and As−Fe−OM complexes.

1125 and 1050 cm^{-1} are caused by the bending mode of hydroxyl groups of Fe−OH (*29–31*). Due to the very low intensity of the 833 cm^{-1} peak in the OM-spectrum and the prominent signal at this wavenumber in the Fe−OM spectrum, we suggest that this peak represents most probably the ν(Fe−O) vibration in Fe−O−C or Fe−O−H. Interestingly, a weak signal at 833 cm^{-1} also exists for freeze-dried FH (SI Figure S3). However, we have to note that this peak has not been mentioned before as an iron-complexation related peak (for a detailed discussion of the peak at 833 cm^{-1} see below where the As−Fe−OM colloids/complexes are discussed). In addition, the FTIR spectra of the OM and Fe−OM samples show broad absorptions in the range of the ν(O−H) vibration (3700−3000 cm^{-1}) stemming from water, in the range of asymmetric carbonyl $\nu_{as}(CO_2^-)$ vibrations (1800−1550 cm^{-1}) and in the range of the symmetric $\nu_s(CO_2^-)$ vibration (~1400 cm^{-1}).

In summary, these results showed that interactions of humic substances with Fe(III) minerals can lead to the formation of dissolved Fe−OM complexes and Fe−OM colloids with a size of <0.45 μm. Similar processes are expected to occur in natural environments. It has been suggested that colloidal and dissolved Fe in groundwater is the result of weathering and leaching of Fe from different Fe-minerals by natural organic matter (NOM) (*32*). It has also been shown in lab experiments and field studies that the interaction of NOM with Fe-minerals can produce stable Fe−OM associations in aqueous systems (*25, 32*). Previous studies by Bauer and Blodau (*16*), where DOC (~2.5 mg C/L) was incubated with acidic solutions of $FeCl_3$ (Fe(total) <5 μM), also lead to the presence of Fe in both dissolved complexes and colloids although the Fe content in the dissolved fraction in our experiments was slightly higher than observed by these authors. The goal of our initial experiments was to reproducibly synthesize Fe−OM aggregates by simulating environmental conditions. While previous studies used acidic solutions of dissolved Fe^{3+} (e.g., $FeCl_3$) as Fe-source for studying the effect of Fe on As complexation by NOM (*8*), we chose FH and humic acids at neutral pH for our experiments for the following reasons: (1) FH is an Fe(III) mineral that is commonly found in the environment in contrast to free Fe^{3+} ions that are present only at very low concentrations at neutral pH without complexing ligands, (2) at circumneutral pH, humic acids are expected to interact with solid-phase Fe(III) minerals but when using dissolved Fe^{3+} at acidic pH, humic acids precipitate and the precipitated humic acids interact with dissolved Fe^{3+}, that is, just the reverse of what is seen in the environment, and (3) starting with acidic solutions followed by readjustments of pH to neutral pH precipitates the Fe^{3+} as $Fe(OH)_3$ at pH values higher than 5, potentially coprecipitating part of the humic acids and in parallel solubilizing another part of the humic acids creating a highly artificial and not reproducible situation compared to the environmentally relevant scenario of reacting ferrihydrite with dissolved humic acids.

Identity of Fe−OM Colloids and Dissolved Fe−OM Complexes. In order to distinguish dissolved Fe−OM complexes from Fe−OM colloids containing FH nanoparticles, we carried out Mössbauer spectroscopy measurements of freeze-dried ^{57}Fe−OM aggregates in comparison to ^{57}Fe−FH. Spectra were recorded at 5 and 77 K (SI Figure S4). At 77 K, a Fe(III) doublet with high quadruple splitting (0.80) for ^{57}Fe−FH and 0.77 for ^{57}Fe−OM was observed (SI Table S5), which is typical for ferrihydrite ((*33*)). At 5 K, magnetically split sextets similar to values previously found for ferrihydrite were observed (SI Figure S5 and Table S5) (*34*). The hyperfine field decreased from 49 T for ^{57}Fe−FH to 47.5 T for ^{57}Fe−OM. A similar decrease was previously reported for FH−OM coprecipitates with increasing OM content (*35*). However, for ^{57}Fe−OM complexes, in addition to the sextet, we found also a Fe(III) doublet (center shift: 0.49, quadrupole splitting: 0.88). This doublet at 5 K does not represent any magnetically ordered structure and likely results from isolated Fe(III) ions associated with the OM suggesting the presence of complexed Fe(III) ions. Quantification of both signals yielded ~95% of the total area for the sextet at 5 K meaning that 95% of the Fe in the Fe−OM fraction is in the form of ferrihydrite, whereas the remaining 5% is attributed to free Fe ions complexed by OM. The presence of complexed Fe(III) ions in Fe−OM (and As−Fe−OM) samples was also confirmed by analysis of As−Fe−OM samples obtained from the 3-kDa filtration step where ~15 μM Fe(III) was measured in the filtrate, that is, the truly dissolved fraction (SI Table S6).

Formation of As−OM and As−Fe−OM Colloids/Complexes. Arsenic can bind to NOM directly in inner-sphere complexes via organic functional groups such as hydroxyl groups (*1, 5*) but it was also suggested that metal cations act as bridges between As to OM forming ternary complexes (*6–8, 13–15*). However, the existence of ternary As−metal−OM colloids/complexes has not yet been validated experimentally. To demonstrate the existence of the ternary colloids/complexes, to understand the mechanism of their formation, and to evaluate their relative importance in comparison to binary As−OM complexes/colloids, we investigated two different experimental setups: (1) As(V) plus OM and (2) As(V) plus Fe−OM systems.

In systems where As(V) was incubated with colloidal/dissolved OM and Fe−OM, we found significant concentrations of free (noncomplexed) As outside the dialysis bag in both systems after one day (approximately 160 μg/L) (Figure 4A and B). On the second day (the solution outside was changed after the first day), the As concentrations outside the dialysis bags dropped significantly and were hardly detectable on the third, fourth, and fifth day in both setups (Figure 4A and B). When we analyzed the As/DOC ratio in the solutions inside the dialysis bags (that contained the OM- and Fe−OM-bound As), As was found in considerable amounts (~3.5−8 μg As/mg DOC) in the As plus Fe−OM systems with slightly higher values for 24 and 48 h of incubation compared to 2, 6, or 12 h of incubation (Figure 4C). In contrast, in systems which consisted of As(V) plus OM (no Fe), the As per DOC ratio was much lower (<0.015 μg As/mg DOC) suggesting that only a minor fraction of As was bound to organic matter directly. This suggests that Fe plays an essential role in As binding to OM confirming a recent study that suggested that As binding to biomass also depends on the presence of Fe bridges (*36*).

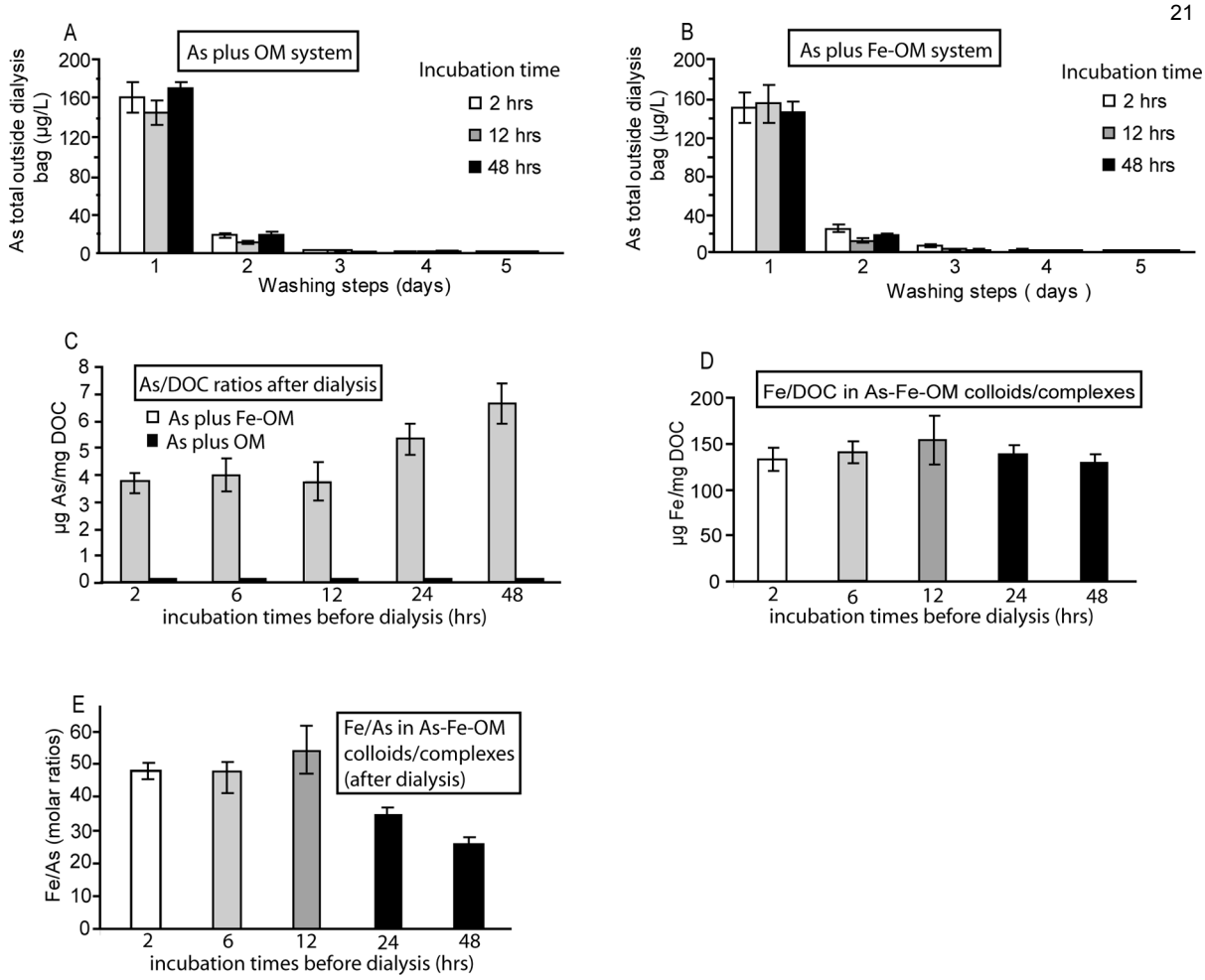

FIGURE 4. As and Fe content in As−OM and As−Fe−OM colloids/complexes after dialysis of mixtures of either As plus OM or As plus Fe−OM colloids/complexes. A and B show As concentrations in washing solutions outside of the dialysis bags for different washing steps for three different experiments with mixtures of As plus OM (A) and As plus Fe−OM (B) incubated before dialysis for either 2, 12, or 48 h. (C) shows total As content per DOC after dialysis in both the As plus OM and As plus Fe−OM systems for experiments with varying incubation times before dialysis. (D) shows Fe content per DOC in As−Fe−OM complexes for experiments with varying incubation times before dialysis. (E) shows the ratio of Fe to As in As−Fe−OM colloids/complexes for experiments with varying incubation times before dialysis. Samples for analysis of As and Fe content in complexes were taken from inside the dialysis bags at the end of the dialysis experiments. Error bars represent standard deviation calculated from three parallel samples.

Additionally to OM-bound As, we also determined the amount of Fe present in the As−Fe−OM colloids/complexes and calculated the Fe:As ratio. We found almost no variation of Fe/DOC ratios in the As−Fe−OM colloids/complexes for different predialysis incubation times between 2 and 48 h with 130−160 μg Fe/mg DOC for all incubation times (Figure 4D). This confirms our first results (Figure 2) that the Fe−OM colloids/complexes were in equilibrium before As(V) addition. From the Fe/DOC and As/DOC values we calculated Fe/As molar ratios of 26 to 55 with slightly decreasing values from 12−48 h of predialysis incubation (Figure 4E). These data suggest a significant excess of Fe bridges or Fe-nanoparticle surface sorption sites compared to the amount of As complexed, meaning that Fe could be responsible for all As complexation/binding with about every 20th to 50th Fe atom functioning as bridge between the OM molecules and the As(V) or as FH surface binding site for the As(V). Additionally, we analyzed the redox speciation of Fe and As in the complexes. However, no significant As and Fe redox reactions took place during the course of the experiment (SI Table S1 and Table S2) and therefore any effect of redox change on complexation of either Fe to OM or As to Fe−OM colloids/complexes can be ruled out.

In order to separate dissolved As−Fe−OM complexes from As−Fe−OM colloids and to quantify As and Fe in both fractions, the As−Fe−OM sample that was incubated for 48 h and then dialyzed, was centrifuged with a 3 kDa filter (*16*). Before ultrafiltration, the As−Fe−OM fraction contained 167.1 μg/L As(V) and 58.3 μM Fe(III) (SI Table S6). After separating this As−Fe−OM sample into dissolved and colloidal fractions via 3 kDa filtration, the supernatant containing the dissolved complexes contained ~10 μg/L As(V) (0.13 μM), ~840 μg/L Fe(III) (15 μM), and ~1 mg C/L DOC (SI Table S6); Fe(II) was below the detection limit of the ferrozine assay. This corresponds to about 6% of As(V) and 25% of Fe(III) in the dissolved As−Fe−OM complexes and 94% As(V) and 75% Fe(III) in the As−Fe−OM colloids suggesting that the fraction of complexed Fe (that was 5% in the Fe−OM fraction) increased to 25% as a consequence of the interaction of the Fe−OM fraction with the added As(V).

This data suggests that the majority of As(V) is bound to Fe−OM colloids, however, a small but still significant fraction of As(V) is complexed to OM via Fe(III) as a cation-bridge. These results are supported by a previous study by Bauer and Blodau (*16*) where comparable values for As distribution in colloidal and dissolved fractions were found upon reaction of DOC (~2.5 mg C/L) with acidic solutions of $FeCl_3$ (Fe(total) <5 μM) and, As(V).

The result of almost no As complexation by Fe-free OM confirms a recent study where As sorption to biomass was

observed only in the presence of Fe-bridges (*36*) but was still rather surprising considering several recent reports on As-complexation by natural organic matter (*13–15*). However, Fe, Mn, or Al in their NOM samples could have acted as bridge in their system (significant amounts of Fe, Mn, and Al were measured in the compost extract used for their study). In contrast, the cation content in PHA from IHSS was found to be very low and close to the detection limit (SI Table S2). As a consequence of this lack of significant amounts of available PHA-bound cation bridges, complexation of As with PHA is close to negligible. For evaluating the two different As-binding scenarios (As−OM and As−Fe−OM), the charges of the three different components involved (As, Fe, and NOM) have to be considered. Arsenate and OM are negatively charged at neutral pH whereas the Fe(III) ions and FH colloids in the Fe−OM fraction provide a positive charge at neutral pH. Therefore, the negatively charged arsenate probably binds more strongly to the Fe-loaded OM, potentially even by electrostatic interactions forming outer-sphere complexes. In contrast, in As plus OM systems, the negatively charged carboxylic or hydroxyl groups will repel the negatively charged arsenate and inner-sphere complexes will be required for strong As(V) binding (*13*).

In order to demonstrate the presence of ternary As−Fe−OM colloids/complexes, ATR-FTIR of the As amended Fe−OM fraction (containing both colloids and dissolved complexes) were compared to Fe−OM samples and OM (Figure 3). Based on X-ray absorption spectroscopy studies of As-binding to biomass via Fe bridges (*36*), ternary complexation of Fe−OM with As is expected to produce a further frequency shift in the COO^- stretching bands compared to the Fe−OM sample. And indeed, in As−Fe−OM samples, absorption peaks can be seen not only at 1585 cm^{-1} but also at 1630 cm^{-1}. The presence of both peaks in the As−Fe−OM sample is probably due to the presence of remaining Fe−OM colloids/complexes (signal at 1585 cm^{-1}) as suggested by the high Fe/As ratio in these samples (Figure 4) and the presence of the newly formed As−Fe−OM colloids/complexes (signal at 1630 cm^{-1}). To support that the 1630 cm^{-1} signal is indicative for the ternary complex formation, we collected FTIR spectra of As(V) sorbed to FH at different FH:As(V) ratios and from FH and As(V) alone (SI Figure S4). We found that pure FH shows a strong, broad signal at 1650 cm^{-1}. Additionally, with increasing As(V) concentrations no prominent peak at 1630 cm^{-1} (e.g., due to FH-sorbed As) is obvious. As(V) itself also gave a broad signal around 1650 cm^{-1} but only at very high As concentrations (1 mM), that is, concentrations much higher than present in our As−Fe−OM samples. Therefore, this data in combination with the fact that the 1630 cm^{-1} peak does not show up in the Fe−OM spectrum (Figure 3) but is present in the As−Fe−OM fraction (Figure 3) provides evidence that the 1630 cm^{-1} signal in the As−Fe−OM fraction is due to a peak shift from 1585 cm^{-1} to 1630 cm^{-1} from the As−Fe−OM fraction to the Fe−OM fraction, and is due to complexation of As to Fe−OM. The peak at 690 cm^{-1} can be attributed to the ν(As−OH) vibration further confirming the presence of As in these colloids/complexes (*37*).

UV absorption measurements of PHA in the As−Fe−OM fraction showed slightly lower E4/E6 values compared to the PHA in the Fe−OM samples (SI Table S3) suggesting a fractionation of the PHA by the loss of DOC during dialysis (leading to a slightly higher aromaticity in the As−Fe−OM fraction). This fractionation of OM could probably have influenced the FTIR spectra of the As−Fe−OM vs the Fe−OM fraction. However, such a fractionation (loss of DOC) is not expected to shift individual peaks (as has been observed after As addition) but rather to lead to the disappearance of certain signals. Therefore, the peak shift observed from the Fe−OM to the As−Fe−OM sample most likely provides evidence for ternary complex formation and is not influenced by the fractionation of the OM.

Additionally to the peaks around 1630 cm^{-1}, some peaks were observed in the FTIR spectra of the As−Fe−OM samples. The signal at 3513 cm^{-1} (not shown) is due to the ν(O−H) vibration of As−OH (*38*). The peak at 940 cm^{-1} in the spectrum obtained for the As−Fe−OM sample (Figure 3) probably belongs to the asymmetric ν_{as}(As−O−Fe) vibration caused by As(V) binding to Fe−OM (reported at 938 cm^{-1} in refs *37, 39*. This 938 cm^{-1} peak is not evident in any of the spectra of As(V) binding directly to ferrihydrite (SI Figure S4), therefore suggesting that OM is involved in the binding of the As(V) to the Fe. In the As−Fe−OM sample, the peak at 1125 cm^{-1} that was observed in the Fe−OM sample disappeared whereas the peak at 833 cm^{-1} is stronger than in the Fe−OM sample. This signal probably corresponds to the As−O stretching vibration suggesting that the 833 cm^{-1} peak involves not only Fe−O vibrations but also the symmetric ν_s(As−O−Fe) vibration that has been reported as an As−O signal (*37, 40*). The two sharp peaks at 1787 and 1725 cm^{-1} correspond to ν(C═O) vibrations in Fe(C═O) (*41*). In summary, the ATR-FTIR measurements demonstrate the formation of ternary As−Fe−OM colloids/complexes by interaction of Fe−OM colloids/complexes with dissolved arsenate.

Environmental Relevance of Dissolved and Colloidal As−Fe−NOM Complex Formation. In the present study we demonstrated the formation of ternary As−Fe−OM colloids and dissolved complexes under environmentally relevant conditions containing arsenate, (natural) organic matter and a Fe(III) mineral (ferrihydrite). The presence of other divalent and trivalent cations such as Ca^{2+}, $Mn^{2+/4+}$, Mg^{2+}, and Al^{3+} in groundwater suggests that there is also vast possibility of formation of ternary complexes of As with other metal−OM complexes as has been postulated and shown in some previous studies (*8, 13–16*). The inability of As to bind directly to OM (without metal bridges) means that As binding to FH−OM colloids and partially to dissolved Fe(III)−OM complexes are possibly the most common mechanisms of As association with NOM in the environment. The formation of binary or ternary complexes of As in flowing conditions as they are present in many aquifers (simulated in column experiments), the stability and mobility of the ternary complexes, and finally whether As(III) or As(V) is more likely to form ternary complexes with metal−OM complexes remains to be answered in further experiments.

Acknowledgments

This work was supported by an IPSWaT fellowship from the German Federal Ministry for Science and Education (BMBF) to P.S. and by funding from the German Research Foundation (DFG) and the BMBF to A.K. We thank J. Breuer, U. Dippon, and P. Larese-Casanova for their help with ICP-MS and Mössbauer spectroscopy, and S. Regenspurg, I. Bauer, J. Jiang, and R. Martinez for valuable comments and suggestions to improve the experiments and the manuscript. C. Zetzsch (University of Bayreuth) is acknowledged for providing access to the ATR-FTIR instrument.

Supporting Information Available

XRD of freeze-dried FH (Figure S1), sorption of PHA to FH (Figure S2), FTIR spectra of freeze-dried As−Fe−OM, Fe−OM, and OM and FH (Figure S3), FTIR spectra of As(V) only, FH only, and samples containing different As(V)−FH ratios (Figure S4), and Mössbauer spectra of freeze-dried ^{57}FH and ^{57}Fe−OM at 5 K (Figure S5). It also contains experimental details for ATR−FTIR analysis (S1), As speciation data for dissolved and colloidal As−Fe−OM (Table S1), speciation data of Fe in PHA, Fe−OM, and As−Fe−OM colloids (Table S2), E4/E6 ratios of PHA (Table S3), As(total), Fe(III) and DOC data for the three kDa fraction after centrifugal filtration

of As−Fe−OM complexes (Table S4), Mössbauer data for ^{57}Fe-labeled FH and ^{57}Fe-OM at 77 and 5 K (Table S5), and particle size data for PHA, and Fe−OM and As−Fe−OM colloids/complexes (Table S6). This material is available free of charge via the Internet at http://pubs.acs.org.

Literature Cited

(1) Warwick, P.; Inam, E.; Evans, N. Arsenic's interaction with humic acid. *Environ. Chem.* **2005**, *2*, 119–124.

(2) Meharg, A. A. Arsenic in rice-understanding a new disaster for South-East Asia. *Trends Plant Sci.* **2004**, *9*, 415–417.

(3) Smedley, P. L.; Kinniburgh, D. G. A review of the source, behaviour and distribution of arsenic in natural waters. *Appl. Geochem.* **2002**, *17*, 517–568.

(4) Dixit, S.; Hering, J. G. Comparison of arsenic(V) and arsenic(III) sorption onto iron oxide minerals: Implications for arsenic mobility. *Environ. Sci. Technol.* **2003**, *37*, 4182–4189.

(5) Goldberg, S. Competitive adsorption of arsenate and arsenite on oxides and clay minerals. *Soil Sci. Soc. Am. J.* **2002**, *66*, 413–421.

(6) Redman, A. D.; Macalady, D. L.; Ahmann, D. Natural organic matter affects arsenic speciation and sorption onto hematite. *Environ. Sci. Technol.* **2002**, *36*, 2889–2896.

(7) Bauer, M. B.; Blodau, C. Mobilization of arsenic by dissolved organic matter from iron oxides, soils, and sediments. *Environ. Sci. Technol.* **2006**, *354*, 179–190.

(8) Ritter, K.; Aiken, G. R.; Ranville, J. F.; Bauer, M.; Macalady, D. L. Evidence for the aquatic binding of arsenate by natural organic matter-suspended Fe(III). *Environ. Sci. Technol.* **2006**, *40*, 5380–5387.

(9) Ilwon, K.; Ju-Yong, K.; Kyoung-Woong, K. Arsenic speciation and sorption kinetics in the As-hematite-humic acid system. *Colloids Surf., A* **2004**, *234*, 43–50. +#.

(10) Ilwon, K.; Davis, A. P.; Ju-Yong, K.; Kyoung-Woong, K. Effect of contact order on the adsorption of inorganic arsenic species onto hematite in the presence of humic acid. *J. Hazard. Mater.* **2006**, *141*, 53–60.

(11) Mueller, F. L. L. Measurement of electrokinetic and size characteristics of estuarine colloids by dynamic light scattering spectroscopy. *Anal. Chim. Acta* **1996**, *331*, 1–15.

(12) Thanabalasingam, P.; Pickering, W. F. Arsenic sorption by humic acids. *Environ. Pollut. Ser.: B* **1986**, *12*, 233–246.

(13) Wang, S.; Mulligan, C. N. Effect of natural organic matter on arsenic release from soils and sediments into groundwater. *Environ. Geochem. Health* **2006**, *28*, 197–214.

(14) Buschmann, J.; Kappeler, A.; Indauer, U.; Kistler, D.; Berg, M.; Sigg, L. Arsenite and arsenate binding to dissolved humic acids: Influence of pH, type of humic acid, and aluminum. *Environ. Sci. Technol.* **2006**, *40*, 6015–6020.

(15) Lin, H.-T.; Wang, M. C.; Li, G.-C. Complexation of arsenate with humic substance in water extract of compost. *Chemosphere* **2004**, *56*, 1105–1112.

(16) Bauer, M.; Blodau, C. Arsenic distribution in the dissolved, colloidal and particulate size fraction of experimental solutions rich in dissolved organic matter and ferric iron. *Geochim. Cosmochim. Acta* **2009**, *73*, 529–542.

(17) Jiang, J.; Bauer, I.; Paul, A.; Kappler, A. Arsenic redox changes by microbially and chemically formed semiquinone radicals and hydroquinones in a humic substance model quinone. *Environ. Sci. Technol.* **2009**, *43*, 3639–3646.

(18) Chen, Z.; Cai, Y.; Solo-Gabriele, H.; Snyder, G. H.; Cisar, J. L. Interactions of arsenic and the dissolved substances derived from turf soils. *Environ. Sci. Technol.* **2006**, *40*, 4659–4665.

(19) Schwertmann, U. C.; Cornell, R. M. *The Iron Oxides*; Wiley-VCH: New York, 2003.

(20) Verdugo, P.; Alldredgeb, A. A.; Azamc, F.; Kirchmand, D. C.; Passowe, U.; Santschif, P. H. The oceanic gel phase: A bridge in the DOM-POM continuum. *Mar. Chem.* **2004**, *92*, 67–85.

(21) Stookey, L. L. Ferozine - A new spectorophotometric reagent for iron. *Anal. Chem.* **1970**, *42*, 779–781.

(22) Kaiser, K.; Mikutta, R.; Guggenberger, G. Increased stability of organic matter sorbed to ferrihydrite and goethite on Aging. *Soil Sci. Soc. Am. J.* **2005**, *71*, 711–719.

(23) Stevenson, F. J. *Humus Chemistry: Genesis, Composition, Reactions*; Wiley: New York, 1994.

(24) Gu, B.; Schmitt, J.; Chen, Z.; Liang, L.; McCarthy, J. Adsorption and desorption of different organic matter fractions on iron oxide. *Geochim. Cosmochim. Acta* **1994**, *59*, 219–229.

(25) Liang, L.; McCarthy, J. F.; Jolley, L. W.; McNabb, J. A.; Mehlhorn, T. L. Iron dynamics: transformation of Fe(II)/Fe(III) during injection of natural organic matter in a sandy aquifer. *Geochim. Cosmochim. Acta* **1992**, *57*, 1987–1999.

(26) Tadanier, C. J.; Roller, J. W. Arsenic mobilization through microbially mediated deflocculation of ferrihydrite. *Environ. Sci. Technol.* **2005**, *39*, 3061–3068.

(27) Hay, M. B.; Myneni, S. C. B. Structural environments of carboxyl groups in natural organic molecules from terrestrial systems. Part 1: Infrared spectroscopy. *Geochim. Cosmochim. Acta* **2007**, *71*, 3518–3532.

(28) Guardado, I.; Urrutia, O.; Garcia-Mina, J. M. Some structural and electronic features of the interaction of phosphate with metal-humic complexes. *J. Agric. Food Chem.* **2008**, *56*, 1035–1042.

(29) Rao, P.; Mak, M. S. H.; Liu, T.; Lai, K. C. K.; Lo, I. M. C. Effects of humic acid on arsenic(V) removal by zero-valent iron from groundwater with special references to corrosion products analyses. *Environ. Sci. Technol.* **2009**, *75*, 156–162.

(30) Nakamoto, K. *Infrared and Raman Spectra of Inorganic and Coordination Compounds*, 3rd ed.; John Wiley: New York, 1978.

(31) Zhang, Y.; Yang, Z. Y.; Dou, X.-M.; He, H.; Wang, D.-S. Arsenate adsorption on an Fe-Ce bimetal oxide adsorbent: role of surface properties. *Environ. Sci. Technol.* **2005**, *39*, 7246–7253.

(32) Rose, A. L.; Waite, T. D. Kinetics of iron complexation by dissolved natural organic matter in coastal waters. *Mar. Chem.* **2003**, *84*, 85–103.

(33) Murad, E.; Schwermann, U. The moessbauer spectrum of ferrihydrite and its relations to those with other iron oxides. *Am. Mineral.* **1980**, *65*, 1044–1049.

(34) Murad, E.; Cashion, J. *Mössbauer Spectroscopy of Environmental Materials and Their Industrial Utilization*; Kluwer Academic Publishers: Boston, 2004.

(35) Eusterhues, K.; Wagner, F. E.; Häusler, W.; Hanzlik, M.; Knicker, H.; Totsche, K. U.; Kögel-Knabner, I.; Schwertmann, U. Characterization of ferrihydrite-soil organic matter coprecipitates by X-ray diffraction and Mössbauer spectroscopy. *Environ. Sci. Technol.* **2008**, *42*, 7891–7897.

(36) Silva, G. C.; Vasconcelos, I. F.; de Carvalho, R. P.; Dantas, M. S. S.; Ciminelli, V. S. T. Molecular modeling of iron and arsenic interactions with carboxy groups in natural biomass. *Environ. Chem.* **2009**, *6*, 350–356.

(37) Myneni, S. C. B.; Traina, S. J.; Waychunas, J. A.; Logan, T. J. Experimental and theoretical vibrational spectroscopic evaluation of arsenate coordination in aqueous solutions, solids, and at mineral-water interfaces. *Geochim. Cosmochim. Acta* **1998**, *62*, 3285–3300.

(38) Siebert, H. *Anwendungen der Schwingungsspektroskopie in der Anorganischen Chemie*; Springer: Berlin, 1966.

(39) Lumsdon, D. G.; Fraser, A. R.; Russell, J. D.; Livesey, N. T. New infrared band assignments for the arsenate ion adsorbed on synthetic goethite (a-FeOOH. *J. Soil Sci.* **1984**, *35*, 381–386.

(40) Jing, C.; Meng, X. Immobilization mechanisms of arsenate in iron hydroxide sludge stabilized with cement. *Environ. Sci. Technol.* **2003**, *37*, 5050–5056.

(41) Socrates, G. *Infrared Characteristic Group Frequencies*; Wiley: New York, 1980.

ES100066S

- Supporting Information -

Formation of binary and ternary colloids and dissolved complexes of organic matter, Fe and As

Prasesh Sharma[1], *Johannes Ofner*[2], *Andreas Kappler*[1]*

[1] Geomicrobiology, Center for Applied Geosciences, University of Tuebingen, Germany

[2] Atmospheric Chemistry Research Laboratory, University of Bayreuth, Germany

For publication in *Environmental Science and Technology*

*To whom correspondence should be sent:

Andreas Kappler, Geomicrobiology, Center for Applied Geosciences

University of Tübingen, Sigwartstrasse 10, D-72076 Tübingen, Germany

Phone: +49-7071-2974992, Fax: +49-7071-295059, email: andreas.kappler@uni-tuebingen.de

Running title: Binary and ternary complexes of OM, Fe and As

- 7 pages (including cover page)
- 5 Figures
- 6 Tables

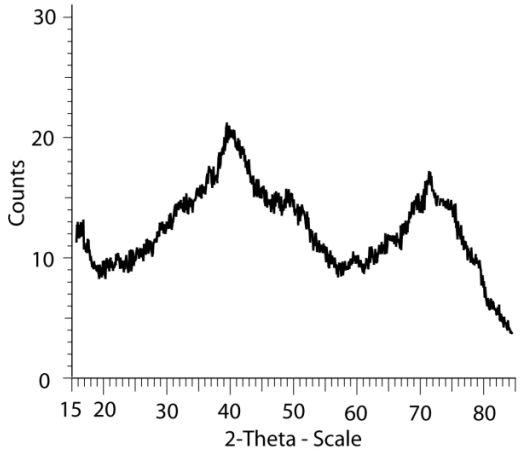

Figure S1: X-ray diffraction analysis of freeze-dried 2-line ferrihydrite used for the experiments.

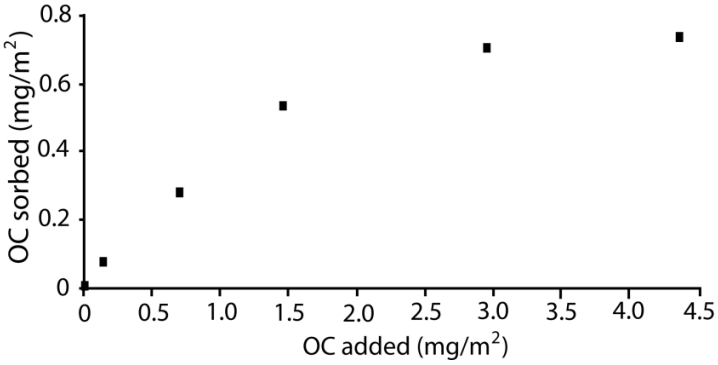

Figure S2: Sorption of Pahokee peat humic acid (PHA) to ferrihydrite presented as the relation between the mass of organic carbon (OC) added and sorbed normalized to the surface area of the ferrihydrite used (239.7 m^2/g).

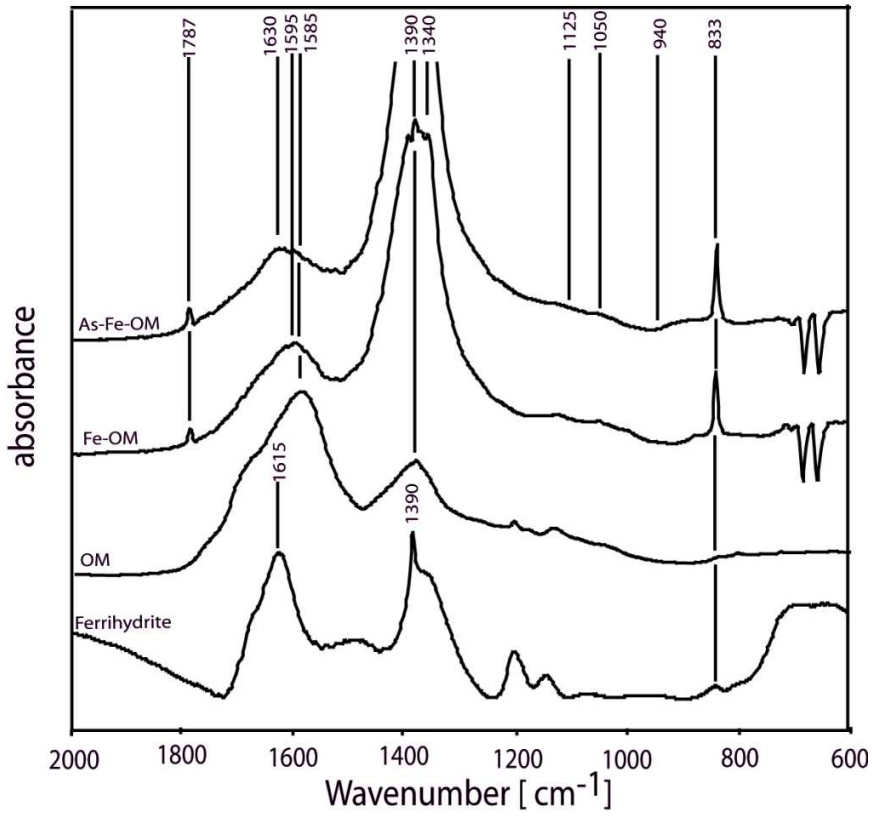

Figure S3: FTIR spectra of freeze-dried ferrihydrite, freeze-dried PHA (sample “OM”), freeze-dried binary Fe-OM colloids/complexes (“Fe-OM”), and freeze-dried ternary As-Fe-OM colloids/complexes (“As-Fe-OM”).

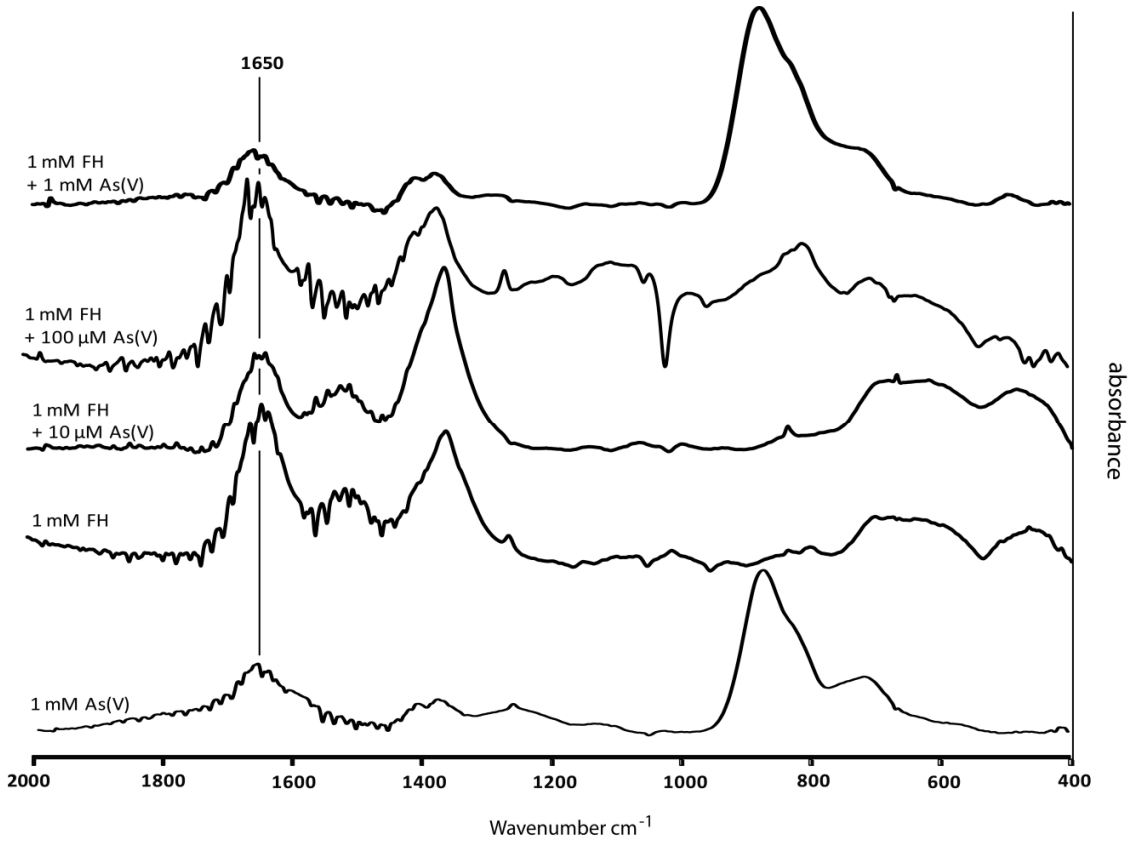

Figure S4: ATR-FTIR spectra of 1 mM As(V), 1 mM ferrihydrite (FH), and spectra for samples with three different FH/As(V) ratios as indicated in the figure. All samples were dried on the ATR crystal in a stream of N_2 for analysis.

Supporting information S1: Experimental details of ATR-FTIR and FTIR spectroscopic analysis: Liquid samples of OM, Fe-OM and As-Fe-OM colloids/complexes (Fig. 3) and liquid samples of dissolved As(V), ferrihydrite suspensions and suspensions of ferrihydrite with different amounts of As(V) sorbed (Fig. S4) were analyzed by ATR-FTIR spectroscopy. To minimize or even avoid absorption of radiation by water, the samples were dried in a stream of N_2 on the KRS5 ATR-crystal (Thallium Bromo-Iodide; surface of 52 x 20 mm and an optical range from 4000 to 600 cm^{-1}) at room temperature. All ATR-FTIR spectra for samples dried under a N_2 stream were recorded using a Bruker IFS 113v FTIR-instrument with a Specac-25 reflection ATR optics (Specac, London, UK) at an optical angle of 60°. The spectral resolution of the infrared spectrometer was adjusted to 2 cm^{-1} and 256 interferograms with an optical range from 4000 to 600 cm^{-1} (both for background as well as sample measurements). Baseline correction and atmospheric compensation of CO_2 and H_2O (liquid phase) was applied using the OPUS 5.0 software of Bruker Optik GmbH.
Additionally, the OM, Fe-OM, and As-Fe-OM samples were freeze-dried and analyzed by FTIR spectroscopy as KBr pellets by mixing 20 mg of freeze-dried material with

200 mg KBr with a Bruker IFS 48 FTIR instrument (Fig. S3). The spectral resolution of the spectrometer was kept constant at 2 cm^{-1} and 256 interferograms with an optical range 4000 to 600 cm^{-1} (both for background as well as sample measurements).
Spectra of liquid samples (without drying at the crystal or freeze-drying) could not be analyzed due to the low concentration of complexes in the samples and the resulting high noise-to-signal ratio. Therefore, in this study we show only the ATR-FTIR data for N_2-stream dried (Figs. 3 and S4) and freeze-dried samples (Fig. S3). It has to be noted, however, that freeze-drying or drying at the ATR-FTIR crystal could potentially have lead to complex formation, i.e. to the formation of the As-Fe-OM colloids/complexes that have not been present before in liquid. However, we believe that it can be ruled out that the complexes only form during drying since in case the sample would have contained only free As and Fe-OM (and no As-Fe-OM complexes) before drying, no differences in As contents inside and outside the dialysis bags would have been observed between Fe-OM-free and Fe-OM-amended samples. The fact that after dialysis we observed As inside the dialysis bags only in setups that also contained Fe-OM demonstrates that As must be associated with the Fe-OM (forming As-Fe-OM colloids/complexes). Therefore, the peak changes observed in the ATR-FTIR data provide evidence for the colloids/complexes formed between As and Fe-OM.

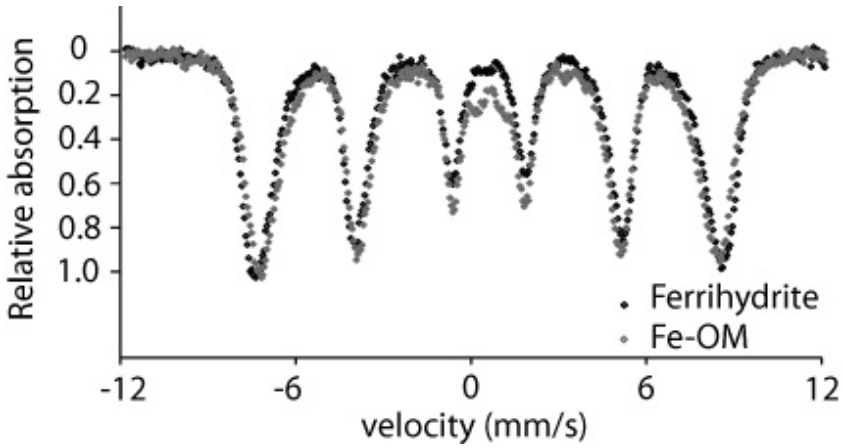

Figure S5: Mössbauer spectra of ^{57}Fe-labelled ferrihydrite (dark black circles) and freeze-dried ^{57}Fe-OM samples (grey circles) at 5 K prepared by incubation of ^{57}Fe-labelled ferrihydrite and PHA.

Table S1. Arsenic concentration and speciation in the fraction that contains both As-Fe-OM colloids and dissolved As-Fe-OM complexes after dialysis determined by IC-ICP-MS. Arsenic was extracted from the colloidal and dissolved As-Fe-OM by adding 500 µL of 2 M HNO_3 to 500 µL of sample and precipitating the OM at 70°C for 30 min. The mixture was then centrifuged at 14,000 RPM for 3 min and the supernatant analyzed for As(III) and As(V) by IC-ICP-MS. (However, it has to be noted that potentially formed As(III) could have been oxidized to some extent by HNO_3).

Incubation time (hrs)	As(III) (µg/L)	As(V) (µg/L)
2	0	91.0 (4.5)*
12	0	95.4 (3.5)
24	0	157.8 (8.9)

* Standard deviations from triplicate measurements are shown in parentheses

Table S2. Fe speciation data in Pahokee peat humic acid (0.1 mg/ml PHA), binary Fe-OM colloids/complexes after filtering with 0.45 µm filters, and ternary As-Fe-OM colloids/complexes after dialysis. Fe was extracted from the colloidal and dissolved aggregates by adding 500 µL of 2 M HCl to 500 µL of sample and precipitating the OM at 70°C for 30 min. The mixture was then centrifuged at 14,000 RPM for 3 min and the supernatant analyzed for Fe(II) and total Fe by ferrozine assay. The efficiency of the HCl extraction compared to total Fe in the samples (determined by ICP-MS) was 90% or higher (see $Fe(tot)^{ICPMS}$).

sample	Fe(II) [µg/mg C]	Fe(tot) [µg/mg C]	Fe(III) [µg/mg C]	$Fe(tot)^{ICPMS}$ [µg/mg C]
PHA	bdl*	4.2(0.6)	2.1(0.7)	5.1(0.8)
Fe-OM	5.1(0.4)	90.0(2.7)	85.3(2.7)	97.3(8.6)
As-Fe-OM	5.7(0.9)	87.9(2.9)	83.8 (3.0)	96.2(6.3)

bdl- below detection limit
*Standard deviations from triplicate measurements are shown in parentheses

Table S3: E4/E6 absorbance ratios of Pahokee peat humic acid (PHA), binary Fe-OM colloids/complexes after filtering with a 0.45 µm filter, and ternary As-Fe-OM colloids/complexes after dialysis.

Sample	**E4/E6 ratio**
PHA (0.1 mg/ml)	3.6 (0.2)*
Fe-OM	3.3 (0.1)
As-Fe-OM	2.8 (0.1)

* Standard deviations from triplicate measurements are shown in parentheses

Table S4: Average particle size of two Pahokee peat humic acid samples (PHA 1: 0.1 mg/ml and PHA 2: 0.5 mg/ml) before incubation with ferrihydrite, of Fe-OM colloids/complexes after filtration with a 0.45 µm filter, and of As-Fe-OM colloids /complexes after dialysis. Three parallels were measured for each sample with a Malvern Instruments ZEN3601 Zetasizer.

sample	PHA 1 [nm]	PHA 2 [nm]	Fe-OM [nm]	As-Fe-OM [nm]
1	35.4 (5.2)*	42.1 (3.5)	102.3 (7.8)	110.3 (8.2)
2	28.6 (2.4)	32.9 (3.4)	98.4 (6.7)	89.1 (4.5)
3	31.2 (4.7)	33.1 (4.5)	82.1 (4.5)	90.3 (2.4)

* Standard deviations from triplicate measurements are shown in parentheses

Table S5: Mössbauer data collected at 77 and 5 K for ^{57}Fe-FH (FH synthesized with ^{57}Fe) and for ^{57}Fe-OM colloids/complexes (Fe-OM synthesized by incubating ^{57}Fe-FH with Pahokee peat humic acid).

77 K

	Center shift mm/s	Quadruple split at 77 K mm/s	Hyperfine field T
^{57}Fe-FH	0.47	0.7996	Not available
^{57}Fe-OM	0.47	0.7654	Not available

5 K

	Center shift mm/s	Quadruple shift at 5 K mm/s	Hyperfine field T
^{57}Fe-FH	0.47	0.001	49.0
^{57}Fe-OM	0.49	-0.0002	47.5

Table S6. DOC, As(V) and Fe(III) determined by TOC analysis, LC-ICP-MS, and the ferrozine assay, respectively, in the total As-Fe-OM fraction collected after 48 hrs of incubation (after completion of dialysis) and in the dissolved fraction (after 3 kDa centrifugal filtration). As and Fe were extracted by adding 500 µL of 2 M HNO_3 (in case of As) and 500 µL of 2 M HCl (in case of Fe) to 500 µL of sample and precipitating the OM at 70°C for 30 min. In both cases, the mixture was then centrifuged at 14,000 RPM for 3 min and the supernatant analyzed for As(III) and As(V) by LC-ICP-MS. No As(III) has been found. It has to be noted, however, that some of the potentially formed As(III) could have been oxidized by the HNO_3.

	As(V) (µg/L)	Fe(III) (µg/L)	DOC (mg C/L)
Total As-Fe-OM fraction	167.1 (12.3)	3256 (329)	39.6 (3.7)
Dissolved fraction	10.2 (0.3)	837 (101)	1.21 (0.0)

* Standard deviations from triplicate measurements are shown in parentheses

3

Influence of natural organic matter on As transport and retention

Prasesh Sharma[1], Massimo Rolle[1], Benjamin Kocar[2], Scott Fendorf[2], Andreas Kappler[1]

[1] Center for Applied Geosciences, University of Tübingen, Germany

[2] Departments of Environmental Earth System Science, Stanford University, Stanford, CA 93405

For submission to *Environmental Science and Technology*

*To whom correspondence should be sent:

Andreas Kappler, Geomicrobiology, Center for Applied Geosciences

University of Tübingen, Sigwartstrasse 10, D-72076 Tübingen, Germany

Phone: +49-7071-2974992, Fax: +49-7071-295059, email: andreas.kappler@uni-tuebingen.de

Running title: Mobility of As in the presence of NOM

Abstract

Natural organic matter (NOM) can affect the behavior of arsenic within surface and subsurface environments. We used batch and column experiments with ferrihydrite-coated sand to determine the effect of peat humic acids (HA), groundwater fulvic acids (GFA), and a soil organic matter (SOM) extract on As sorption and transport. A reactive transport model was used to quantitatively interpret the breakthrough experiments. We found that As(III) breakthrough was faster than As(V) by up to 18 and 14% with and without OM, respectively. The fastest breakthrough occurred in systems containing SOM and GFA. Dialysis and ultrafiltration of samples from breakthrough experiments showed that in systems containing OM, As was transported mostly as free (non-complexed) dissolved As but also as ternary As-Fe-OM colloids and dissolved complexes. In OM-free systems, As was transported in colloidal form or as free ion. During desorption, As(III) desorbed to a greater extent (23-37%) than As(V) (10-16%), with SOM showing highest and OM-free the lowest amount of desorption. Overall, the results demonstrate that (i) NOM can mobilize As as dissolved complexes/colloids, (ii) different fractions of NOM are capable of As mobilization and (iii) freshly extracted SOM (from a forest soil) had greater impact on As transport than purified FA/HA.

Introduction

Arsenic is a toxic element that poses an environmental threat due to its contamination of surface and ground waters worldwide used for domestic consumption *(1)*. In many areas of the world, concentrations of As are higher than the WHO drinking water limit of 10 µg/L *(1)*. The understanding and quantification of physical and biogeochemical processes governing the transport and mobility of this element in complex natural *(2)* and engineered systems *(3)* still remain a challenging task.

Arsenic is present in the environment mainly as inorganic As(III) and As(V), and to a lesser extent organic forms. At neutral pH, As(III) exists as H_3AsO_3 with pK_a values of 9.2, 12.7 and 13.4, whereas As(V) is present as $H_2AsO_4^-$ and $HAsO_4^{2-}$ with pK_a values (for H_3AsO_4) of 2.2, 6.9 and 11.5 *(4)*. Both oxidation states of As can co-exist in solution, with As(III) considered to be generally more mobile than As(V) *(1,5,6)*. The mobility of both species of As is controlled by sorption onto, and redox reactions with, metal oxides and clay minerals *(7,8)*, by competitive sorption of anions such as phosphate (*8-10*), and by redox and complexation reactions with natural organic matter (NOM) *(11-13)***.**

NOM is ubiquitous in both aquatic and terrestrial environments, and can be part of the dissolved or solid phase. The concentration of NOM in groundwater (aquifers) and surface water (rivers and lakes) ranges from 0.1 mg C/L to several hundred mg C/L *(14)*. Soil organic matter (SOM) refers to the organic compounds present in soil from decomposed plant/animal products and soil biomass with fulvic acids (FA) and humic acids (HA) as two of its operationally defined fractions. FA are soluble at all pH values, whereas HA are only soluble in base and insoluble in acid. Both FA and HA bind strongly to metal oxides and clay minerals *(14,15)*.

The interaction of As with metal oxides and minerals in presence of HA and FA has been widely studied in batch experiments *(11,16-22)*. However, it has been less extensively studied in flow-through systems**.** In batch systems, in presence of HA and FA, sorption of both As(V) and As(III) to minerals was found to decrease due to competition of As and NOM for sorption sites at mineral surfaces such as in hematite

(11,19), goethite *(16,22)* and ferrihydrite *(18)*. However, unlike other findings, Grafe (2002) *(17)* found no significant impact of HA or FA in As(III) or As(V) sorption to ferrihydrite in batch systems. Also, HA did not have any discernable effect in transport of As(V) in comparison to As(V) only column systems despite the competitive nature of HA on As sorption to Fe-oxy(hydr)oxides *(17)*. NOM can also leach Fe from Fe-oxy(hydr)oxides forming Fe-NOM/FH-NOM colloids as well as dissolved Fe-NOM complexes (*23,24*). This can in turn form ternary As-Fe-NOM colloids/complexes by interacting with As *(11,24-26)*. Additionally, NOM has been proposed to bind As directly *(27)*, although recent experiments demonstrated that this complex formation is of minor importance in Fe-free humic substances *(24)*.

Despite the recognized importance of As interactions with Fe-(hydr)oxides such as ferrihydrite (FH) in presence of NOM, a comprehensive study of the influence of varying concentrations of different fractions of NOM on As transport/desorption in iron (hydr)oxide dominated systems is lacking. Additionally, almost all studies with NOM have been carried out with purified HA and FA and not with environmentally relevant SOM extracts that were not treated/purified under harsh conditions as it has usually been done with HA and FA. Also, it is unclear in which form the As is mobilized in the environment (i.e. as free As ion or as dissolved or colloidal As-OM, As-Fe-OM, As-FH, or As-FH-OM colloids/complexes).

Therefore, the objectives of this study are: (1) to quantify sorption, desorption and transport of As in ferrihydrite-coated sand (FH-sand) in presence and absence of OM in both batch and flow-through systems, (2) to determine whether SOM, as fulvic and humic acids, can be as competitive in As transport and desorption from FH-sand, (3) to describe As transport and its competitive interaction with different OM fractions with a reactive transport model, and (4) to determine in which form (speciation) As is mobilized in a flow through system, as free (dissolved) As or as dissolved/colloidal As-OM, As-Fe-OM, As-FH, or As-OM-FH.

Material and methods

Reagents. Stock solutions of 1 mM As(III) ($NaAsO_2$) and As(V) ($Na_2HAsO_4 \cdot 7H_2O$) were prepared. Pahokee peat humic acid (HA) was purchased from the International Humic Substances Society (IHSS) (Minnesota, USA) and Gorleben groundwater fulvic acid (GFA) was kindly provided by Prof. Dr. Manfred Wolf (Institute for Groundwater Ecology, Munich, Germany). The extraction procedure for the GFA can be found in *(28).* All stock solutions of As, HA and GFA were prepared in solutions containing both 5 mM NaCl and 1 mM PIPES in deionized water. HA and GFA solutions were readjusted to pH 7.0 using 1 M NaOH and filtered with a 0.45 µm mixed cellulose ester (MCE) filter. Dissolved organic carbon (DOC) concentrations of 5 and 50 mg C/L were chosen since they represent environmentally relevant concentrations of dissolved OM in aquifer systems *(14,29)***.**

Soil organic matter (SOM) extraction. The SOM protocol and chemical data of the SOM extract is given in the Supporting Information (SI) S1 and Table S1).

Synthesis of ferrihydrite-coated sand. Two-line ferrihydrite (FH) was synthesized by hydrolyzing 0.2 M $Fe(NO_3)_3 \cdot 9H_2O$ with 1 M KOH to circumneutral pH (7-7.5) *(30)***.** The required amount of quartz sand (Unimin Corp., Spruce Pine, NC) was washed with DI water twice and then mixed with ferrihydrite to prepare ferrihydrite-coated sand (FH-sand) *(5)* with a total Fe content of ~0.1 % (~1030 µg/g).

Sorption isotherms. Arsenic(III) and As(V) sorption isotherms were determined by equilibrating 1 g FH-sand with 30 mL of As(III) and As(V) solutions with concentrations ranging from 10-5000 µM; the isotherms were conducted in either OM-free solutions or in presence of 30 ml of either 50 mg C/L HA, 50 mg C/L GFA or the SOM extract (SI Table S2). After equilibrating the mixtures for 48 h (23°C, 100 rpm) on a horizontal shaker, samples were taken, filtered with a 0.45 µm MCE filter and prepared for As total measurements (see analytical section). Sampling from As(III) sorption experiments was conducted in an anoxic glovebox.

Column experiments. Breakthrough of As through FH-sand and desorption of As from As-loaded FH-sand in presence of OM (HA, GFA and SOM) and absence of OM (OM-free) was studied under flow conditions (flow rate of 24 µl/min following *(5)* using columns (Kontes Flex-column economy columns, 1.3 cm diameter, 10 cm length) containing ~15 g FH-sand (sand porosity of 0.44). All As(III) related experiments were carried out in an anoxic glovebox. Also, all breakthrough and desorption experiments were carried out in duplicates (SI Table S3). The pH of the effluent remained circumneutral throughout the experiments in all setups.

To study transport (breakthrough) of As through FH-sand, 15 g of FH-sand was filled in columns and equilibrated with 5 mM NaCl and 1 mM PIPES solution for 48 h after which the solutions from the respective experimental setup were injected (SI Table S3). Concentrations of As used in all breakthrough experiments were 10 µM (750 µg/L), which is representative of As concentrations observed in As-contaminated aquifers *(1)*. Breakthrough was considered complete when concentration of As in the eluate for each column was equivalent to that of the influent.

To study desorption of As from FH-sand, As(III) and As(V) were individually presorbed to FH-sand, targeting a surface loading of 60-65% (compared to the maximum value based on sorption isotherms – Figure 1 and Table SI S2) for both As species (yielding 10.1 and 7.6 mmol As/kg FH-sand for As(III) and As(V), respectively). Columns were filled with 15 g of the FH-sand that was presorbed with As(III) or As(V) and the As was then desorbed by OM and OM-free solutions (SI Table S3). Desorption was considered to be complete once the concentration of As in the eluate did not decrease further. A cumulative plot was obtained by summing-up the total moles of As desorbed from samples collected.

Dialysis and ultra-filtration of samples from breakthrough experiments. To quantify in which fraction (colloidal/dissolved) As gets mobilized during breakthrough experiments, selected samples were subjected to dialysis and ultrafiltration following Tufano et al., (2008)*(24)* (SI S2, Table SI S6).

Modeling of batch and column experiments. A two-site Langmuir model, including strong and weak sorption sites, was used to describe the sorption batch experiments of As(III) and As(V) in the absence and presence of different OM fractions (eq 1 and eq 2 in SI S4.1). The same two-site Langmuir model was adopted, as a source/sink term in the one-dimensional transport equation, to simulate the breakthrough column experiments *(31,32)*. However, in our experimental setup the characteristic time of advection (~2×10^4 s) is shorter than the one of sorption (~2×10^5 s) indicating that sorption of As to FH-sand in the columns cannot be considered at local equilibrium. Therefore, a kinetic description based on a linear driving force approach was adopted to describe the mass-transfer between the aqueous and the solid phases (further detail on the model formulation and fitting procedure is provided in SI 4.1, 4.2 and 4.3).

Analytical methods. Samples from batch, breakthrough, desorption and dialysis experiments were filtered with a 0.45 µm filter (MCE, Millipore), acidified with 0.25 M HNO_3 and analyzed for total As by ICP-OES. Samples from ultrafiltration were acidified without filtration. Selected samples were analysed for As speciation by LC-ICP-MS by following standard protocols *(33)*. DOC was quantified using a TOC analyzer. To quantify total Fe, Fe was extracted by 1 M HCl at 90ºC at 150 rpm. After 30 min the suspension was centrifuged at 14,000 g for 5 minutes and the supernatant was analyzed for total Fe (and/or Fe(II)) by the spectrophotometric ferrozine assay *(34)*. The ratio of the absorbance at 465 and 665 nm (E4/E6) was determined by a plate reader (FlashScan 550, Jena Analytik, Germany). Particle size measurements were carried out by a Mastersizer 2000 (Malvern, Germany).

Results and Discussion

Effect of GFA and HA on As sorption to ferrihydrite-coated sand. To quantify sorption of As to FH-sand, As(III) and As(V) were incubated with FH-sand in presence and absence of OM **(**Figure 1).

For both As(III) and As(V), the sorption maximum in presence of HA and GFA was appreciably lower than that for OM-free systems (Figure 1a-c and Figure 1e-g; Table S2). Arsenic(III) showed greater sorption than As(V) on FH-sand in As-only (16.2 compared to 11.4 mmol As/kg sand) and in As-HA systems (11.8 compared to 8.5 mmol As/kg FH-sand). In presence of GFA, As(III) and As(V) sorption was even lower, yielding 4.5 and 3.8 mmol As/kg FH-sand respectively. The total Fe content of the FH-sand did not decrease extensively after addition of HA/GFA, and in all cases less than 5% of the total Fe in the FH-sand was reduced to Fe(II) (data not shown).

The comparison between observed and simulated results (SI S4.1 - Eq. 1 and Eq. 2) shows that a two-site isotherm model (including one weak and one strong binding site, distributed according to the ferrihydrite data provided by Dzombak and Morel, (1990) *(35)*) reasonably describes the measured As concentrations in both absence and presence of OM (Figure 1). In the presence of OM, sorption of both As(III) and As(V) to FH-sand decreased significantly, thus indicating the competitive effects of both HA, GFA and SOM on arsenic sorption. A competitive effect of OM on As adsorption to Fe-oxy(hydr)oxides has been previously reported *(18-20,22)*. However, in a study by *(17)*, FA did not affect As(V) sorption onto ferrihydrite, but only affected As(III) sorption. In this study, no influence of HA on As(III) or As(V) sorption was found. The authors attributed this to the fact that saturation of FH surface sites by As leads to adsorption onto microporous structures of FH which are not accessible to FA or HA for competitive adsorption.

The two As species As(III) and As(V) show different sorption behavior to Fe(III)-(hydr)oxides. With our FH-sand, we saw higher sorption of As(III) compared to As(V) in both OM-containing and OM-free systems confirming previous studies *(10,36,37)*. The adsorption maxima in OM-free systems for As(III) (16.7 mmol/kg) and As(V) (12.1 mmol/kg) FH-sand correspond to 0.87 mol As(III) and 0.65 mol As(V) per mol Fe. These values for As per mol Fe are slightly larger than the ones reported by Dixit and Hering (2003) *(10)* who obtained 0.16 mol As(III) and 0.13 mol As(V) per mol Fe (calculated from their

sorption values of ~1500 µmol/g for As(III) and ~1200 µmol/g for As(V)). This is probably due to the fact that the FH in our systems is distributed on sand particles preventing aggregation of FH particles, and thus providing more exposed surface area for As binding. Alternatively, it could be due to the higher concentration of As we used for sorption isotherms (up to 3 mM As) in comparison to 100 µM used by Dixit and Hering, (2003) *(10)*.

Effect of GFA and HA on As transport and desorption in Fe(III) ferrihydrite systems. After having quantified sorption of As(III) and As(V) to FH-sand in batch experiments, we conducted breakthrough experiments where As enriched solutions were injected into FH-sand filled columns in presence and absence of OM to quantify transport behavior of As in column flow-through systems. In the column experiments, the total time for arsenic breakthrough was up to 700 h which is considerably larger than the time scale of our conservative tracer (i.e., bromide), whose breakthrough occurred in less than 5.5 h. The asymmetrical shape of the measured breakthrough curves is consistent with a rate-limited sorption behavior (Figure 2), and is well described by the reactive transport simulations (Eq. 3 and 4) with the fitted values of the affinity constants for As(III) of 1.2×10^{-3} mol/L and 4.2×10^{-6} mol/L for the weak and strong sites, respectively, and 5.2×10^{-4} mol/L and 9×10^{-7} mol/L for As(V) (SI S4.3 and SI Table S8).

In systems with OM present in the influent, we observed more rapid breakthrough of both As(V) and As(III) compared to OM-free systems (Figure 2). The rapid breakthrough in the presence and absence of OM is given as mean arrival time of the advective front (i.e. arrival time of 50% of the inflowing As concentration; Table S4). Breakthrough of both As(III) and As(V) was faster in presence of HA and GFA than in OM-free systems. In fact, in the OM-free systems the longest breakthrough times were observed: 522 h for As(III) and 609 h for As(V), respectively. In the presence of OM, breakthrough times were significantly shorter: ≤470 h for As(III) and ≤531 h for As(V), respectively. GFA were more

effective than HA in causing more rapid arsenic breakthrough; this effect can be attributed to the smaller molecule size and higher polarity of GFA which results in a stronger competition with As(III) and As(V) for the available sorption sites on the FH-sand. Furthermore, we also found that As(III) breakthrough was generally faster than As(V) by up to 23 and 14% in systems with and without OM respectively which shows that As(III) is more mobile than As(V).

For each OM fraction, concentrations of 5 and 50 mg C/L were injected in the columns (SI Table S3). The breakthrough of arsenic was always faster in the presence of higher OM concentrations. This was particularly true for As(III) with HA (Figure 2a), resulting in a 13 and 26% shorter breakthrough time in 5 and 50 mg C/L HA, respectively. For As(V) breakthrough time was shorter by 10, 34, 32 and 40% in presence of 5 and 50 mg C/L HA, or 5 and 50 mg C/L GFA, respectively, compared to OM-free systems (Figure 2d and 2e, SI Table S4). This behavior is described by the competitive sorption description given in Eq. 2 and Eq. 4 where the competitive effects depend on both sorption affinity and concentration of OM. Although similar values of the affinity constants were obtained from fitting both batch and flow-through experiments (SI Table S7 and S8), it was not possible to obtain a satisfactory match of the column breakthrough curves directly using the parameters determined in the isotherm experiments. Such discrepancies between sorption behavior in batch and flow-through systems have been frequently observed Hanna et al., (2010) *(38)* and may be attributed to factors including different soil/solution ratios, presence of immobile water regions in the porous medium, and changes in sorption site accessibility.

To further understand arsenic mobilization in flow-through systems, As desorption from FH-sand was examined for OM and OM-free solutions. The time scale for desorption experiments was shorter than for the breakthrough experiments (about ~220 h for desorption as compared to ~700 h for breakthrough). With the exception of the experiments with 5 mg C/L HA, the results of the desorption experiments were consistent with what we observed in the breakthrough experiments. We found that the

223 amount of As desorbed in presence of OM was significantly higher than in OM-free systems (Figure 3a
224 and 3b, and SI Table S5). 50 mg C/L GFA showed the largest amount of desorption with 32% in As(III)
225 and 16% in As(V) systems. A concentration of 5 mg C/L GFA was equally effective in desorbing both
226 redox species of As than 50 mg C/L HA with 30% As(III) and 13% desorbed As(V) by 5 mg C/L GFA
227 compared to desorption of 26% As(III) and 11% As(V) by 50 mg C/L HA despite the 10-fold
228 concentration difference between GFA and HA. This can again be explained by the differences in size
229 and polarity of the GFA and HA molecules as described above already for batch (sorption) and
230 breakthrough experiments. Besides their higher polarity due to their higher content in carboxylic groups,
231 FA have a smaller molecule size than HA and thus are situated closer to the oxide surface causing
232 stronger repulsive electrostatic interactions compared to HA *(14,22)*.
233 In our experiments we found that As(III) was more mobile than As(V) at pH 7, confirming findings
234 from previous studies *(5,6,10,38,39)*. In the desorption experiments we carried out, the cumulative
235 amount of As(III) desorbed from the FH-sand was almost twice as much as that for As(V) (~21-37% for
236 desorbed As(III) and 10-16% for As(V)) (Figure 3a and 3b, Table S5). These results confirm previous
237 studies (Herbel and Fendorf, (2006) *(37)*) where the total amount of As desorbed in abiotic columns by
238 mineral media was reported between 22-27% for As(III) and 10-12% for As(V). Interestingly, our initial
239 sorption (batch) experiments showed that more As(III) than As(V) binds to FH-sand. The two different
240 experimental setups (batch sorption vs desorption experiments) therefore show that although As(III) is
241 initially sorbed to a larger extent, the binding to the FH-sand is weaker than As(V) binding and As(III)
242 is more mobile and transported faster than As(V) in the environment.
243
244 **Effectiveness of SOM in desorbing As from ferrihydrite-coated sand in comparison to GFA and**
245 **HA.** To investigate the effect of NOM for transport/mobilization of As under more environmentally
246 relevant conditions, we extracted SOM from a forest soil (SI S1, SI Table S1) and carried out sorption

247 (batch), breakthrough and desorption experiments with the SOM extract. We then compared the results
248 from these experiments to the results obtained with HA/FA, two highly purified and thus chemically
249 modified fractions of NOM. The SOM extract contained 11.5 mg C/L representing typical
250 concentrations of DOC in soils/aquifers. The maximum sorption of As in presence of SOM (4.3 and 3.6
251 mmol/kg FH-sand for As(III) and As(V), respectively) was only slightly lower than that for 50 mg C/L
252 GFA (4.5 and 3.8 mmol/kg FH-sand for As(III) and As(V) respectively) and represented ~50 % and
253 ~25% of the maximum As sorption values in presence of 50 mg C/L HA and OM-free systems,
254 respectively, for both As(III) and As(V) (Figure 1, SI Table S2). In breakthrough experiments, the time
255 needed for breakthrough of As in the presence of SOM was in the same range as observed for the other
256 OM sources (Figure 2A and 2B, SI Table S4). Specifically, in case of As(III), the 50% breakthrough
257 time with 11.5 mg C/L SOM was 287 h which was faster than the breakthrough time obtained with 50
258 mg C/L GFA which was 312 h. In case of As(V), the breakthrough time obtained in presence of 50 mg
259 C/L GFA was slightly more rapid, with 50% breakthrough at 352 h compared to 372 h for SOM. In
260 desorption experiments (Figure 3A and 3B, SI Table S5), SOM and 50 mg C/L GFA desorbed similar
261 amounts of As(V) from FH-sand (both 16%) whereas for As(III), 50 mg C/L GFA desorbed slightly
262 more (37% for 50 mg C/L GFA) compared to 32% for SOM).
263 Our results suggest that the SOM extract was more, or at least equally effective as other OM in
264 transporting and desorbing As. This result is even more significant given the low DOC concentration of
265 SOM that was 11.5 mg C/L which is almost five times lower than the highest concentration (50 mg C/L)
266 of HA and GFA used. The strong competitive effect of SOM on sorption of both As(III) and As(V) is
267 also substantiated by the fitted values of the affinity constants for SOM, which yielded smaller values
268 than the ones for other OM fractions in both batch and flow-through experiments.
269 Results from ion chromatography showed that the SOM extract did not have high concentrations silicate
270 (below detection limit) or phosphate (~100 µg/L) (SI Table S1), two ions which could potentially

271 compete with As for sorption sites *(9)*. The E4/E6 ratio of 6.4 and a DOC concentration of 9.9 mg C/L
272 after 6M HCl addition (82.1% of the original DOC value) shows that the SOM to a large extent had a
273 FA character probably consisting of small, polar organic molecules. This explains why the SOM is more
274 effective than the HA tested. Additionally, the average, molecule size of the SOM was ~95 nm as
275 compared to ~80 nm for the 50 mg C/L GFA and ~160 nm for the 50 mg C/L HA (Table SI S1). This
276 suggests that with a smaller particle size, the SOM is more effective than the HA in competing with and
277 desorbing As. Most importantly, while SOM was extracted in an environmentally relevant manner
278 (extraction with DI water), the HA and GFA used were extracted by repeated additions of concentrated
279 acids and bases including treatment with hydrofluoric acid followed by sorption to hydrophobic XAD
280 resins (e.g. Kappler et al., (2001) *(40)*). This harsh and selective isolation protocol probably destroys
281 and removes environmentally relevant polar organic fractions of HA and GFA which could otherwise be
282 present and probably more effective in influencing arsenic mobility *(41)*. In our SOM extract, these
283 fractions were present since no purification of the SOM was carried out and therefore explain the high
284 efficiency of the SOM extract.
285 The greater effectiveness of the SOM in affecting As transport and desorption from FH-sand in
286 comparison to GFA/HA shows that results obtained from extracted and purified humics could possibly
287 underestimate the effects of SOM on As transport. In some of the As contaminated areas in the world,
288 for example in Bangladesh, the effect of SOM on As mobilization/desorption could be even stronger
289 where high phosphate and silicate concentrations are present in surface water infiltrating the aquifers
290 thus even increasing the effect of SOM and causing a cumulative effect on the mobilization of As *(42)*.
291
292 **Speciation of As mobilized by OM under flow-through conditions.** The interaction of OM with FH
293 can produce FH-OM colloids and dissolved Fe-OM complexes *(23, 24)*. Free As ions can bind to
294 FH/FH-OM-colloids or dissolved Fe-OM complexes to form ternary As-Fe-OM complexes/colloids

295 *(24,43)*. In flow-through systems, however, it is unclear which fraction (dissolved As,
296 dissolved/colloidal As-OM, dissolved As-Fe-OM complexes, As-FH colloids or As-OM-FH colloids)
297 dominates As transport. Therefore we selected samples from breakthrough experiments (samples from
298 pore volume 25) and used dialysis and ultracentrifugation to separate the different fractions (Table SI6).
299 The highest total Fe concentrations (before dialysis) were found in the eluates from columns running
300 with OM. This suggests that OM is able to leach Fe from FH-sand and form Fe-OM/FH-OM colloids as
301 well binary Fe-OM complexes also in flow-through systems similar as observed recently in batch
302 systems (*24*). Dialysis of column eluates showed that As was present (and thus transported) mostly
303 (>90%) as a free ion with less than 10% of total As remaining in the dialysis bags (i.e. As probably
304 bound to OM molecules larger than 0.45 µm) (Table SI S6). After dialysis, >70% of total Fe stayed in
305 the dialysis bags in samples stemming from columns running with OM (Table SI6) suggesting that also
306 most of the Fe was present in OM molecules/aggregates larger than 0.45 µm. Quantification of As in the
307 fractions separated by dialysis showed that after completion of dialysis, ~3.5-20 µg/L of total As and
308 ~110-330 µg/L of total Fe remained inside with highest concentration of As and Fe in setups with SOM
309 followed by GFA, HA and lastly OM-free system for both As(III) and As(V) related setups (Table SI6).
310 When comparing the setups containing different OM sources we found that the highest concentrations
311 of total Fe after dialysis were present in systems containing SOM (284 for As(III) and 334 µg/L for
312 As(V)), followed by setups running with GFA (192 for As(III) and 251 µg/L for As(V)) and HA (141
313 for As(III) and 165 µg/L for As(V)). This demonstrates that OM with smaller molecular weight
314 fractions (i.e. GFA and SOM) was able to leach out more Fe from FH-sand than HA. A small fraction of
315 As even remained inside the dialysis bag in the OM-free system together with very low concentrations
316 of Fe suggesting that As can also be transported by colloidal FH particles in absence of OM.
317 To quantify the amount of As in the truly dissolved fraction compared to the colloidal fraction, all
318 samples that were dialysed were subjected to 3 kDa filtration. We found that approximately ~15-55%

(1.5-7.3 µg/L) of total As and ~35-67% (~90-140 µg/L) of total Fe from the dialysed fraction remained in the 3 kDa filtrate (i.e. the dissolved fraction) in setups containing OM. Analysis of DOC contents in the colloidal and dissolved fractions showed that between 0.9-1.2 mg C/L remained in the 3 kDa filtrate (i.e. the dissolved fraction) corresponding to ~2% of the HA, 2% of the GFA and ~10% of the SOM of the colloidal fraction. These values in the 3 kDa filtrate are comparable to values that have been reported earlier by *(24,43)* for similar studies. The results obtained in the present study with samples from breakthrough experiments confirm the formation of both ternary colloids/complexes of As-Fe-OM which have been proposed previously *(11,24,26,43)*. Dissolved As-Fe-OM complexes can form when Fe ions act as a cation-bridge to bind As to Fe-OM complexes. Colloids containing FH and Fe-OM complexes can form when OM interacts with FH-sand. Interaction of free As with the Fe-OM complexes or FH-OM colloids can then form As-FH-OM colloids or As-Fe-OM complexes. Release of FH colloids from FH by OM was described previously *(23)*.

In samples with SOM, even more total As was found in dissolved fraction (6.7 µg/L in As(V) and 7.3 µg/L in As(III)) compared to GFA (5.5 µg/L in As(V) and 3.6 µg/L in As(III)) and HA (1.5 µg/L in As(V) and 1.9 µg/L As(III)). This again confirms the efficiency of SOM in comparison to other purified OM fractions, in affecting arsenic transport. There were no significant differences in the amount of As total in dissolved fraction between As(III) and As(V) setups. In samples from OM-free systems, no detectable total As and total Fe was obtained which shows that As was only transported as free dissolved species in setups containing no OM.

Environmental relevance of effects of NOM on As transport. In this study we demonstrated the effect of different fractions of NOM on As transport and mobilization. Experiments with SOM extracted from forest soil showed that fresh OM from natural soils can be as effective as FA or even more effective in affecting As transport and desorption from Fe-oxide minerals than more hydrophobic and

large molecule-sized HA. This suggests that fresh NOM infiltrating from surface waters (e.g. from surface ponds or during monsoon) into aquifers, subject to excessive groundwater use *(44)***,** may promote efficient and rapid As mobilization. Our data also suggests that results solely based on experiments obtained with purified HA and FA may underestimate the role of NOM in As-contaminated aquifers.

Acknowledgements

This work was supported by an IPSWaT fellowship from the BMBF to PS and by funding from the DFG and BMBF to AK. We would like to thank J. Breuer (University of Hohenheim), P. Kühn and F. Baumann (University of Tuebingen), B. Daus (UFZ, Leipzig) for their help with As-analytics respectively and G. Chiogna, R. Martinez, M. Mühe, M. Emmerich, E.D. Melton, U. Dippon (Tuebingen) and Y. Masue-Slowey, G. Li (Stanford) for sampling and/or valuable suggestions to improve the experiments and the manuscript. Support for work conducted at Stanford University was provided by the Stanford NSF Environmental Molecular Science Institute (NSF-CHE-0431425).

Supporting information available

Soil organic matter (SOM) extraction (section S1) and chemical data of the SOM extract (Table S1). Sorption and column experimental setups (section S2) with sorption maxima of As(III) and As(V) to FH-sand (Table S2). Setups and experimental conditions for breakthrough and desorption experiments (Table S3). Average As breakthrough times for different experimental setups (Table S4). Total amount of As desorbed from FH-sand in desorption experiments (Table S5). Dialysis and ultra-filtration of samples from breakthrough experiments (section S2) with As(total) and Fe(total) in samples from breakthrough experiments before and after dialysis, and after 3 kDa centrifugal filtration (Table S6). Modeling approach and fitting procedure (SI section S4) with Modeling of batch and column

367 experiments (S4.1). Fitting parameters for isotherm experiments (SI S4.2, Table S7) and column
368 experiments (S4.3, Table S8) are available.
369

370 ## References

371

372 1 Smedley, P. L.; Kinniburgh, D. G. A review of the source, behaviour and distribution of arsenic
373 in natural waters. *App. Geochem.* **2002**, *17*, 517-568.
374 2 Fendorf, S.; Michael, H.A..; van Green, A. Spatial and Temporal Variations of Groundwater
375 Arsenic in South and Southeast Asia. *Science* **2010**, *328*, 1123-1127.
376 3 Wallis, I.; Prommer, H.; Simmons, C. T.; Post, V.; Stuyfzand, P. J. Evaluation of conceptual and
377 numerical models for arsenic mobilization and attenuation during managed aquifer recharge.
378 *Environ. Sci. Technol.* **2010**, *44*, 5035-5041.
379 4 Warwick, P.; Inam, E.; Evans, N. Arsenic's interaction with humic acid. *Environ. Chem.* **2005**,
380 *2*, 119-124.
381 5 Tufano, K.J.; Fendorf, S. Confounding impacts on iron reduction on arsenic retention. *Environ.*
382 *Sci. Technol.* **2008**, *42*, 4777-4783.
383 6 Tufano, K.J.; Reyes, C.; Saltikov, C.W.; Fendorf, S. Reductive processes controlling arsenic
384 retention: Revealing Importance of Iron and Arsenic Reduction. *Environ. Sci. Technol.* **2008**, *42*,
385 8322-8289.
386 7 Goldberg, S. Competitive adsorption of arsenate and arsenite on oxides and clay minerals. *Soil*
387 *Sci. Soc. of Am. J.* **2002**, *66*, 413-421.
388 8 Amstaetter, K.; Borch, T.; Larese-Casanova, P.; Kappler, A. Transformation of Arsenic by
389 Fe(II)-Activated Goethite (α-FeOOH). *Environ. Sci. Technol.* **2010**, *44*, 102–108.
390 9 Violante, P.; Pigna, M. Competitive Sorption of Arsenate and Phosphate on Different Clay

391 Minerals and Soils. *Soil Sci. Soc. Am. J.* **2002**, *66*, 1788–1796.
392 10 Dixit, S.; Hering, J. G. Comparison of Arsenic(V) and Arsenic(III) Sorption onto Iron Oxide
393 Minerals: Implications for Arsenic Mobility. *Environ. Sci. & Technol.* **2003**, *37*, 4182-4189.
394 11 Redman, A. D.; Macalady, D. L.; Ahmann, D. Natural organic matter affects arsenic speciation
395 and sorption onto hematite. *Environ. Sci. & Technol.* **2002**, *36*, 2889-2896.
396 12 Wang, S.; Mulligan, C. N. Effect of natural organic matter on arsenic release from soils and
397 sediments into groundwater. *Environ. Geochem. and Health* **2006**, *28*, 197-214.
398 13 Jiang, J.; Bauer, I.; Paul, A.; Kappler, A. Arsenic Redox Changes by Microbially and
399 Chemically Formed Semiquinone Radicals and Hydroquinones in a Humic Substance Model
400 Quinone. *Environ. Sci. & Technol.* **2009**, *43*, 3639-3645.
401 14 Stevenson, F.J. *Humus Chemistry: Genesis, Composition, Reactions*. Wiley: New York, 1994.
402 15 Gu, B.; Schmitt, J.; Chen, Z.; Liang, L.; McCarthy, J. Adsorption and desorption of different
403 organic matter fractions on iron oxide. *Geochim. Cosmochim. Acta* **1994**, *59*, 219-229.
404 16 Grafe, M.; Eick, M.J.; Grossl, P.R. Adsorption of Arsenate (V) and Arsenite (III) on
405
406 Goethite in the Presence and Absence of Dissolved Organic Carbon. Soil Sci. Soc. Am. J. **2001**,
407
408 *65*, 1680–1687.
409
410 17 Grafe, M.; Eick, M.; Gross, P.R.; Saunders, A.M. Adsorption of arsenate and arsenite on
411 ferrihydrite in the presence and absence of dissolved organic carbon. *J. Environ. Qual.* **2002**,
412 *31*, 1115–1123.
413 18 Simeoni, M. A.; Batts, B. D.; McRae, C. Effect of groundwater fulvic acid on the adsorption of
414 arsenate by ferrihydrite and gibbsite. *Appl. Geochem.* **2003**, *18*, 1507–1515.
415 19 Ilwon, K.; Ju-Yong, K.; Kyoung-Woong, K. Arsenic speciation and sorption kinetics in the As–
416 hematite–humic acid system. *Colloids Surf. A* **2004**, *234*, 43-50.
417 20 Gustafsson, J. P. Arsenate adsorption to soils: Modelling the competition from humic

418 substances. *Geoderma* **2006**, *136*, 320–330.

419 21 Ilwon, K.; Davis, A. P.; Ju-Yong, K.; Kyoung-Woong, K. Effect of contact order on the
420 adsorption of inorganic arsenic species onto hematite in the presence of humic acid. *J. Hazard.*
421 *Mater.* **2006**, *141*, 53-60.

422 22 Weng, L.; Riemsdijk, W.H.V.; Hiemstra, T. Effects of Fulvic and Humic Acids on Arsenate
423
424 Adsorption to Goethite: Experiments and Modeling. *Environ. Sci. Technol.* **2009**, 43, 7198–
425
426 7204.
427
428 23 Liang, L.; McCarthy, J. F., Jolley, L. W.; McNabb, J. A.; Mehlhorn, T. L. Iron dynamics:
429 transformation of Fe(II)/Fe(III) during injection of natural organic matter in a sandy aquifer.
430 *Geochim. Cosmochim. Acta* **1992**, *57*, 1987-1999.

431 24 Sharma, P.; Ofner, J.; Kappler, A.; Formation of binary and ternary colloids and dissolved
432 complexes of organic matter, Fe and As. *Environ. Sci. and Technol.* **2010**, *44*, 4479-4485.

433 25 Bauer, M. B.; Blodau, C. Mobilization of arsenic by dissolved organic matter from iron oxides,
434 soils and sediments. *Environ. Sci. & Technol.* **2006**, *354*, 179-190.

435 26 Ritter, K.; Aiken, G. R.; Ranville, J. F.; Bauer, M.; Macalady, D. L. Evidence for the aquatic
436 binding of arsenate by natural organic matter-suspended Fe(III). *Environ. Sci. & Technol.* **2006**,
437 *40*, 5380-5387.

438 27 Buschmann, J.; Kappeler, A.; Indauer, U.; Kistler, D.; Berg, M.; Sigg, L. Arsenite and Arsenate
439 Binding to Dissolved Humic Acids: Influence of pH, Type of Humic Acid, and Aluminum.
440 *Environ. Sci. & Technol.* **2006**, *40*, 6015-6020.

441 28 Kim, J.I.; Buckau, G.; Li, G.H.; Duschner, H.; Psarro, N. Characterization of humic and fulvic
442 acids from Gorleben groundwater. *J. Anal. Chem.* **1990**, *338*, 245- 252.

443 29 Mladenov, N.; Zheng, Y.; Miller, M.P.; Nemergut, D.R.; Simone, B.; Hageman, C.; Rahman,
444 M.M.; Ahmed, K.M.; Mcknight, D.M. Dissolved Organic Matter Sources and Consequences for

Iron and Arsenic Mobilization in Bangladesh Aquifers. *Environ. Sci. Technol.* **2010**, *44*, 123-128.

30 Schwertmann, U. C.; Cornell, R. M. The Iron oxides; Wiley-VCH: New York, 2003.

31 Radu, T.; Kumar, A.; Clement, T. P.; Jeppu, G.; Barnett, M. O. Development of a scalable model for predicting arsenic transport coupled with oxidation and adsorption reactions. *J. Contam. Hydrol.* **2008**, *95*, 30–41.

32 Mikutta, C.; Wiederhold, J.G.; Cirpka, O.A.; Hofstetter, T.B.; Bourdon, B.; Von Gunten, U. Iron isotope fractionation and atom exchange during sorption of ferrous iron to mineral surfaces. *Geochim. Cosmochim. Acta* **2009**, *73*, 1795–1812.

33 Daus, B.; Mattusch, J.; Wennrich, R.; Weiss, H. Investigation on stability and preservation of arsenic species in iron rich water samples. *Talanta* **2002**, *58*, 57-65.

34 Stookey, L. L. Ferozine - A new spectorophotometric reagent for iron. *Anal. Chem.* **1970,** *42*, 779-781.

35 Dzombak, D. A.; Morel, F.M.M. Surface Complexation Modeling; Wiley and Sons: New York, 1990.

36 Raven, K.P.; Jain, A.; Loeppert, R.H. Arsenite and Arsenate adsorption on Ferrihydrite: Kinetics, Equililibrium, and Adsorption envelopes. *Environ. Sci. Technol.* **1998**, *32*, 344-349.

37 Herbel, M.; Fendorf, S. Biogeochemical processes controlling the speciation and transport of arsenic within iron coated sands. *Chem. Geol.* **2006**, *228*, 16–32.

38 Hanna, K.; Rusch, B.; Lassabatere, L.; Hofmann, A.; Humbert, B. Reactive transport of gentisic acid in a hematite-coated sand column: Experimental study and modeling. *Geochim. Cosmochim. Acta.* **2010**, *74*, 3351–3366.

39 Kocar, B.D.; Herbel, M.J.; Tufano, K.J.; Fendorf, S. Contrasting effects of Dissimilatory Iron(III) and As(V) reduction on Arsenic Retention and Transport.

40 Kappler, A.; Ji, R.; Schink, B.; Brune, A. Dynamics in composition and size-class distribution of humic substances in profundal sediments of Lake Constance. *Org. Geochem.* **2001**, *32*, 3–10.

41 Kappler, A.; Brune, A. Influence of gut alkalinity and oxygen status on mobilization and size-class distribution of humic acids in the hindgut of soil-feeding termites. *Appl. Soil Ecol.* **1999**, *13*, 219–229.

42 Hossain, M. F. Arsenic contamination in Bangladesh – an overview. *Agricult. Ecosys. Environ.* **2006**, *113*, 1-16.

43 Bauer, M.; Blodau, C. Arsenic distribution in the dissolved, colloidal and particulate size fraction of experimental solutions rich in dissolved organic matter and ferric iron. *Geochim. Cosmochim. Acta* **2009**, *73*, 529-542.

44 Burgess, W.G.; Hoque, M.A.; Michael, H.A.; Voss, C.J.; Breit, G.N.; Ahmed, K.M. Vulnerability of deep groundwater in the Bengal aquifer system to contamination by arsenic. *Nature Geosci.* **2010**, *3*, 83-87.

Figures

Figure 1. Sorption isotherms of As(III) and As(V) onto FH-sand in organic-matter-free systems compared to systems containing Pahokee Peat Humic Acids (HA), Gorleben Groundwater fulvic acids (GFA) and extracted soil organic matter (SOM).

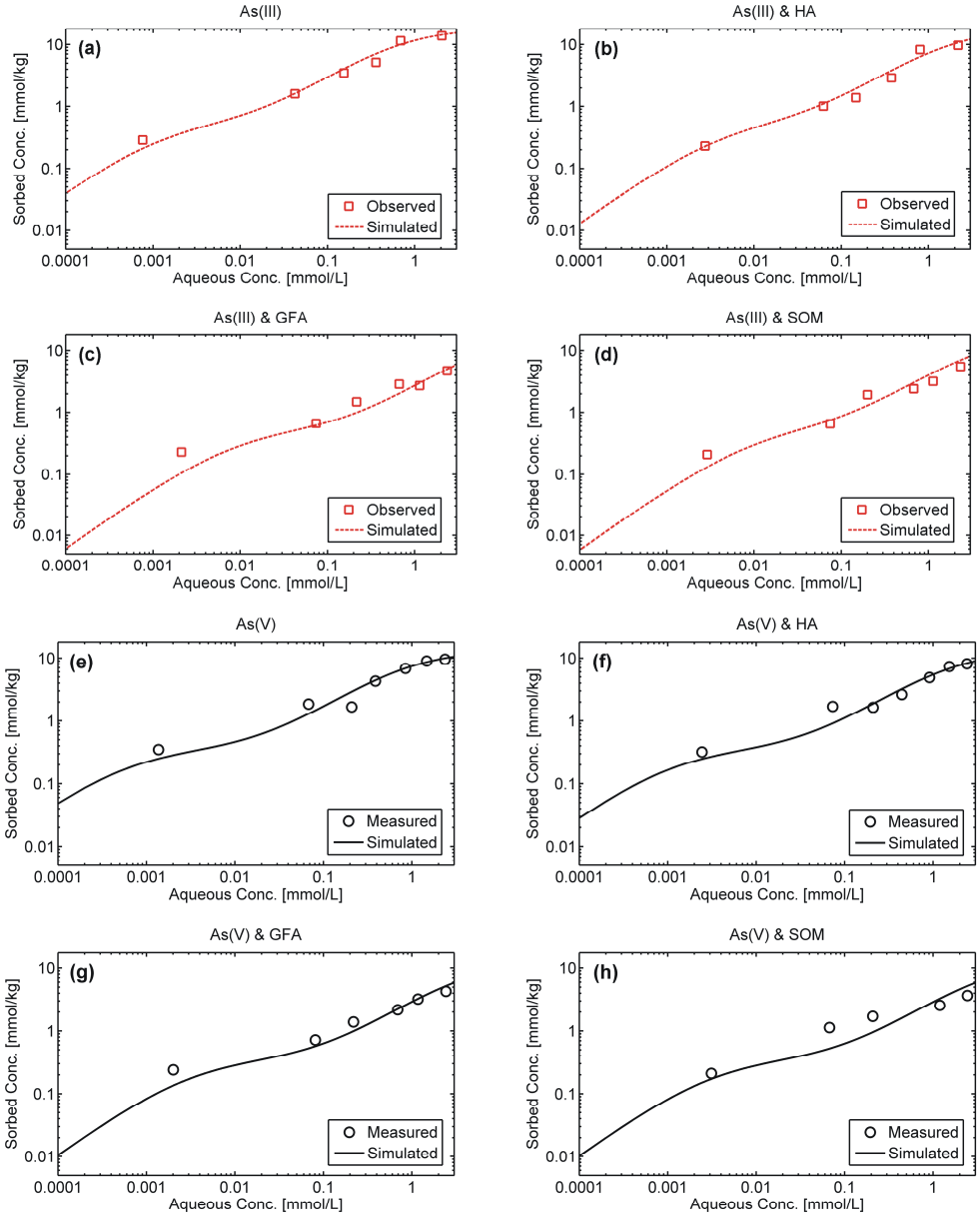

504

505

506 Figure 2. Breakthrough curves of 10 µM As(III) (left) and As(V) (right) in FH-sand filled columns in
507 presence and absence of various concentrations and types of OM: Pahokee Peat Humic Acids (HA),
508 Gorleben Groundwater fulvic acids (GFA) and extracted soil organic matter (SOM).

509

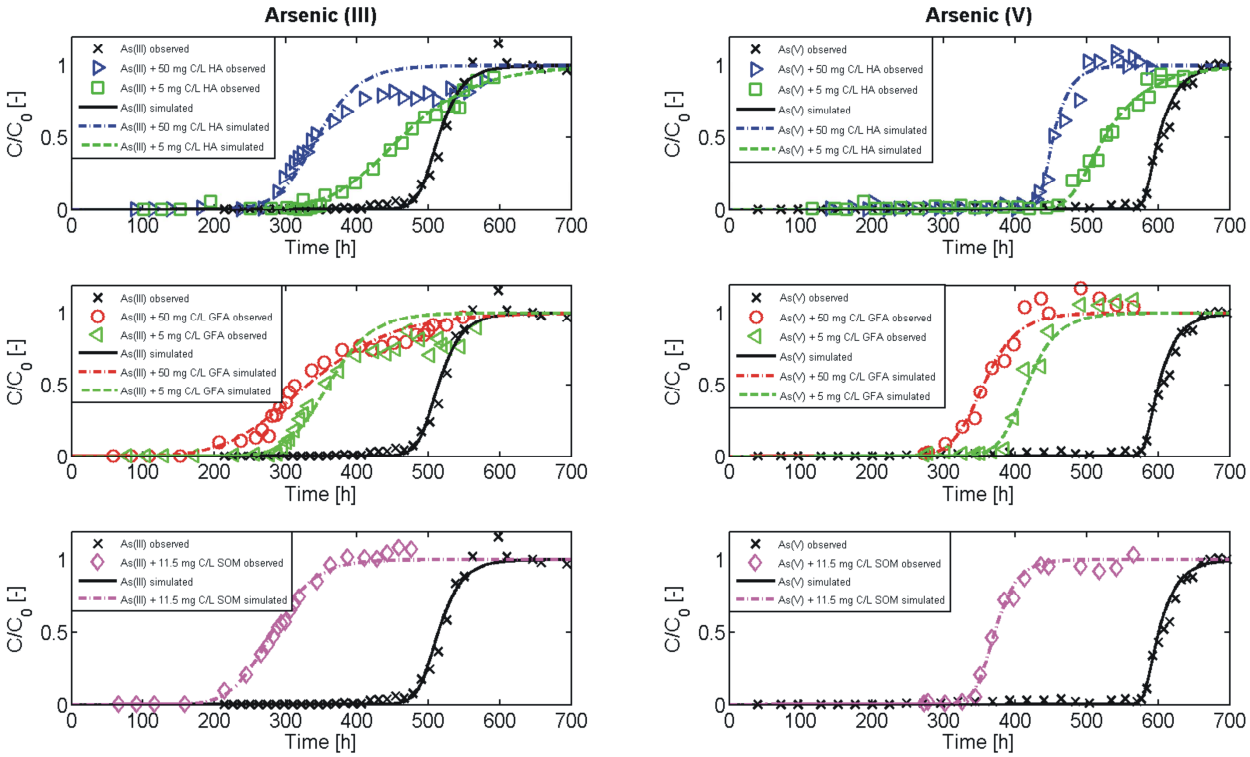

510

Figure 3. Desorption curves of As(III) (a) and As(V) (b) from FH-sand filled columns in presence and absence of various concentrations of Pahokee Peat Humic Acids (HA), Gorleben Groundwater fulvic acids (GFA) and extracted soil organic matter (SOM).

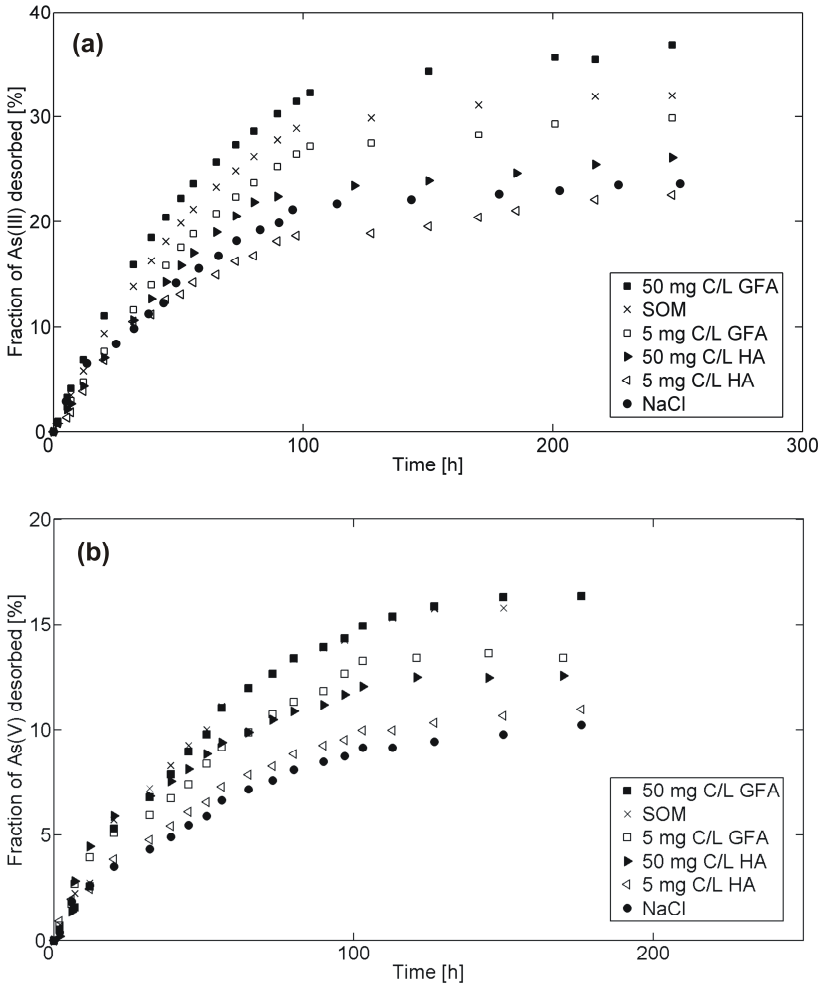

- Supporting Information -

Influence of natural organic matter on As transport and retention

Prasesh Sharma[1], Massimo Rolle[1], Benjamin Kocar[2], Scott Fendorf[2], Andreas Kappler[1]

[1] Center for Applied Geosciences, University of Tübingen, Germany

[2] Departments of Environmental Earth System Science, Stanford University, Stanford, CA 93405

For submission to *Environmental Science and Technology*

*To whom correspondence should be sent:
Andreas Kappler, Geomicrobiology, Center for Applied Geosciences
University of Tübingen, Sigwartstrasse 10, D-72076 Tübingen, Germany
Phone: +49-7071-2974992, Fax: +49-7071-295059, email: andreas.kappler@uni-tuebingen.de

Running title: Running title: Mobility of As in the presence of NOM

- pages (11 including cover page)
- Figures (0)
- Tables (8)

Section S1. Soil organic matter (SOM) extraction and chemical data.

Supporting Information S1: Extraction of SOM. The SOM was extracted as described by Kaiser et al. (2005). Top soil was collected from the O-horizon from a forested area in Schönbuch (close to the city of Tübingen, Germany). The organic matter rich moist soil was sieved (<2 mm) to remove coarse particles. 500 g of the freshly sieved soil was added to 2 L of deionised water in a 2.5 L glass bottle and shaken (under oxic conditions) for 24 hours in a rotable shaker at 15 rpm. The suspension was left to settle for another 24 hours before passing the supernatant through a 0.45 µm MCE filter. The SOM filtrate contained 11.5 mg C/L dissolved organic carbon (DOC), the pH was 7.2 and the E4/E6 ratio was 6.4 (Table S1). To determine whether the humic acid or the fulvic acid fraction is the dominant fraction of the SOM, an aliquot of SOM was acidified to pH 1 by 6 M HCl to precipitate the humic acids. The acidified solution was incubated for 48 hrs at room temperature after which the mixture was centrifuged and the supernatant analyzed for DOC which yielded 9.9 mg C/L meaning that the humic acid fraction represented about 14% in the SOM extract.

Table S1. Major elemental concentration in SOM extract measured with ICP-OES (a); Concentrations of anions in the SOM extract (measured with IC) (b); Dissolved organic carbon concentration (DOC) of the SOM extract before and after 6 M HCl extraction (c); pH and E4/E6 values of the SOM extract (d); and average particle size of the SOM extract compared to GFA and HA (e).

a) Major elements concentration in the SOM extract (all values are given in mg/L)

Ca	Fe	K	Mg	Na	P	Si	Mn
105.1	0.6	6.9	9.4	4.2	0.1	4.8	<0.1

b) Concentration of anions in the SOM extract (mg/L)

F^-	Cl^-	NO_2^-	Br^-	NO_3^-	PO_4^{3-}	SO_4^{2-}
0.1 (0.0)	24.2 (0.9)	0.1(0.0)	n.a.	56.2(2.3)	0.10(0.0)	10.4 (0.7)

* Standard deviations from triplicate measurements are shown in parentheses

c) DOC in the SOM extract before and after 6 M extraction (mg C/L)

before	after
11.5 (0.8)	9.9 (1.2)

* Standard deviations from triplicate measurements are shown in parentheses

d) pH and E4/E6 values of the SOM extract	
pH	7.2 (0.2)
E4/E6	6.4 (0.5)

* Standard deviations from triplicate measurements are shown in parentheses

559

e) Particle size of the molecules in the SOM extract compared to GFA and HA (in nm)	
SOM	95 (8)
50 mg C/L GFA	78 (5)
50 mg C/L HA	162 (13)

* Standard deviations from triplicate measurements are shown in parentheses

560

561

562 **Section S2. Sorption and column experiments - setups and results.**

563

Table S2. As(III) and As(V) sorption maxima (mmol/kg FH-sand) from batch experiments.

setup	As(III) [mmol/kg]	As(V) [mmol/kg]
OM-free	16.7	11.3
50 mg C/L HA	11.8	8.5
50 mg C/L GFA	4.5	3.8
SOM	4.3	3.6

Solid to liquid density - 1 g FH-sand: 30 ml solution. Background was 1 mM PIPES and 5 mM NaCl in all experiments. The sorption maxima was obtained via a two-sites Langmuir model approach (Detailed information in SI 4.1)

564

Table S3. Setups and experimental conditions for As(III) and As(V) breakthrough and desorption experiments.

Breakthrough experiments	Desorption experiments
OM-free*	OM-free*
5 mg C/LHA	5 mg C/L HA
50 mg C/L HA	50 mg C/L HA
5 mg C/L GFA	5 mg C/LGFA
50 mg C/L GFA	50 mg C/L GFA
SOM	SOM

*OM-free systems: 1 mM PIPES + 5 mM NaCl. For breakthrough experiments the solutions contained either 10 µM As(III) or As(V). For desorption experiments, the FH-sand was presorbed with As(III) or As(V) separately before desorbed by the solutions above. Solutions for all setups (breakthrough and desorption) were prepared in a background of 1 mM PIPES and 5 mM NaCl. All experiments were carried out in duplicates.

565

Table S4. Time required (in hours) for 50% As breakthrough in different setups.

setups	As(III)	As(V)
OM-free	609	522
5 mg C/L	531	470
50 mg C/L HA	452	347
5 mg C/L GFA	408	354
50 mg C/L GFA	352	312
SOM	372	287

566

567

568

Table S5. Total amount of As desorbed (in %) from columns at the end of the experiment in different setups.

setups	As(III)	As(V)
OM-free	21	10
5 mg C/L HA	21	11
50 mg C/L HA	26	11
5 mg C/L GFA	29	13
50 mg C/L GFA	32	16
SOM	37	16

569

570 **Section S3. Dialysis and ultra-filtration of samples from breakthrough experiments.**

571 **Supporting Information S2:** Selected **s**amples from breakthrough experiments (for both As(III) and
572 As(V) column experiments) were dialyzed following Sharma et al. (2010) using 1000 MWCO
573 Regenerate Cellulose ester membrane dialysis bags (Roth, Germany) after washing the membranes first
574 with DI water and then with 5 mM NaCl. 10 ml aliquots samples from As only, As + 50 mg C/L HA;
575 As + 50 mg C/L GFA; and As + SOM setups were placed in the dialysis bags separately and were
576 dialyzed. The solution outside was replaced daily by fresh 5 mM NaCl solution until no detectable As
577 was present outside the dialysis bags (this took 7 days). Samples from inside the dialysis bags were
578 analyzed for OM-bound Fe and OM-bound As. An aliquot from the samples from inside the dialysis
579 bags was subjected to centrifugal filtration with a nominal 3 kDa (~2 nm) filter (Millipore) to quantify
580 dissolved vs colloidal fractions of As (see Bauer and Blodau, (2009)). The pH of the solution did not
581 change upon ultrafiltration.

582

Table S6. As(total) and Fe(total) in samples before and after dialysis and after 3 kDa centrifugal filtration.

As(total)

setups	before dialysis	after dialysis	after dialysis	after 3 kDa	after 3 kDa
	µg/L	µg/L	%	µg/L	%
As(V) only	453	2.2	0.5	bdl	-
As(III) only	477	1.6	0.3	bdl	-
As(V) and SOM	263	17.4	6.6	6.7	38.7
As(III) and SOM	298	20.7	6.9	7.3	35.2
As(V) and HA	641	10.4	1.6	1.5	14.7
As(III) and HA	742	8.7	1.2	1.9	21.7
As(V) and GFA	258	10.9	4.2	5.5	50.5
As(III) and GFA	225	15.8	7.0	3.5	22.1

Fe(total)

setups	before dialysis	after dialysis	after dialysis	after 3 kDa	after 3 kDa
	µg/L	µg/L	%	µg/L	%
As(V) only	77	bdl	-	0	0
As(III) only	82	bdl	-	0	0
As(V) and SOM	487	334	68.5	140	41.8
As(III) and SOM	342	284	83.2	101	35.4
As(V) and HA	185	141	76.3	bdl	-
As(III) and HA	188	165	87.7	bdl	-
As(V) and GFA	210	192	91.2	129	66.9
As(III) and GFA	265	251	94.6	96	38.1

DOC

setups	before dialysis	after dialysis	after dialysis	after 3 kDa	after 3 kDa
	mg C/L	mg C/L	%	mg C/L	%
As(V) only	0	bdl	-	0	0
As(III) only	0	bdl	-	0	0
As(V) and SOM	11.7	11.2	95.7	0.9	8.0
As(III) and SOM	11.1	10.8	97.3	1.3	12.0
As(V) and HA	48.7	47.1	96.7	1.1	2.3
As(III) and HA	50.1	48.1	96.0	1.2	2.5
As(V) and GFA	52.3	48.9	93.5	1.4	2.9
As(III) and GFA	47.1	46.4	98.5	0.9	1.9

*bdl: below detection limit. All samples were measured in duplicates. Setups containing 50 mg C/L HA and 50 mg C/L GFA were chosen for the experiments for HA and GFA. $\%^{+}$: total As, total Fe and DOC remaining in the bag after dialysis, $\%^{\#}$: fraction of total As, total Fe and DOC in the 3 kDa filtrate of that was remaining in the dialysis bags.

S4. Modeling approach and fitting procedure.

Supporting Information S4.1 - Modeling of batch and column experiments. Different modeling approaches to simulate the sorption experiments were screened and preliminarily tested. Under the specific conditions of this study, where the pH was maintained constants using buffered solutions in both batch a flow-through systems, a surface complexation model (SCM) explicitly taking into account the effects of electrostatic terms was deemed unnecessary. An approach based on the Langmuir sorption isotherm equation was selected. This simple sorption model provided a reasonable fit of the experimental batch observations for both As(III) and As(V). However, the good agreement was limited to the high concentrations whereas the environmental significant low concentrations, at which the column breakthrough experiments have been performed (i.e., 10 μM), were poorly matched. Therefore, a two-site Langmuir model, including strong and weak sorption sites, was selected and used to describe sorption in both batch and flow-through experiments carried out in this study.

The sorption isotherms for As(III) and As(V), without the presence of OM, read as:

$$q_{As}^{eq} = \frac{q_{\max,s} c_{As}}{K_{L,s} + c_{As}} + \frac{q_{\max,w} c_{As}}{K_{L,w} + c_{As}} \quad (1)$$

where q_{As}^{eq} [MM^{-1}] is the sorbed arsenic concentration at equilibrium, $q_{max,s}$ and $q_{max,w}$ [MM^{-1}] are the sorption capacities of the strong and weak sites, $K_{L,s}$ and $K_{L,w}$ [ML^{-3}] the affinity constants (i.e. inverse of the equilibrium constants) and c_{As} [ML^{-3}] is the concentration of arsenic in the aqueous phase. The competitive effects of the different fractions of NOM influencing arsenic sorption to the FH-sand were described with the following multi-component isotherm:

$$q_{As}^{eq} = \frac{q_{\max,s} c_{As}}{K_{L,s}(1 + c_{OM} / K_{OM,s}) + c_{As}} + \frac{q_{\max,w} c_{As}}{K_{L,w}(1 + c_{OM} / K_{OM,w}) + c_{As}} \quad (2)$$

where c_{OM} [ML^{-3}] represents the aqueous concentration of the organic matter (i.e. HA, GFA and SOM, respectively) and $K_{OM,s}$ and $K_{OM,w}$ [ML^{-3}] its affinity for the strong and weak sites.

The same two-site isotherm model was adopted to simulate the breakthrough column experiments. In these systems the transport of As(III) and As(V), continuously injected in absence and/or presence of different OM fractions, is described by the one-dimensional advection-dispersion equation including sorption as a source/sink term (Radu et al., 2008; Mikutta et al., 2009). In our experimental setup the characteristic time of advection (~2×10^4 s) is shorter than the one of sorption (~2×10^5 s), thus indicating that sorption of As to FH-sand in the columns cannot be considered at local equilibrium. Therefore, a

kinetic description based on a linear driving force approach was adopted to describe the mass-transfer between the aqueous and the solid phases. The equations describing As reactive transport read as:

$$\frac{\partial c_{As}}{\partial t} + v\frac{\partial c_{As}}{\partial x} - D\frac{\partial^2 c_{As}}{\partial x^2} = -\frac{(1-n_e)\rho_s}{n_e}\lambda\left(q_{As}{}^{eq} - q_{As}\right) \quad (3)$$

$$\frac{\partial q_{As}}{\partial t} = \lambda\left(q_{As}{}^{eq} - q_{As}\right) \quad (4)$$

where x [L] and t [T] are the spatial and temporal coordinates, v [LT^{-1}] is the seepage velocity, n_e [-] the effective porosity, ρ_s the mass density of the solids [ML^{-3}] and λ [T^{-1}] the mass-transfer coefficient. The equilibrium As concentration in the solid phase, $q_{As}{}^{eq}$, is expressed as Eq. 1 for the OM-free column systems or as Eq. 2 to describe the competitive effects of HA, GFA and SOM on arsenic transport.

Supporting Information S4.2 - Isotherm Experiments. The batch experiments performed with As(III) and As(V) in the absence and presence of different fractions of OM were simulated using a two-sites Langmuir model without and with competition (Eq. 1 and Eq. 2, respectively). The Nelder-Mead simplex algorithm was used as optimization scheme. In the experiments with arsenic alone, the fitted parameters were the sorption maximum capacity for the weak and strong ferrihydrite sites, distributed according to the experimental database of Dzombak and Morel (1990), and the affinity constants of arsenic for the weak and strong sites. These parameters were held constant for the following experiments in which sorption of arsenic(III) and arsenic(V) was investigated in the presence of OM. During the simulation of these competitive sorption experiments the parameters fitted were the affinity constants of the different OM fractions for the sorption sites. A summary of the fitted parameters during the batch experiments is reported in Table S7.

Table S7. Fitted Sorption Parameters – Batch Experiments.

Experiment	Parameter			
	Maximum sorption capacity [mol/kg FH sand]		Affinity Constants [mol/L]	
	weak sites[a]	strong sites[a]	weak sites	strong sites
As(III)	1.81×10^{-2}	4.82×10^{-4}	$K_{As(III)w}=6.2\times10^{-4}$[b]	$K_{As(III)s}=1.2\times10^{-6}$[b]
As(III) & 50 mg C/L HA	1.81×10^{-2}	4.82×10^{-4}	$K_{HAw}=2.5\times10^{-3}$	$K_{HAs}=1.8\times10^{-3}$
As(III) & 50 mg C/L GFA	1.81×10^{-2}	4.82×10^{-4}	$K_{GFAw}=4.0\times10^{-4}$	$K_{GFAs}=7.2\times10^{-4}$
As(III) & 11.5 mg C/L SOM	1.81×10^{-2}	4.82×10^{-4}	$K_{SOMw}=1.7\times10^{-4}$	$K_{SOMs}=1.5\times10^{-4}$
As(V)	1.32×10^{-2}	3.29×10^{-4}	$K_{As(V)w}=8.52\times10^{-4}$[c]	$K_{As(V)s}=6\times10^{-7}$[c]
As(V) & 50 mg C/L HA	1.32×10^{-2}	3.29×10^{-4}	$K_{HAw}=3.8\times10^{-3}$	$K_{HAs}=3.5\times10^{-3}$
As(V) & 50 mg C/L GFA	1.32×10^{-2}	3.29×10^{-4}	$K_{GFAw}=1.1\times10^{-3}$	$K_{GFAs}=9.9\times10^{-4}$
As(V) & 11.5 mg C/L SOM	1.32×10^{-2}	3.29×10^{-4}	$K_{SOMw}=2.5\times10^{-4}$	$K_{SOMs}=2.2\times10^{-4}$

[a] parameter fitted for the experiments with As alone

[b] value used in the competitive sorption experiments with As(III) and different OM fractions

[c] value used in the competitive sorption experiments with As(V) and different OM fractions

Supporting Information S4.3. Column Experiments. A similar approach was applied to simulate the arsenic breakthrough curves during the flow-through experiments. The governing transport equations (Eq. 3 and Eq. 4) were solved in Matlab using an operator split approach. The experimentally determined conservative transport parameters (i.e., seepage velocity, $v=5.14\times10^{-6}$ m/s, porosity, n=0.44, dispersion coefficient, $D_L=1.73\times10^{-9}$ m^2/s) were not included in the fitting procedure. Also the maximum sorption capacity for the weak and strong sites was assumed to be the same as determined in the batch experiments. Therefore, the fitting parameters were the affinity constants of the different solute species for the weak and strong sorption sites and the mass-transfer coefficients, expressing the kinetic limitation of arsenic partitioning between the aqueous and solid phases. These parameters were determined by trial and error calibration. As for the batch experiments, the affinity constants of arsenic to the weak and strong ferrihydrite sites were obtained for the experiments where only As(III) and As(V) were transported in the ferrihydrite-coated sand columns. For the subsequent runs with transport and competitive sorption between arsenic and different fractions of organic matter, these values were kept constant and the affinity constants of the humic acids, fulvic acids and soil organic matter were used to fit the observed profiles of arsenic concentrations. Table S8 reports the fitted parameters for the breakthrough experiments. To quantify the agreement between the observed and simulated concentrations, the root mean square error was selected as measure of the goodness of fit which is :

$$RMSE = \sqrt{\frac{1}{n}\sum_{i=1}^{n}(obs_i - sim_i)^2} \qquad (5)$$

where n is the number of observations (i.e., measured samples), obs_i are the observed concentrations (i.e., average between duplicate flow-through experiments) and sim_i are the simulated values.

Table S8. Fitted Sorption Parameters – Column Experiments.

Experiment	Parameter			Goodness of Fit
	Affinity Constants [mol/L]		Mass Transfer	RMSE
	weak sites	strong sites	Coeff., $\lambda[s^{-1}]$	[mol/L]
As(III)	$K_{As(III)w}=1.2\times10^{-3}$[a]	$K_{As(III)s}=4.2\times10^{-6}$[a]	3×10^{-5}	5.26×10^{-7}
As(III) & 5 mg C/L HA	$K_{HAw}=1.62\times10^{-3}$	$K_{HAs}=6.1\times10^{-4}$	1×10^{-5}	2.92×10^{-7}
As(III) & 50 mg C/L HA	$K_{HAw}=5.6\times10^{-3}$	$K_{HAs}=2.1\times10^{-3}$	3×10^{-5}	1.02×10^{-6}
As(III) & 5 mg C/L GFA	$K_{GFAw}=9\times10^{-4}$	$K_{GFAs}=2.1\times10^{-4}$	3×10^{-5}	1.08×10^{-6}
As(III) & 50 mg C/L GFA	$K_{GFAw}=8.2\times10^{-3}$	$K_{GFAs}=1.9\times10^{-3}$	1×10^{-5}	5.21×10^{-7}
As(III) & 11.5 mg C/L SOM	$K_{SOMw}=9.1\times10^{-4}$	$K_{SOMs}=3.2\times10^{-4}$	3×10^{-5}	3.91×10^{-7}
As(V)	$K_{As(V)w}=5.15\times10^{-4}$[b]	$K_{As(V)s}=9\times10^{-7}$[b]	3×10^{-5}	3.97×10^{-7}
As(V) & 5 mg C/L HA	$K_{HAw}=6.7\times10^{-4}$	$K_{HAs}=6.3\times10^{-4}$	1×10^{-5}	3.02×10^{-7}
As(V) & 50 mg C/L HA	$K_{HAw}=4.8\times10^{-3}$	$K_{HAs}=4.5\times10^{-3}$	3×10^{-5}	5.46×10^{-7}
As(V) & 5 mg C/L GFA	$K_{GFAw}=6.3\times10^{-4}$	$K_{GFAs}=9\times10^{-5}$	3×10^{-5}	6.55×10^{-7}
As(V) & 50 mg C/L GFA	$K_{GFAw}=4.2\times10^{-3}$	$K_{GFAs}=6\times10^{-4}$	3×10^{-5}	7.98×10^{-7}
As(V) & 11.5 mg C/L SOM	$K_{SOMw}=9.5\times10^{-4}$	$K_{SOMs}=3\times10^{-4}$	3×10^{-5}	5.16×10^{-7}

[a] value used in the transport and competitive sorption experiments with As(III) and different OM fractions
[b] value used in the transport and competitive sorption experiments with As(V) and different OM fractions

References

1 Kaiser, K.; Mikutta, R.; Guggenberger, G. Increased stability of organic matter sorbed to ferrihydrite and goethite on aging. *Soil Sci. Soc. Am. J.* **2005,** *71*, 711-719.

2 Sharma, P.; Ofner, J.; Kappler, A.; Formation of binary and ternary colloids and dissolved complexes of organic matter, Fe and As. *Environ. Sci. and Technol.* **2010**, *44*, 4479-4485.

3 Bauer, M.; Blodau, C. Arsenic distribution in the dissolved, colloidal and particulate size fraction of experimental solutions rich in dissolved organic matter and ferric iron. *Geochim. Cosmochim. Acta.* **2009**, 73, 529-542

4 Radu, T.; Kumar, A.; Clement, T. P.; Jeppu, G.; Barnett, M. O. Development of a scalable model for predicting arsenic transport coupled with oxidation and adsorption reactions. *J. Contam. Hydrol.* **2008**, *95*, 30–41.

5 Mikutta, C.; Wiederhold, J.G.; Cirpka, O.A.; Hofstetter, T.B.; Bourdon, B.; Von Gunten, U. Iron isotope fractionation and atom exchange during sorption of ferrous iron to mineral surfaces. *Geochim. Cosmochim. Acta* **2009**, *73*, 1795–1812.

6 Dzombak, D. A.; Morel, F.M.M. Surface Complexation Modeling; Wiley and Sons: New York, 1990.

4

The effect of humic acids on desorption of As(V) from ferrihydrite-coated sand at different ionic strength

Prasesh Sharma[1] and Andreas Kappler[1]

[1]Center for Applied Geosciences, University of Tübingen, Germany

Abstract

Natural organic matter (NOM) is liable to changes in its structure upon variations/fluctuations in geochemical conditions such as ionic strength. NOM can affect the mobility of contaminants such as arsenic in the environment, e.g. via competitive sorption processes at mineral surfaces. Since the interactions of NOM with mineral surfaces also depends on its structural properties (size, composition etc), it is expected that changing ionic strength will also influence the effect of NOM on arsenic sorption to minerals. Therefore, column experiments with As(V) presorbed ferrihydrite-coated sand were carried out to determine the desorption of As(V) in presence (5 and 50 mg C/L) and absence of humic acid (HA-free) at different ionic strength (5 and 100 mM NaCl). The total amount of As(V) desorbed from As-preloaded, ferrihydrite-coated sand systems that contained 50 mg C/L humic acid (HA) decreased slightly with increasing ionic strength (5 to

100 mM NaCl) from 12.9 to 12.2%. This decrease can be possibly explained by the decreased negative charge of humic molecule at higher ionic strength. In presence of 5 mg C/L HA, the amount of As(V) desorbed decreased from 11.1 to 10.6% with increasing ionic strength. In contrast, in systems that contained NaCl only (HA-free), 10.2 and 9.9% As(V) desorbed in 5 and 100 mM NaCl containing systems, respectively. Results from these experiments showed that increasing concentrations of HA increases total amount of As(V) mobilized at environmentally relevant ionic concentrations. However, fluctuations in ionic strength (within environmentally relevant concentration limits), affect arsenic (im)mobilization only to a minor extent.

Keywords: arsenic, organic matter, humics, columns,(im)mobilization

Introduction

Arsenic is a toxic element that poses a worldwide environmental threat due to its contamination of drinking, surface and ground waters worldwide (Smedley and Kinniburgh, 2002). In many areas of the world, concentrations of As are higher than the WHO drinking water limit of 10 µg/L, which is considered harmful for human health (Smedley and Kinniburgh, 2002).

Arsenic is present in the environment mainly as inorganic As(III) and As(V) and to a lower extent also in organic forms. At neutral pH, As(III) exists as H_3AsO_3 with pK_a values of 9.2, 12.7 and 13.4, whereas As(V) is present as $H_2AsO_4^-$ and $HAsO_4^{2-}$ with pK_a values of 2.2, 6.9 and 11.5 (Warwick, 2005). Both oxidation states of As can co-exist in solution with As(III) considered to be more mobile than As(V) at neutral pH (Smedley and Kinniburgh, 2002). However, the mobility of both species of As is controlled by sorption onto and redox reactions

with metal oxides and clay minerals, as well as by competitive sorption of anions such as phosphate (Amstaetter et al., 2010; Violante et al., 2002; Goldberg and Johnston, 2002; Dixit and Hering 2003), and by redox and complexation reactions with natural organic matter (NOM) (Redman et al., 2002; Wang et al., 2006; Jiang et al., 2009; Sharma et al. 2010).

Natural organic matter is ubiquitous in both aquatic and terrestrial environments. The concentration of NOM in groundwater (aquifers) and surface water (rivers and lakes) ranges from 0.1 mg C/l to several hundred mg C/l (Stevenson, 1994). Humic acid (HA) is the fraction of NOM which is soluble at high pH and precipitates at lower pH. HA binds strongly to metal oxides and clay minerals (Stevenson, 1994; Gu et al., 1994) and its structure can undergo modifications upon changes in ionic strength (Myneni et al., 1999; Ceccanti et al., 1989; Bauer et al., 2009 (submitted)). The changes in humic acid structure can also enhance reactivity of the humic acid molecules, which can consequently affect transport of contaminants like As (Myneni et al., 1999).

The influence of changes in ionic strength on As sorption have been studied by various researchers. In sorption and desorption experiments carried out in batch systems, changes in ionic strength did not significantly change the amount of As sorbed onto natural soils and minerals surfaces such as in alfisol (Smith and Naidu, 2009), TiO_2 (Liu et al., 2008), Al_2O_3 (Arai et al., 2001), Goethite (Antelo et al., 2001) and Al/Fe-oxides (Goldberg and Johnston, 2001). However, in flow-through systems, a significant effect of ionic strength on As(III) and As(V) transport was demonstrated. As(III) (Zhang and Selim, 2007) and As(V) (Puls and Powell, 1992) transport was studied in soil columns where it was found that replacing background solutions

with deionised water enhanced As transport. With respect to humic acid, interaction of As with metal oxides and minerals in presence of humic acid at constant ionic strength has been widely studied in batch and column systems (Grafe et al., 2001, 2002; Redman et al., 2002; Simeoni et al., 2003; Ko et al., 2004, 2006; Gustaffson et al., 2006; Weng et al., 2009; Sharma et al., 2010 (submitted)). However, the effect of HA on As transport/desorption at different ionic strengths has not yet been quantified.

Therefore, the objective of this study was to quantify desorption of As(V) from ferrihydrite-coated sand in presence and absence of HA at different ionic strengths. This study presents follow-up experiments to Sharma et al., 2010 (submitted).

Material and methods

Reagents: Stock solutions of 1 mM As(V) ($Na_2HAsO_4 \cdot 7H_2O$) and 1 M NaCl were prepared (both purchased from Fluka, Germany). Pahokee peat humic acid (HA) was purchased from the International Humic Substances Society (IHSS) (Minnesota, USA). Stock solutions of As(V) used for pre-sorption to the ferrihydrite-coated sand (FH-sand) were prepared in 1 mM PIPES. Stock solutions of HA used for desorption were prepared in either 5 mM NaCl and 1 mM PIPES, or 100 mM NaCl and 1 mM PIPES solution. HA solutions were readjusted to a pH of ~7.0 using 1 M NaOH and filtered with a 0.45 µm mixed cellulose ester (MCE) filter to remove any larger colloidal particles. HA-free solutions with 5 mM NaCl and 1 mM PIPES, and 100 mM NaCl and 1 mM PIPES was also prepared.

Synthesis of ferrihydrite-coated sand. Ferrihydrite-coated sand (FH-sand) was prepared as described in Sharma et al., 2010 (submitted).

Column (desorption) experiments: Desorption of As(V) from FH-sand in the presence (5 and 50 mg C/L HA) and absence of OM (HA-free) solutions was studied under flow through conditions (flow rate of 24 µl/min following Tufano et al. (2006) using columns (Kontes Flex-column economy columns, 1.3 cm diameter, 10 cm length) containing ~15 g FH-sand (sand porosity: 0.44). All desorption experiments were carried out in duplicates. The pH of the effluent remained circumneutral throughout the experiments in all setups (Table 1).

To study desorption of As from FH-sand, As(V) was presorbed to FH-sand, targeting a sorption coverage of 60-65% which amounted to ~7.6 mmol/kg FH-sand (based on sorption isotherms from Sharma et al., 2010(submitted). Columns were filled with 15 g of the FH-sand that was presorbed with As(V) and then desorbed by 5 and 50 mg C/L HA and HA-free solutions prepared in both 5 mM and 100 mM NaCl concentrations separately (Table 1). HA concentrations of 5 mg and 50 mg C/L and were chosen for desorbing As(V) from columns as they represent the average and higher end of environmentally relevant concentrations of dissolved OM in aquifer systems (Mladenov et al., 2010; Stevenson, 1994). The lower and higher ionic strength solutions of 5 mM and 100 mM NaCl were chosen on a similar environmental relevance basis (Anwar et al., 2003). Desorption was considered to be complete once the concentration of As in the eluate did not decrease further. A cumulative plot was obtained for each setup by adding the total moles of As desorbed from the collected samples.

Analytical methods. Samples from the desorption experiments were filtered with a 0.45 µm filter (MCE, Millipore), acidified with 0.25 M HNO_3 and analyzed for total As by ICP-OES. Samples from ultrafiltration were acidified without filtering. DOC was quantified using a TOC analyser (highTOC II, Elementar Analysensysteme, Hanau, Germany). To quantify total Fe, Fe was extracted by adding 1 M HCl at 90ºC at 150 RPM in a thermomixer. After 30 min the suspension was centrifuged at 14,000 g for 5 minutes and the supernatant was analyzed for total Fe (and/or Fe(II)) by the spectrophotometric ferrozine assay (Stookey, 1970).

Results and Discussion

Effect of ionic strength on desorption of As in presence and absence of HA. Ionic strength is an important geochemical parameter which is known to affect the molecular structure of humic substances (Myneni et al., 1999, Ceccanti et al., 1989), as well as the sorption and transport of contaminants like As (Puls and Powell, 1992; Zhang and Selim, 2001, Smith and Naidu, 2009). To study the effect of ionic strength on As mobilization by humic substances, desorption of As(V) from FH-sand was quantified in presence and absence of 5 and 50 mg C/L HA at two different ionic strengths, 5 and 100 mM NaCl. We found that desorption of As(V) in 100 mM NaCl solutions were consistent with what we observed in previous experiments carried out with 5 mM NaCl in presence or absence of HA (Fig. 1A, Table 2 and Sharma et al., 2010 (submitted)). At 5 mM NaCl, As(V) desorbed by 10.2, 11.1 and 12.9% and at 100 mM NaCl by 9.9, 10.6 and 12.2% in HA-free, 5 and 50 mg C/L systems respectively. The slight but significant decrease (0.8%) in the amount of As(V) desorbed was observed in 100 mM NaCl containing systems compared to 5 mM NaCl systems in presence of 50 mg C/L HA (Fig 1B). This can be

explained by the decreased negative charge of humic molecule at higher ionic strength. Zeta potential measurements of non-reduced HA (from peat soil) by (Bauer et al., 2009 (submitted) prepared in 0-60 mM NaCl solutions showed slight decrease in zeta potential values with increasing ionic strength. It is possible that in our system with 100 mM NaCl concentrations, due to decreased negative charge of the HA molecules, HA did not interact with the positively-charged FH-sand containing As as strongly as in case of 5 mM NaCl concentrations thereby desorbing less As. In presence of 5 mg C/L, the decrease of 0.5% in As(V) desorbed from 5 mM to 100 mM NaCl systems was questionable as the results were not significantly different (Fig. 1 – note that error bars were not shown as the desorption values were very close and the standard deviations overlapped). The amount of As(V) desorbed in all experiments, regardless of ionic strength, is between 9.9 to 12.7%. Similar results for As(V) desorption from As-presorbed FH-sand have been reported previously for abiotic systems with FH-sand (Sharma et al., 2010(submitted); Herbel and Fendorf, 2006).

Although the results show a slight decrease in As desorption in presence of HA, changes in ionic strength did not show any distinct decrease in the amount of As(V) desorbed upon increase of ionic strength from 5 to 100 mM in absence of HA (Fig. 1A). This was expected since the effect of ionic strength seen in our systems is probably due to structural changes of the HA and without HA, there was no significant difference between 5 mM and 100 mM NaCl HA-free systems. This is concurrent with what has been reported previously with regards to adsorption and desorption of As in batch studies with natural soils with slightly higher Fe-content (~0.2% compared to ~0.1% in our study) (Smith and Naidu, (2009)). Smith and Naidu, (2009) showed

that increasing the background salt concentration from 30 mM to 300 mM $NaNO_3$ had negligible effects in adsorption or desorption of As in absence of humics.

Effect of ionic strength on HA structure. The particle size and charge of organic molecules which ultimately affects its aggregation behavior can also change upon changing ionic strength concentrations. The particle size measurements carried out by Bauer et al., 2009 (submitted) showed that at similar HA concentrations for non-reduced HA, varying ionic strength solutions from 0-60 mM NaCl did not change the average particle size significantly. However, at very low ionic strengths, a small fraction of particles in the size range of 1-2 nm were observed. These fractions disappeared at higher ionic strength. These small fractions, because of their size, could be effective in desorbing As in our systems and the reason why there is a small but significant increase in total amount of As desorbed in 5 mM NaCl containing compared to 100 mM NaCl containing systems.

Effect of ionic strength on colloidal mobilization. Changes in ionic strength can also affect colloid facilitated transport of contaminants in the environment, i.e. lower ionic strength increases repulsive electrostatic force between the colloidal particles, increases dispersion and ultimately mobilization of colloids (Sposito, 1989). This was experimentally demonstrated in several studies where upon changing ionic strength enhanced contaminant transport (e.g. Pb^{2+}, Ni^{2+}, As(V)) (Grolimund et al., 1992; Puls and Powell, 1992; Roy and Dzombak, 1997). In our systems, Fe-colloids were mobilized in all cases as seen in the differences in Fe(total) values of FH-sand before and after desorption was complete. The amount of Fe(total) in the FH-sand decreased in 5 mM NaCl systems from 1070 µg/g to 721, 698 and 643 µg/g and in 100 mM

NaCl systems from 1070 µg/g to 756, 682 and 656 µg/g in HA-free, 5 and 50 mg C/L HA containing systems respectively (Table 3). The effect of increased HA concentrations on amount of Fe leached from FH-coated is evident in our systems (Table 3). The differences between HA-free, 5 and 50 mg C/L in 5 mM and 100 mM ionic strength concentrations is <5% suggesting that any effect of colloidal mobilization due to changes in ionic strength is not significant in our systems.

Environmental relevance of ionic strength on As transport in presence of NOM. In this study we demonstrated that humic acids affect the amount of As mobilized only slightly but significantly upon changes in ionic strength within environmentally relevant concentrations. In deltaic areas like that of Bangladesh and Vietnam which are also i) monsoon affected and ii) heavily irrigated; infiltration of rainwater or freshwater into the subsurface could cause fluctuations in ionic strength due to mixing with the saline (or brackish) water from aquifers (Burgess et al., 2010). These fluctuations could affect sorption/desorption processes of As. In addition, the infiltrating waters might contain NOM which could further enhance mobilization of As depending upon the concentration of OM. Our data, suggests that changes in OM concentrations is more important than changes in ionic strength in desorption of As. However, the results from this study are inadequate to make a general conclusion on impact of changes in ionic strength on As geochemistry in flow through systems. To fully understand the effect of ionic strength changes on mobilization of As in the environment more experiments are necessary. Sorption and column (desorption and breakthrough) studies carried out with different NOM, cations, minerals and As loadings will give a comprehensive overview of impacts of ionic strength on As(V) (im)mobilization in the environment. In addition to the experiments

mentioned, further structural analyses of HA via techniques used in this study (combination of IR, particle size and zeta potential measurements) plus will give a better understanding of varying ionic strength on As sorption and transport.

Acknowledgements

This work was supported by an IPSWaT fellowship from the German Federal Ministry for Science and Education (BMBF) to PS and by German Research Foundation (DFG) and BMBF to AK. We would like to thank J. Breuer (University of Hohenheim), P. Kühn and F. Baumann (University of Tuebingen), for their help with ICP-MS and ICP-OES.

References

1 Amstaetter, K.; Borch, T.; Larese-Casanova, P.; Kappler, A. Transformation of arsenic by Fe(II)-activated goethite (α-FeOOH). *Environ. Sci. Technol.* **2010**, *44*, 102–108.

2 Antelo, J.; Ayena, M.; Fiol, S.; L'opez, R.; Arce, F. Effect of pH and ionic strength on the adsorption of phosphate and arsenate at the goethite-water interface. *J. Coll. Interf. Sci.* **2005**,*285***,** 476-486**.**

3 Anwar, Z.; Hassan, M.Q.; Balke, K.-D.; Flegr, M.; Clark, D.W. Groundwater chemistry and occurrence of arsenic in the Meghna floodplain aquifer, southeastern Bangladesh. *Environ. Geol.*, **2007**, *54*, 1247-1260.

4 Arai, Y.; Elzinga, E.J.; Sparks, D. L. X-ray absorption spectroscopic investigation of arsenite and arsenate at the aluminum oxide-water interface. *J. Coll. Interf. Sci.* **2001**, *235*, 80-88.

5 Bauer, I.; Amstaetter, K.; Haderlein, S.; Kappler, A. Influence of ionic strength on structure and redox activity of humic substances. **Submitted to** *Geochim. Cosmochim. Acta* **2009**.

6 Burgess, W.G., Hoque, M.A., Michael, H.A., Voss, C.J., Breit, G.N., Ahmed, K.M, 2010. Vulnerability of deep groundwater in the Bengal aquifer system to contamination by arsenic. *Nature Geosci.* **2010**, *3*, 83-87.

7 Ceccanti, B.; Calcinai, M.; Bonmati-Pont, M.; Ciardi, C.; Tarsitano, R. Molecular size distributions of soil humic substances with ionic strength. *Sci.Total Environ.* **1989**, *81/82*, 471-479.

8 Dixit, S.; Hering, J. G. Comparison of arsenic(V) and arsenic(III) sorption onto iron oxide minerals: implications for arsenic mobility. *Environ. Sci. & Technol.* **2003**, *37*, 4182-4189.

9 Dixit, S.; Hering, J. G. Comparison of arsenic(V) and arsenic(III) sorption onto iron oxide minerals: implications for arsenic mobility. *Environ. Sci. & Technol.* **2003**, *37*, 4182-4189.

10 Goldberg, S.; Johnston, C. T. Mechanisms of arsenic adsorption on amorphous oxides evaluated using macroscopic measurements, vibrational spectroscopy and surface complexation modeling. *J. Coll. Interf. Sci.* **2001**, *234*, 204–216.

11 Goldberg, S. Competitive adsorption of arsenate and arsenite on oxides and clay minerals. *Soil Sci. Soc. of Am. J.* **2002**, *66*, 413-421.

12 Grafe, M.; Eick, M.J.; Grossl, P.R. Adsorption of Arsenate (V) and Arsenite (III) on goethite in the presence and absence of dissolved organic carbon. *Soil Sci. Soc. Am. J.* **2001**, *65*, 1680–1687.

13 Grafe, M.; Eick, M.; Gross, P.R.; Saunders, A.M. Adsorption of arsenate and arsenite of ferrihydrite in the presence and absence of dissolved organic carbon. *J. Environ. Qual.* **2002**, *31*, 1115–1123.

14 Grolimund, D.; Borkovec, M.; Barmettler, K.; Sticher, H. Colloid-facilitated transport of strongly sorbing contaminants in natural porous media: A laboratory column study. *Environ. Sci. and Technol.* **1996**, *30*, 3118-3123.

15 Gu, B.; Schmitt, J.; Chen, Z.; Liang, L., McCarthy, J. Adsorption and desorption of different organic matter fractions on iron oxide. *Geochim. Cosmochim. Acta* **1994**, *59*, 219-229.

16 Gustafsson, J. P. Arsenate adsorption to soils: Modelling the competition from humic substances. *Geoderma* **2006**, *136*, 320–330.

17 Herbel, M.; Fendorf, S. Biogeochemical processes controlling the speciation and transport of arsenic within iron coated sands. *Chem. Geol.* **2006**, *228*, 16–32.

18 Ilwon, K.; Ju-Yong, K.; Kyoung-Woong, K. Arsenic speciation and sorption kinetics in the As–hematite–humic acid system. *Colloids Surf. A* **2004,** *234*, 43-50.

19 Ilwon, K.; Davis , A. P.; Ju-Yong, K.; Kyoung-Woong, K. Effect of contact order on the adsorption of inorganic arsenic species onto hematite in the presence of humic acid. *J. Hazard. Mater.* **2006**, *141*, 53-60.

20 Jiang, J., Bauer, I., Paul, A., Kappler, A. Arsenic redox changes by microbially and chemically formed semiquinone radicals and hydroquinones in a humic substance model quinone. *Environ. Sci. & Technol.* **2009**, *43*, 3639-3645.

21 Liang, L.; McCarthy, J. F., Jolley, L. W.; McNabb, J. A.; Mehlhorn, T. L. Iron dynamics: transformation of Fe(II)/Fe(III) during injection of natural organic matter in a sandy aquifer. *Geochim. Cosmochim. Acta* **1992**, *57*, 1987-1999.

22 Liu, G.J.; Zhang, X.R.; Mcwilliams, L.; Talley, J.W.; Neal, C.R. Influence of ionic strength, electrolyte type, and NOM on As(V) adsorption onto TiO_2. *J. Environ. Sci. Health, Part A: Environ. Sci. Eng.* **2008**, *43*, 430-436.

23 Mladenov, N.; Zheng, Y.; Miller, M.P.; Nemergut, D.R.; Simone, B.; Hageman, C.; Rahman, M.M.; Ahmed, K.M.; Mcknight, D.M. Dissolved organic matter sources and consequences for iron and arsenic mobilization in Bangladesh aquifers. *Environ. Sci. Technol.* **2010**, *44*, 123-128.

24 Myneni, S. C. B.; Brown, J. T.; Martinez, G. A.; Meyer-Ilse, W. Imaging of humic substance macromolecular structures in water and soils. *Science* **1999**, *286*, 1335-1337.

25 Puls, R.W.; Powell, R.M. Transport of inorganic colloids through natural aquifer material: Implication for contaminant transport. *Environ. Sci. Technol.* **1992**, *26*, 614-621**.**

26 Redman, A. D.; Macalady, D. L.; Ahmann, D. Natural organic matter affects arsenic speciation and sorption onto hematite. *Environ. Sci. & Technol.* **2002**, *36*, 2889-2896.

27 Roy, S.B.; Dzombak, D.A. Chemical factors influencing colloid-facilitated transport of contaminants in porous media. *Environ. Sci. and Technol.* **1997**, *31*, 656-664.

28 Schwertmann, U. C.; Cornell, R. M. The Iron oxides; Wiley-VCH: New York, 2003.

29 Sharma, P.; Rolle, M.; Kocar, B.; Fendorf, S.; Kappler, A. Influence of organic matter on As transport and retention. **Submitted to** *Environ. Sci. Technol.* **2010.**

30 Sharma, P.; Ofner, J.; Kappler, A.; Formation of binary and ternary colloids and dissolved complexes of organic matter, Fe and As. *Environ. Sci. and Technol.* **2010**, *44*, 4479-4485.

31 Simeoni, M. A.; Batts, B. D.; McRae, C. Effect of groundwater fulvic acid on the adsorption of arsenate by ferrihydrite and gibbsite. *Appl. Geochem.* **2003**, *18*, 1507–1515.

32 Smedley, P. L.; Kinniburgh, D. G. A review of the source, behaviour and distribution of arsenic in natural waters. *App. Geochem.* **2002**, *17*, 517-568.

33 Smith, E.; Naidu, R. Chemistry of inorganic arsenic in soils: kinetics of arsenic adsorption-desorption. *Environ. Geochem. Health* **2009**, *31*, 49-59.

34 Sposito, G. The chemistry of soils. Oxford Univ. Press, New York, 1994.

35 Stevenson, F.J. *Humus Chemistry: Genesis, Composition, Reactions*. Wiley: New York, 1994.

36 Stookey, L. L. Ferozine - A new spectorophotometric reagent for iron. *Anal. Chem.* **1970,** *42*, 779-781.

37 Tufano, K.J.; Reyes, C.; Saltikov, C.W.; Fendorf, S. Reductive processes controlling arsenic retention: revealing the relative importance of iron and arsenic reduction. *Environ. Sci. Technol.* **2008**, *42*, 8283-8289.

38 Violante, P.; Pigna, M. Competitive sorption of arsenate and phosphate on different clay minerals and soils. *Soil Sci. Soc. Am. J.* **2002**, *66*, 1788–1796.

39 Wang, S.; Mulligan, C. N. Effect of natural organic matter on arsenic release from soils and sediments into groundwater. *Environ. Geochem. and Health* **2006**, *28*, 197-214.

40 Warwick, P.; Inam, E.; Evans, N. Arsenic's interaction with humic acid. *Environ. Chem.* **2005**, *2*, 119-124.

41 Weng, L.; Riemsdijk, W.H.V.; Hiemstra, T. Effects of fulvic and humic acids on arsenate adsorption to goethite: experiments and modeling. *Environ. Sci. Technol.* **2009**, 43, 7198–7204.

42 Zhang, H.; Selim, H.M. Colloid mobilization and arsenite transport in soil columns: effect of ionic strength. *J. of Environ. Qual.* **2007**, *36*, 1273-1280.

Figures and tables

Figure 1 (A) Desorption curves of As(V) from FH-sand filled columns in presence and absence of Pahokee Peat Humic Acid (HA) prepared in 5 mM and 100 mM NaCl concentrations; (B) Desorption curves from 1A plotted from time point 50-250 h to show the statistical differences between '5mM NaCl + 50 mg C/L HA' and '100 mM NaCl + 50 mgC/L' systems with 50 mgC/L HA. Other plots are not shown as the standard deviations overlapped and therefore were not statistically significant.

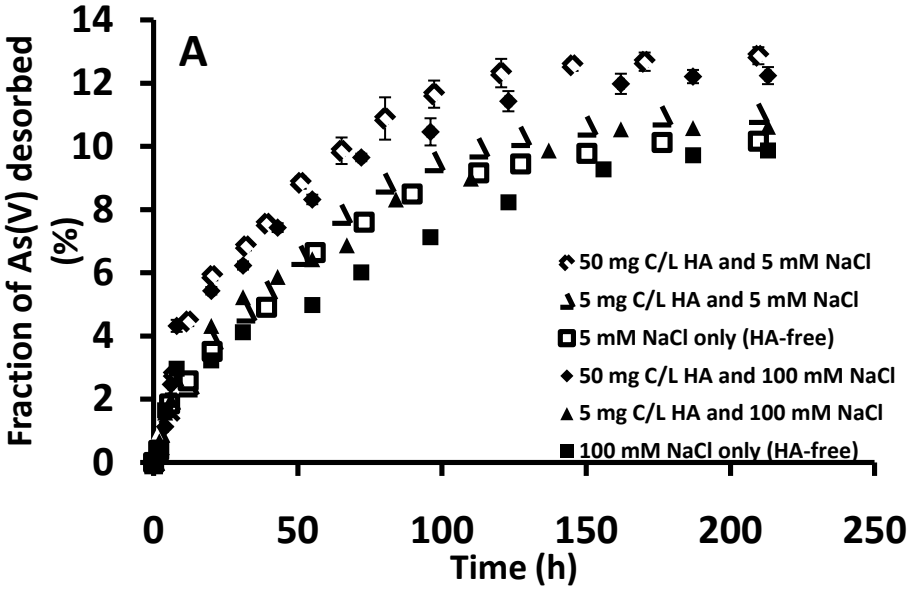

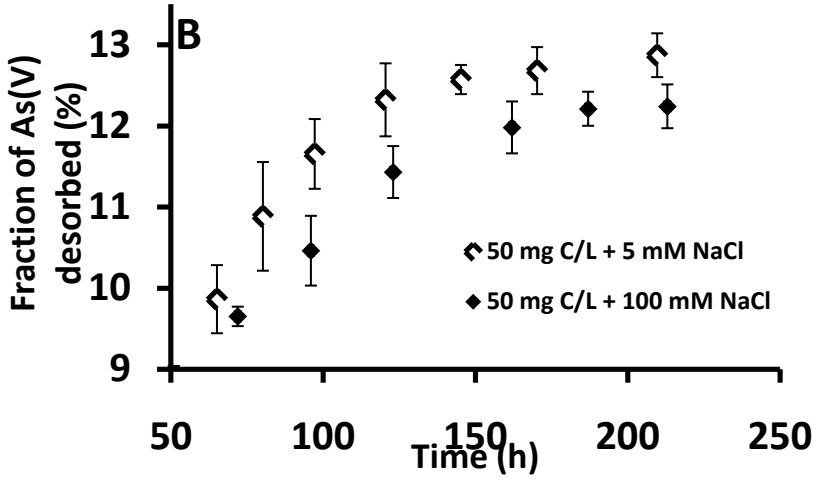

Table 1. Setups and experimental conditions for desorption experiments.

Desorption by
5 mM NaCl (HA-free)
5 mg C/L HA + 5 mM NaCl
50 mg C/L HA + 5 mM NaCl
100 mM NaCl (HA-free)
5 mg C/L HA + 100 mM NaCl

For desorption experiments, the FH-sand was presorbed with As(V) before desorbing by the solutions mentioned above. Solutions for all setups were prepared in a background of 1 mM PIPES. All experiments were carried out in duplicates.

Table 2. Total amount of As(V) desorbed (in %) from FH-sand at the end of desorption experiments in presence of HA (5 and 50 mg C/L), and absence of HA (HA-free) in 5 mM and 100 mM NaCl solutions .

setups	As(V) desorbed [%]
5 mM NaCl only (HA-free)	10.2
5 mg C/L HA + 5 mM NaCl	11.1
50 mg C/L HA + 5 mM NaCl	12.9
100 mM NaCl only (HA-free)	9.9
5 mg C/L HA + 100 mM NaCl	10.8
50 mg C/L HA + 100 mM NaCl	12.2

Table 3. Amount of Fe(total) leached from 5 mM and 100 mM NaCl containing setups in presence and absence of HA at the completion of desorption experiments.

	amount of Fe leached [µg/g]	
setup	**in 5 mM NaCl**	**in 100 mM NaCl**
NaCl (HA-free)	721(23)	756(24)
5 mg C/L HA	698(29)	682(17)
50 mg C/L HA	643(17)	656(12)

The amount of Fe(total) in FH-sand before desorption for all setups was 1030 µg/g. The numbers in parentheses show standard deviations from triplicate measurements.

5

Surface binding site analysis of Ca^{2+}-homoionized clay-humic acid complexes

*Raul E. Martinez, Prasesh Sharma, Andreas Kappler**

Published in *Journal of colloids and interface science*

10.1016/j.jcis.2010.08.082

Journal of Colloid and Interface Science xxx (2010) xxx–xxx

Contents lists available at ScienceDirect

Journal of Colloid and Interface Science

www.elsevier.com/locate/jcis

Surface binding site analysis of Ca^{2+}-homoionized clay–humic acid complexes

Raul E. Martinez, Prasesh Sharma, Andreas Kappler *

Geomicrobiology, Center for Applied Geosciences, University of Tuebingen, Germany

ARTICLE INFO

Article history:
Received 3 August 2010
Accepted 28 August 2010
Available online xxxx

Keywords:
Kaolinite
Illite
Humic acid–clay complexes
Surface complexation modeling
FTIR
Zeta potential

ABSTRACT

Clay–humic substance complexes play a major role in controlling the mobility of toxic metals in contaminated soils. However, our understanding of the underlying mechanisms is limited. Binding site analysis of clay and clay–mineral–humic composites, in this study, revealed an enhanced surface reactivity for the clay surface by the sorbed humic substances. Kaolinite and illite had three binding sites with pK_a values ranging from ~4.5 to 9.6 at Ca^{2+} concentrations of 0.01 and 0.1 M respectively. In the presence of peat humic acid (PHA), four or five binding sites were observed for humics sorbed kaolinite surface at Ca^{2+} concentrations of 0.01 and 0.1 M respectively. pK_a values ranged from ~4.4 to 9.6 for humic acid concentration of 0.01 and 0.1 mg/mL. For illite, four or five binding sites were found with pK_as ranging from ~4.1 to 9.4. From zeta potential measurements of PHA-kaolinite or PHA-illite suspensions, the already negative potential decreased by 30 mV from pH 4 to 7, and by 10 mV for pH values greater than 7. For illite the initial negative surface potential decreased by 15 mV up to a pH of 9. Above this pH, the potential decrease diminished to 2 or 5 mV. These changes in surface potential confirm the adsorption of PHA to the clay mineral surface. FTIR measurements of clay samples were able to identify the kaolinite and illite phases. In addition, FTIR absorption bands found in the range of 1950–1800 cm^{-1}, suggest the interaction of PHA with kaolinite and illite surfaces. The results of this study indicate that the sorption of humic substances increases the availability of clay surface functional groups for deprotonation and potential sorption of toxic metal cations.

1. Introduction

Kaolinite and illite are clay minerals that represent major constituents of soils and sediments [1–4]. These are examples of reactive geochemical solids whose interactions with soil organic matter play a key role in the transport of toxic substances [5–9]. Kaolinite has a 1:1 tetraoctahedral aluminosilicate structure with the general formula: $Al_2Si_2O_5(OH)_4$, with two different basal cleavage faces. One face consists of tetrahedral siloxane (—Si—O—Si—) species, while the other of an octahedral, alumina (Al_2O_3) sheet. At the edges of kaolinite particles, octahedral alumina and silica tetrahedral sheets expose reactive functional moieties including aluminol (Al—OH) and silanol (Si—OH) groups. The hydroxyl (—OH) groups can be deprotonated to generate a net negative charge. The edge faces are estimated to occupy approximately 10% of the whole kaolinite surface. The basal face of kaolinite, carries a net negative charge as a result of isomorphous substitution of Si^{4+} by Al^{3+} groups [10–15].

Illite is an aluminum–potassium mica-like, non-expanding, dioctahedral mineral, usually present in the clay fraction. Illite has been described as an interlayer deficient mica and it crystallizes in the monoclinic system, where two tetrahedral sheets sandwich an octahedral sheet. An approximate formula for illite is: $K_{0.88}Al_2(Si_{3.12}Al_{0.88})O_{10}(OH)_2$. In this 2:1 layered system, the illite surface has been proposed to be heterogeneous, with different binding affinities for protons or other ions. The morphology of the illite crystal and the complexity of its surface suggest a number of surface reactive sites, including weakly acidic basal planes and amphoteric silanol and aluminol sites on the edge surface [16–19]. For the most part, however, because of the clay structural complexity and the limited ability of current surface complexation models (SCMs), and optimization routines such those included, for example, in the FITEQL® code [20], to predict the number of reactive sites, two binding sites have been assumed on clay mineral surfaces [16,17,21,22]. In order to better understand the nature of metal and organic matter complexation to clays, not only the number of available sites, but their most accurate apparent pK_a values and concentrations must be first defined. The inclusion of electrostatic parameters enhances the flexibility of optimization routines. This, coupled to the need for a close initial input guess on the number and concentration of sites renders, both the SCM models (which in most cases assume only one or two binding sites)

* Corresponding author. Address: Geomicrobiology, Center for Applied Geosciences, University of Tübingen, Sigwartstrasse 10, D-72076 Tübingen, Germany. Fax: +49 7071 295059.
E-mail address: andreas.kappler@uni-tuebingen.de (A. Kappler).

0021-9797/$ - see front matter © 2010 Published by Elsevier Inc.
doi:10.1016/j.jcis.2010.08.082

and their respective optimization approaches (e.g. FITEQL® [20]), at the least, questionable. A mathematical fit of experimental data, based on a more flexible model, means that the resulting optimized parameters may not be representative of the system being studied.

Organic coating of the clay surface by sorbed humic substances plays a key role in partitioning and transport of toxic metals in soils. However, very few studies have quantified humic sorption onto the clay surface [4,5,13,23–27]. Humic substances are mixtures of polydisperse, heterogeneous polyelectrolytes [23,28–30]. They are negatively charged due to the presence of carboxylic acid and phenolic groups on aromatic residues and aliphatic chains. The solubility and conformation of humic substances in aqueous media are determined by pH, background electrolyte concentration, and the interaction of the deprotonated functional groups (carboxyl and hydroxyl) with metals and polyvalent cations [1,23,28–30]. For example, Ca^{2+} has been proposed to cause condensation of humic acid molecules. This may increase the amount of humics adsorbed to the clay surface and influence the conformation and orientation of sorbed organic molecules. This process would then dominate the ability of the organic coating and the clay surface to complex trace metal cations in the soil [5,23,26].

Major cations in soils including Ca^{2+}, Mg^{2+}, and Na^{+} are readily sorbed on clay surfaces by ion exchange mechanisms. Clay minerals have also shown a generally ineffective adsorbing of anions, including Cl^{-} and I^{-} [23,31–33]. As mentioned previously, polyvalent cation generated changes in molecular conformation play a key role in the quantity of humics that can adsorb to the mineral surface. In addition, recent studies have postulated that the organic coating of clays changes the nature of the mineral surface binding sites for metal contaminants, providing a mechanism for the removal of potentially toxic substances from the environment [32–35].

However, our understanding of the interaction between clays and humic substances, and the effect of humic binding on trace metal sorption by clay mineral surfaces is limited because of our incomplete knowledge of the formation and chemical behavior of humic–clay aggregates and their surfaces. Therefore, the goal of this study is to identify and quantify the reactive functional groups on the kaolinite and illite mineral surfaces responsible for humic acid and trace metal sorption. A discrete site surface complexation modeling approach aided by linear programming optimization (without the need of a pre-defined "initial input guess") was complemented by zeta potential determinations and Fourier transform infrared (FTIR) spectroscopy to account for surface functional groups on clay surfaces upon interaction with peat humic acid (PHA).

2. Materials and methods

2.1. Reagents

Peat humic acid (PHA) was purchased from the International Humics Substances Society (IHSS, USA). Clay minerals (kaolinite KGa-1b and illite Imt-1) were obtained from the Clay Mineral Society Source Clay Repository (University of Missouri, USA). The composition of the kaolinite (KGa-1b) consisted mainly of SiO_2 (44.2%), Al_2O_3 (39.7%) and TiO_2 (1.4%), and the major components of illite (Imt-1) were SiO_2 (49.3%), Al_2O_3 (24.3%) Fe_2O_3 (7.3%) and TiO_2 (0.6%) as described by the source clay physical/chemical data of the Mineral Society Source Clay Repository (University of Missouri, USA). The $CaCl_2$ used in these experiments was 99.99% trace metal basis (Sigma–Aldrich). The surface area of clay minerals was measured by BET, with corresponding values of 9.2 m^2/g and 24.2 m^2/g for kaolinite and illite respectively. The organic matter content in clay minerals was determined to be less than 0.05% using a TOC analyzer (highTOC II, Elementar Analysensysteme GmbH, Hanau, Germany).

2.2. Homoionization of clay minerals

The protocol from Saada et al. (2003) was followed for homoionization of the clay minerals [26]. 0.75 g of clay were shaken (at 150 rpm) with 7.5 mL of 1 M $CaCl_2$ (solid:liquid ratio 1:10) to obtain Ca^{2+}-homoionised kaolinite and illite. This process was repeated three times with 2 h of shaking in between. Excess chloride was removed after the last homoionization step by washing with deionized water until $AgNO_3$ addition to the washing water indicated absence of Cl^{-}.

2.3. Preparation of peat humic acid (PHA) stock solutions

PHA solutions of 0.01 mg/mL (5.5 mg C/L) and 0.1 mg/mL (57.9 mg C/L) were prepared by dissolving 10 and 100 mg of PHA in 1 L deionized water. The pH of the two stock solutions was adjusted to ~7 with 1 M NaOH.

2.4. Preparation of PHA-clay complexes

The Ca^{2+}-homoionized clay was added to the pH-neutral PHA solutions at a ratio of 1:40 (i.e. 0.75 g of dry clay with 30 mL of 0.01 or 0.1 mg/mL PHA). The PHA-clay suspensions were incubated for 48 h at 150 rpm in a horizontal shaker. The suspension was then centrifuged at 5000 rpm for 15 min. The supernatant was sampled for dissolved organic carbon (DOC) measurements to quantify the non-sorbed PHA. To remove loosely bound humics from the PHA-clay, the pellet containing the PHA-clay aggregates was resuspended and gently shaken with deionized water. The suspension was then centrifuged again for at 5000 rpm for 15 min and the supernatant was removed. The supernatant was again sampled for DOC measurements. DOC measurements were carried out by a TOC analyzer (highTOC II, Elementar Analysensysteme GmbH, Hanau, Germany).

2.5. Acid–base titration of clay mineral surfaces

Acid–base titration experiments were conducted at two different calcium chloride concentrations (0.01 and 0.1 M $CaCl_2$), with kaolinite or illite clay, with or without PHA. 0.75 g of clay mineral or PHA-clay aggregates were suspended in 100 mL of the corresponding $CaCl_2$ solution. Aliquots containing 40 mL of suspension were placed inside a Metrohm® glass titration vessel and covered with a Metrohm® lid through which a pH electrode, a custom designed N_2 gas line interface, and a stirrer were fitted. The solution was acidified with 0.01 M HCl to a pH of 4. The pH electrode was calibrated with fresh National Institute of Standards and Technology (NIST) buffer solutions of pH 4.01, 6.86, 9.18 at room temperature, before each experiment. Before the start of the acid–base titration, the system was allowed to reach equilibrium by maintaining a constant pH for a period of 1 h. The pH electrode drift criteria was that the 0.1 M NaOH titrant solution was added only if the change in potential was less than 0.1 mV/min. The titrations were conducted at $4 < pH < 10$ to avoid dissolution of clay minerals.

Previous studies analyzing clay surface acid–base titration data have, for the most part, coupled one or two site pK_a models along with adjustable electrostatic parameters and an *a priori* set of pK_a and site concentration values to provide more flexibility to the optimization of the experimental data fit. In recent works, for example, two site pK_a models have been implemented and com-

bined with electrostatic parameters to fit acid–base titration data arising from the illite surface, as follows:

$$\equiv SOH_2^+ \leftrightarrow \equiv SOH + H^+, Ka_1 \quad (1)$$

$$\equiv SOH \leftrightarrow \equiv SO^- + H^+, Ka_2 \quad (2)$$

where $\equiv SOH_2^+$ and $\equiv SOH$ are considered to be the amphoteric hydroxyl groups from ionized surface sites on the clay mineral surfaces, with their corresponding apparent acidity constants Ka_1 and Ka_2 for the deprotonation reactions at the solid/water interface [6,17,21,22,36–38]. These apparent proton equilibrium constants are usually corrected for electrostatic effects and translated into intrinsic acidity constants through the optimization of an approximate value of the mineral surface charge (Ψ) and the use of electrostatic models, such as the constant capacitance model (CCM) which has been one of the most used routines to describe acid base titration data in the presence of geochemically reactive solids, including mineral surfaces and bacterial cells [21,22,36–38]. This, however, has served to minimize the physico-chemical significance of resulting optimized parameters, as the increased mathematical flexibility of optimization routines, obtained due to the inclusion of electrostatic parameters, permits, almost in all cases, an acceptable fit of experimental data as shown previously [39–41].

In the present study, however, for $j = 1 \ldots m$ binding sites on the clay surface, the dissociation mechanism of protons from mineral surface sites is proposed to occur as a combination of j monoprotic reactions:

$$HS_j \overset{K_a}{\rightarrow} H^+ + S_j^- \quad (3)$$

where HS_j and S_j^- represent the protonated or deprotonated jth functional group as a function of increasing pH. $K_{a,j}$ is the apparent acidity constant as described below:

$$K_{a,j} = \frac{[S_j^-] \cdot [H^+]}{[HS_j]} \quad (4)$$

where $pK_a = -\log_{10} K_{a,j}$ is a measure of acid strength for each binding site, not yet properly determined for the clay mineral surface.

Therefore apparent pK_a values, embedding electrostatic parameters, and site concentrations on the Ca^{2+}-homoionized clay mineral surface were calculated from the surface charge excess obtained from the raw titration data using:

$$b_{meas,i} = Cb_i - Ca_i + [H^+]_{bulk,i} - [OH^-]_{bulk,i} \quad (5)$$

where $b_{meas,i}$ represents net hydroxide (OH^-) ions consumed by the clay mineral surfaces, Ca_i and Cb_i correspond to the acid and base concentrations respectively at the ith addition of titrant and $[H^+]_{bulk,i}$ and $[OH^-]_{bulk,i}$ denote the concentration of protons and hydroxide in solution calculated from the measured solution pH. Modeling of transformed acid–base titration data was performed using a multi-site Langmuir isotherm approach along with a linear programming optimization method, as described in detail in Kramer et al. [2], Martinez and Ferris [40], Martinez et al. [42], Cox et al. [43].

In order to model transformed acid–base titration data, the surface charge excess, $b_{meas,i}$ in Eq. (5) can be calculated as a function of speciation parameters:

$$b_{calc,i} = \sum_{j=1}^{m} \left(\frac{S_{Tj} K_{a,j}}{K_{a,j} + [H^+]_i} \right) + S_o \quad (6)$$

where S_{Tj} is the concentration of each binding site, and K_{aj} is the acidity constant of each site defined in Eq. (2) as the acid dissociation constant. The constant offset term, S_o, accounts for positive charges on the clay surface. For a true monoprotic system, S_o corresponds to the difference between the sites that are always protonated and those that are always deprotonated over the course of the titration. The model in Eq. (6) was fitted to the experimental data in Eq. (5) using a multi-site Langmuir isotherm and linear programming optimization. No assumptions were made *a priori* regarding the number, pK_a values or concentrations of the deprotonating sites on the clay mineral or on humic-coated clay surfaces [40,42–44].

2.6. Zeta potential measurements

Zeta potentials of Ca^{2+}-homoionized kaolinite and illite clays, in absence or presence of PHA, were measured using a CAD Instrumentation "Zetaphoremeter IV" Z 4000, microelectrophoremeter. Clay suspensions were prepared from previously freeze-dried samples. These solutions were comprised of kaolinite and illite and clay-PHA, with a concentration of 0.01 mg of clay/mL and a 0.01 M $CaCl_2$ concentration. The suspensions were acidified to a pH of 4 with 0.1 M HCl to determine the isoelectric point via interpolation or extrapolation of zeta–pH dependences. The electrophoretic measurements were performed in a quartz cell connecting two Pd electrode chambers. The clay particles were illuminated by a 2 mW He/Ne laser. During the measurements, an electric field of 80 V cm^{-1} was applied in each direction and the images of moving clay particles were transmitted to a computer via a CCD camera. The zeta potential of the clay suspensions was measured by timed image analysis of an average of 20 ± 5 particles for each pH value analyzed. Experiments were performed at pH ranging from 4 to 10.5 with a resolution of 0.3–0.4 pH units. The pH of these suspensions was increased manually by adding 2–10 μL aliquots of 0.1–1 M NaOH. Three replicates were carried out and each was performed with a renewed clay suspension. The uncertainty of zeta potential measurements ranged from 5% to 10%.

2.7. FTIR spectroscopy

All IR spectra were recorded using a Bruker IFS 148 FTIR spectrometer. The spectral resolution of the infrared spectrometer was adjusted to 2 cm^{-1} and 256 interferograms with an optical range from 4000 to 400 cm^{-1} were recorded, both for background and sample measurement. To prepare clay (kaolinite and illite), and PHA-clay samples for FTIR measurement, 2 mg of clay or PHA-clay freeze-dried sample were homogeneously mixed and with 250 mg of dry potassium bromide (KBr – 99.9% Sigma–Aldrich) to prepare a KBr pellet for FTIR measurements. The samples had to be freeze-dried in order to remove water for FTIR measurements, however, slight changes in structure during this procedure cannot be ruled out.

3. Results and discussion

3.1. PHA adsorption to kaolinite and illite

Dissolved organic carbon (DOC) measurements were performed on PHA-clay samples to assess the degree of adsorption of PHA to the kaolinite and illite surfaces under changing conditions of ionic strength and PHA concentration. As shown in Tables 1 and 2, at low PHA concentrations, i.e. 0.01 mg PHA/mL (5.5 mg C/L), the percentage of PHA adsorbed to the mineral surface decreased as the Ca^{2+} concentration increased from 10 to 100 mM. Compared to a maximum PHA sorption to kaolinite of 82% at 10 mM Ca^{2+}, only 74% of the PHA was adsorbed to kaolinite at 100 mM Ca^{2+}. A more pronounced effect was observed for illite (Table 2). In this case, sorption of PHA to the mineral surface decreased from maximum sorption percentages of 79% at 10 mM Ca^{2+} respectively, to 65% at 100 mM. A lower sorption of PHA to the mineral surface may suggest a more open conformation of the PHA molecules [23,26].

Table 1
DOC measurements for 0.01 mg/mL (5.5 mg C/L) and 0.1 mg/mL (57.9 mg C/L) PHA in the presence of kaolinite as a function of increasing Ca^{2+} concentrations.

$[Ca^{2+}]$ (M)	[PHA][a] (mg C/L)	Sorbed [PHA][a] (mg C/L)	% PHA sorbed
0.01	5.5	4.5	82
	5.5	4.4	80
0.1	5.5	4.0	74
	5.5	4.0	73
0.01	57.9	55.8	96
	57.9	55.3	96
0.1	57.9	54.9	95
	57.9	55.3	96

These measurements were carried out at circumneutral pH, and the error in the DOC measurements ranges from 5% to 10%.
[a] [PHA] refers to the concentration of peat humic acid, obtained as described previously.

Table 2
DOC measurements for 0.01 mg/mL (5.5 mgC/L) and 0.1 mg/mL (57.9 mgC/L) PHA in the presence of illite as a function of increasing Ca^{2+} concentrations.

$[Ca^{2+}]$ (M)	[PHA][a] (mg C/L)	Sorbed [PHA][a] (mg C/L)	% PHA sorbed
0.01	5.5	4.3	79
	5.5	4.2	77
0.1	5.5	3.9	71
	5.5	3.6	65
0.01	57.9	54.1	94
	57.9	53.8	93
0.1	57.9	53.8	93
	57.9	53.7	93

These measurements were carried out at circumneutral pH, and the error in the DOC measurements ranges from 5% to 10%.
[a] [PHA] refers to the concentration of peat humic acid, obtained as described previously.

An excess of Ca^{2+}, in the presence of lower PHA concentrations of 0.01 mg/mL (5.5 mg C/L) may imply that sorption occurs through electrostatic attraction of open conformation humic molecules to the clay surface.

At higher PHA concentrations of 0.1 mg/mL (57.9 mg C/L) in the presence of kaolinite and illite (Tables 1 and 2 respectively), more than 95% of the PHA was adsorbed to the kaolinite surface and at least 90% of the PHA was adsorbed to the illite surface for Ca^{2+} concentrations of 10 and 100 mM. The higher sorption of PHA to the kaolinite and illite surfaces at higher PHA concentrations (0.1 mg/mL) and for 10 and 100 mM Ca^{2+} suggests, as mentioned earlier [23,26], that calcium may promote a more compact structure of humic substances. This mechanism, proposed to occur through carboxylate site saturation and intersite bridging by Ca^{2+}, may lead to the changes in PHA conformation required to enhance the quantity of PHA adsorbed to the mineral surface [23,26].

3.2. Acid–base titration of clay and PHA-clay complexes

In order to determine the number and identity of clay surface functional groups and quantify the effects of PHA binding on the clay mineral with respect to surface reactivity, acid base titration experiments were performed. Tables 3–5 present a summary of the results obtained from acid base titration of clay minerals (kaolinite and illite), and PHA-clay complexes. As shown in Table 3, three binding sites were found for both kaolinite and illite mineral phases. For kaolinite, average pK_a values of 4.63 ± 0.07, 8.06 ± 0.07 and 9.38 ± 0.07 were obtained from replicate experiments for Ca^{2+} concentrations of 0.01 and 0.1 M. In the case of illite, complexing sites had pK_a values in the order of 6.39 ± 0.07, 7.90 ± 0.07, and 8.97 ± 0.09 at the same Ca^{2+} concentrations as for kaolinite. Individual fits of pK_a values for both illite and kaolinite were affected

Table 3
Summary of parameters optimized from acid base titration data for kaolinite and illite.

Mineral phase	$[Ca^{2+}]$ (M)	pK_a[a]	SD (μmoles/mg)[b] × 10^{-4}	Total SD[c]
Kaolinite	0.01	4.50 ± 0.07	1.60	5.22
		7.85 ± 0.05	1.13	
		9.15 ± 0.07	2.49	
	0.1	4.75 ± 0.05	1.55	4.36
		8.25 ± 0.07	1.22	
		9.61 ± 0.07	1.59	
Illite	0.01	6.15 ± 0.05	4.29	8.76
		7.65 ± 0.05	2.37	
		8.80 ± 0.05	2.11	
	0.1	6.65 ± 0.05	1.03	4.59
		8.15 ± 0.05	0.91	
		9.15 ± 0.07	2.65	

[a] pK_a is the apparent acid dissociation constant calculated for each site j as described.
[b] SD is the binding site concentration for each site j at the assigned pK_a.
[c] Total SD is the sum of the individual SD values for each site j in Eq. (6).

Table 4
Summary of parameters optimized from acid base titration data for kaolinite in the presence of peat humic acid (PHA).

$[Ca^{2+}]$ (M)	PHA (mg/mL)	pK_a[a]	SD (μmoles/mg) × 10^{-4}[b]	Total SD[c]
0.01	0.01	5.25 ± 0.05	1.03	5.76
		7.10 ± 0.07	1.50	
		8.15 ± 0.09	1.13	
		9.05 ± 0.05	2.11	
	0.1	4.40 ± 0.07	1.43	7.86
		5.31 ± 0.05	1.12	
		6.50 ± 0.07	1.40	
		7.43 ± 0.09	1.33	
		8.78 ± 0.07	2.58	
0.1	0.01	4.75 ± 0.05	1.87	9.49
		6.85 ± 0.07	1.68	
		8.25 ± 0.07	2.45	
		9.55 ± 0.05	3.49	
	0.1	4.60 ± 0.05	1.55	9.33
		5.05 ± 0.07	1.16	
		6.55 ± 0.07	1.73	
		7.55 ± 0.09	1.64	
		8.65 ± 0.07	3.25	

[a] pK_a is the apparent acid dissociation constant calculated for each site j as described.
[b] SD is the binding site concentration for each site j at the assigned pK_a.
[c] Total SD is the sum of the individual SD values for each site j in Eq. (6).

by varying background electrolyte concentration. However, optimized total site concentration ($S_{T,j}$) values in Eq. (6), for illite decreased from 8.76 to 4.59 × 10^{-4} μmoles/mg of clay as a function of increasing Ca^{2+} concentration from 0.01 to 0.1 M. This suggests that the pK_a values are affected by Ca^{2+} concentrations either by electrostatic effects due to increased ionic strength or by Ca^{2+} competition for sorption sites on the clay surface. A similar effect was observed in the case of kaolinite, however, total site concentrations decreased to a lesser extent within the range of 4.36–5.22 × 10^{-4} μmoles/mg of clay (Table 3). This may be explained by the increased electrostatic interaction of background electrolyte cations with the mineral surface as function of ionic strength. This results in a reduced jth binding site concentration available for detection with acid base titration experiments as observed previously for bacterial cell surfaces [39–43].

Because of differences in the clay minerals (kaolinite or illite) in terms of composition, structure and varying acid–base titration

Table 5
Summary of parameters optimized from acid base titration data for illite in the presence of peat humic acid (PHA).

[Ca^{2+}] (M)	PHA (mg/mL)	pK_a[a]	SD (μmoles/mg) × 10^{-4}[b]	Total SD[c]
0.01	0.01	4.45 ± 0.07	2.07	6.45
		6.35 ± 0.09	1.04	
		7.45 ± 0.05	1.46	
		9.05 ± 0.05	1.88	
	0.1	4.15 ± 0.05	2.35	7.37
		5.25 ± 0.05	0.98	
		6.40 ± 0.07	2.04	
		7.75 ± 0.07	1.55	
		8.95 ± 0.07	0.45	
0.1	0.01	4.45 ± 0.05	3.60	9.77
		5.25 ± 0.07	0.82	
		6.45 ± 0.07	1.63	
		8.05 ± 0.07	1.07	
		9.05 ± 0.05	2.65	
	0.1	4.35 ± 0.07	3.91	10.18
		5.85 ± 0.07	1.15	
		6.85 ± 0.05	1.60	
		8.35 ± 0.09	1.52	
		9.35 ± 0.05	2.00	

[a] pK_a is the apparent acid dissociation constant calculated for each site j as described.
[b] SD is the binding site concentration for each site j at the assigned pK_a.
[c] Total SD is the sum of the individual SD values for each site j in Eq. (6).

experiment equilibration times, direct comparison of clay pK_a and total site concentration data with literature values is difficult [38]. However, kaolinite pK_a values form this study are in good agreement with intrinsic and apparent parameters reported by Kramer et al. [2] and Tertre et al. [38] and Wehrli et al. [45]. Average pK_a values of 4.63 ± 0.07 and 8.06 ± 0.07 (Table 3) describe the deprotonation of aluminol ($\equiv AlOH_2^+ \rightarrow \equiv AlOH + H^+$) and silanol ($\equiv SiOH \rightarrow \equiv SiO^- + H^+$) sites at the edge octahedral alumina and silica tetrahedral sheets on kaolinite respectively, whereas the value of 9.38 ± 0.07 is comparable to that reported by Kramer et al. [2], and may provide evidence for a third binding site corresponding to a deprotonation mechanism of AlOH ($\equiv AlOH \rightarrow \equiv AlO^- + H^+$) at alkaline pH [2,38,45]. This suggests a heterogeneous functional group reactivity of the kaolinite surface, and a greater number of surface group ligands available to complex toxic metal cations in soils.

Only a few studies have addressed the illite surface chemistry. These works have relied on one or two pK_a surface complexation models and the FITEQL® optimization routine to quantify the number and concentration of illite surface functional groups [6,11,16,17,20,46]. Acid base titration data, in this study, for Ca^{2+} concentrations of 0.01 and 0.1 M, yielded pK_as of 6.39 ± 0.07 and 8.97 ± 0.09 (Table 3), which suggest the deprotonation of aluminol and silanol groups on the illite surface, as mentioned previously for kaolinite [10–14]. The observed illite pK_a value of 7.90 ± 0.07 is consistent with that reported by Liu et al. 1997 and Du et al. 2001 [16,17]. In their work, however, a three site model was found not to be suitable to describe protonation reactions on the illite surface, as their optimal result set would differ as a function of the initial input guess values of the FITEQL® nonlinear least squares optimization. In this study, however, the multi-site Langmuir isotherm model, was able to establish the presence of a third binding site on the illite surface, therefore, emphasizing the robustness of this semi-empirical model [40,43,44]. The finding of a third reactive site on the clay mineral surface, without the need for prior knowledge of the number or concentration of the sites, may imply a further deprotonation reaction ($AlOH \rightarrow AlO^- + H^+$) on the clay surface, as suggested previously through computer simulation studies of these minerals [10,16–19].

Tables 4 and 5 show the results obtained from the modeling of acid base titration experiments in the presence of kaolinite or illite respectively, and 0.01 or 0.1 mg/mL PHA at Ca^{2+} concentrations of 0.01 and 0.1 M. For kaolinite in the presence of 0.01 mg/mL PHA (Table 4) four binding sites were found with pK_as ranging from 5.25 ± 0.05 to 9.05 ± 0.05 and from 4.75 ± 0.05 to 9.55 ± 0.05 for background electrolyte concentrations of 0.01 and 0.1 M $CaCl_2$ respectively. The average pK_a values observed in Table 4 at 6.98 ± 0.10 and 8.20 ± 0.11, for 0.01 and 0.1 M Ca^{2+} respectively, at 0.01 mg/mL PHA, suggest an additive character to the binding of PHA functional groups to the kaolinite surface. This may indicate a partial sorption of humics to the clay surface, where both functional groups from the mineral and organic fraction could be detected through high resolution acid base titration data analysis, as presented in this study. PHA has been shown to contain carboxylic (—COOH) and phenolic (—OH) groups in different coordination environments, with pK_a values ranging between 4–6, and 9–11 respectively [1,30]. Five binding sites are shown in Table 4 for the kaolinite setups containing 0.1 mg/mL PHA. The presence of the most acidic sites, with average pK_as of 4.40 ± 0.07 and 4.60 ± 0.05 at calcium chloride concentrations of 0.01 and 0.1 M respectively, could be attributed to the adsorption of PHA to the clay mineral surface and subsequent exposure of deprotonating —COOH surface groups. This observation is consistent with the increase in percent of PHA adsorbed on the clay mineral for high ionic strength and PHA concentration, as observed from previous DOC results. Conformational modifications of the PHA molecules upon interaction with dissolved Ca^{2+} have been suggested to increase the quantity of humic acids adsorbing to the clay particle surface [23,26], however, in addition, the presence of Ca^{2+} may lead to bridging of clay and humic functional groups, and to the condensation/aggregation of humic molecules.

Table 5 shows the optimized binding site concentrations, along with their corresponding pK_a values for illite in the presence of 0.01 and 0.1 mg/mL PHA, and varying Ca^{2+} concentration. Four or five binding sites were obtained for background electrolyte concentrations of 0.01 and 0.1 M Ca^{2+} respectively, with total number and concentration of binding sites increasing proportionally as a function of PHA concentration (Table 5). The presence of five binding sites is indicative of exposed PHA functional groups on the clay surface. This is indicative of an additive nature of the PHA adsorption on the clay mineral surface. This is suggested by the increase in total binding site concentration observed in Tables 4 and 5 for PHA-coated kaolinite and illite respectively, as described previously for bacteriogenic iron oxides [47,48]. At high calcium chloride concentrations and high PHA concentration, the interaction of PHA molecules with background electrolytes, Ca^{2+}, may increase the quantity of PHA adsorbed on the clay surface and therefore the binding site concentration [23,26].

Individual and total binding site concentrations are reported in Tables 3–5 for kaolinite and illite, as well as for PHA-coated clay mineral in the presence of 0.01 or 0.1 mg/mL PHA. The three sites reported in Table 1 for kaolinite at 0.01 and 0.1 M $CaCl_2$, show decreasing total site concentrations of 5.22 and 4.36×10^{-4} μmol/mg clay respectively. Similarly for illite, decreasing values of total binding site concentrations were observed at 8.76 and 4.59×10^{-4} μmoles/mg clay for the increasing concentrations of 0.01 and 0.1 M $CaCl_2$. Tables 4 and 5 show variations of the total complexing site density as a function of increasing PHA and background electrolyte concentrations. In general for both kaolinite and illite total binding site concentrations increase to maximum values of 9.33 and 10.18×10^{-4} μmol/mg clay, respectively at conditions of high PHA concentration (0.1 mg/mL) and 0.1 M $CaCl_2$. A similar increase in site density concentration is also observed for the lower

PHA concentration from 5.76 to 9.49, and 6.45 to 9.77 μmol/mg clay, for kaolinite and illite respectively (Tables 4 and 5). This is indicative of an enhancement of PHA adsorption to the clay mineral surface with increasing background electrolyte concentration as confirmed by DOC analysis, and may also suggest changes in PHA molecule conformation at higher Ca^{2+} concentrations as suggested previously [23,26]. As mentioned earlier, a higher background electrolyte concentration, given by increasing Ca^{2+} in this study, may cause humic molecules to condense and sorb to the mineral surface, increasing the total binding site concentration. From the site density values in Tables 3–5, an additive, rather than a masking of clay surface functional groups could be inferred [23,26].

3.3. Zeta potential measurements of clay and PHA-clay suspensions

Zeta potential measurements of clay suspensions (kaolinite or illite) in the presence and absence of PHA indicate the development of a net particle negative surface charge as a function of increasing pH. Fig. 1 presents zeta potentials measured for Ca^{2+}-homoionized kaolinite, and for PHA-kaolinite complexes at a concentration of 0.01 M Ca^{2+}.

The zeta potential values shown for kaolinite were obtained in the pH range of 4–10. Those contained in the pH range of 4–7, show a general decrease in surface potential with increasing pH, as shown from the initial value of −30.1 ± 5.8 mV at pH 4.4 to that of −36.1 ± 1.6 mV at pH 6.6. This is consistent with the result obtained previously for kaolinite where a single acidic site was available to undergo deprotonation reactions at a $pK_a \sim 4.6$. At pH 7, a drop in surface potential, to −50.8 ± 3.0 mV, is observed, suggesting the deprotonation of a further available surface site as shown in Table 1. The surface potential then decreases only slightly to reach a value of −53.2 ± 6.6 mV at pH 9.1. Further measurements of zeta potential values for kaolinite, within the pH range of 9.1–10.4, show increasing surface potentials which scale up from −47.8 ± 2.2 to a maximum of −42.1 ± 2.8 mV at pH 10.4. This increase in potential to more positive values for kaolinite at alkaline pH, may suggest the further deprotonation of AlOH groups as described earlier and the electrostatic interaction of background Ca^{2+} electrolyte cations. This effect should be able to generate a more apparent positive charge on the clay mineral surface.

Fig. 1 shows, in addition, the results of measured zeta potential values for kaolinite in the presence of 0.1 mg/mL PHA and a background electrolyte concentration of 0.01 M Ca^{2+}. The zeta potential values obtained in the presence of PHA are more negative than those for the clay mineral phase. From an initial potential of −54.3 ± 4.1 mV at pH 4.5, surface potential values of −57.2 ± 3.7, −60.8 ± 3.1, −63.1 ± 5.9 and −60.5 ± 3.8 mV were recorded at pH 5.7, 6.8, 8.8 and 10.4 respectively. This confirms an enhanced negative surface charge on the PHA-coated kaolinite surface and further emphasize the ability of humic substances to sorb to the clay mineral surface. An electrostatic interaction of organic carboxylate functional groups with the clay surface can be inferred from the more negative zeta potentials measured for the PHA-kaolinite sample as a function of increasing pH. At alkaline pH values, functional groups in humic acid (e.g. phenolic groups) would deprotonate and further interact with background electrolyte cations giving rise to a less negative particles surface potential (Fig. 1). The lower potential observed at pH 10.4 for PHA-kaolinite compared to kaolinite may indicate the deprotonation of high pK_a humic surface functional groups.

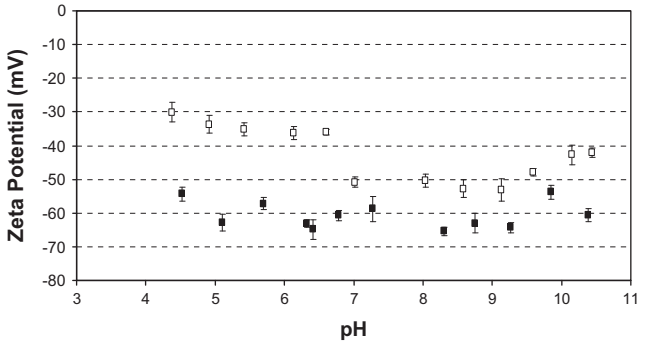

Fig. 1. Measured zeta potential of kaolinite (□) and PHA-kaolinite (■) in the pH range of 4 < pH < 10.5 and the kaolinite or PHA-kaolinite concentrations used were in the order of 0.01 mg/mL, in 0.01 M $CaCl_2$ as the background electrolyte.

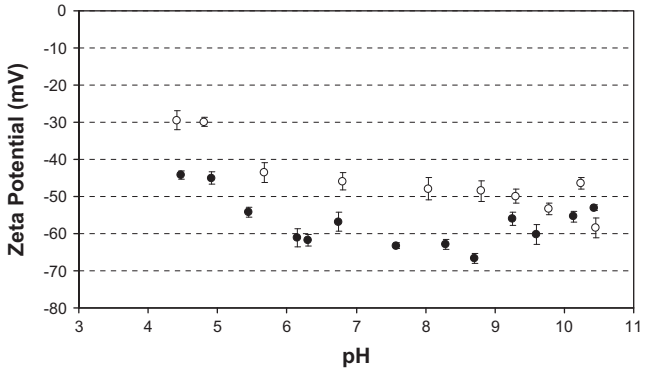

Fig. 2. Measured zeta potential of illite (○) and PHA-illite (●) in the pH range of 4 < pH < 10.5 and the illite or PHA-illite concentrations used were in the order of 0.01 mg/mL in 0.01 M $CaCl_2$ as the background electrolyte.

Fig. 2 shows the results of zeta potential measurements for illite in absence and presence of 0.1 mg/mL PHA respectively.

These measurements were recorded at a concentration of 0.01 M Ca^{2+}. Values for illite alone show a decrease in surface potentials in the pH range of 4.4–10.4. An initial zeta potential of −29.5 ± 2.4 mV was recorded at a pH of 4.4. A decrease in potential occurs at a pH of 5.7 to −43.5 ± 4.6 mV. This drop in potential is consistent with the deprotonation of the most acidic site for the illite surface, reported in Table 1, with a pK_a of ∼6.2. Significant differences are observed in the illite and PHA-illite zeta potential values in the range of pH 4–9. No significant differences in the zeta potential values are observed for illite in Fig. 2 at alkaline pH values higher than 9. The observation of a more negative potential suggests the complexation of humics to the illite surface, as described previously for kaolinite.

Zeta potential values for illite in the presence of PHA, also described in Fig. 2, confirm the interaction of organic matter with the mineral surface. An initial potential of −44.2 ± 2.3 mV was measured for illite at pH 4.5. The surface potential for this mineral decreased to −54.2 ± 2.6 mV at a pH of 5.6, suggesting the presence of a weakly acidic site on the illite surface, as mentioned previously. Values of zeta potential fluctuate within the narrow range of −60 to −65 mV in the pH range of 5.6–10.4, as shown in Fig. 2. This fluctuation represents an approximate decrease of 20 mV in the presence of PHA. This implies a similar effect of humic substance adsorption to the illite mineral surface, as that described previously for kaolinite-humics systems. Comparison of zeta potentials from pure mineral phases and PHA-bound clays show a general decrease of surface charge in the presence of PHA. This effect may be attributed to the interaction of humic substances with deprotonated aluminol and silanol functional groups on the clay surface, as suggested previously [5,27,49,50].

Please cite this article in press as: R.E. Martinez et al., J. Colloid Interface Sci. (2010), doi:10.1016/j.jcis.2010.08.082

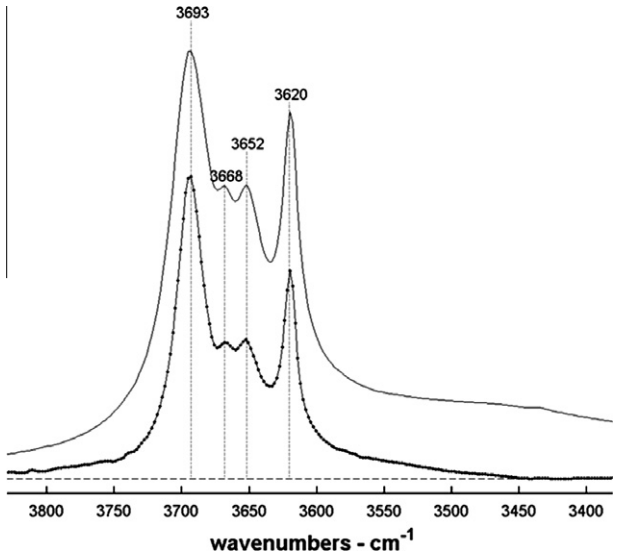

Fig. 3a. Dotted and solid lines represent Fourier transform infrared (FTIR) spectra of kaolinite and PHA-kaolinite respectively depicting absorbance values ranging from 4000 to 3400 cm^{-1}. These peaks are characteristic of kaolinite as described previously.

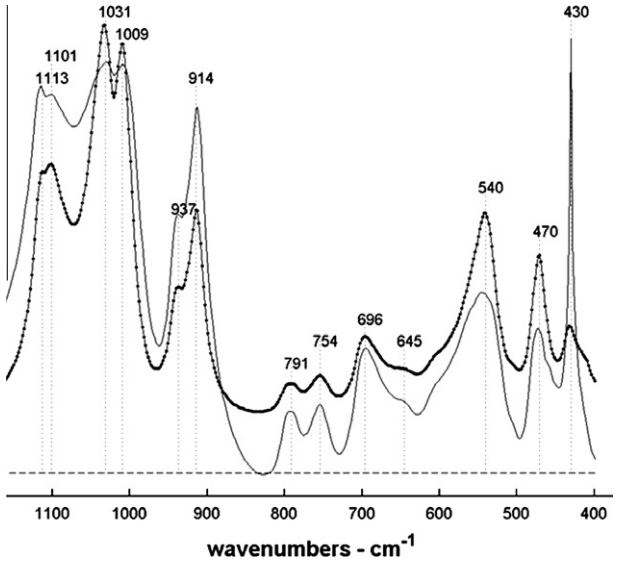

Fig. 3b. Dotted and solid lines represent Fourier transform infrared (FTIR) spectra of kaolinite and PHA-kaolinite respectively depicting absorbance values ranging from 1200 to 400 cm^{-1}. These peaks are characteristic of kaolinite as describe previously.

3.4. FTIR spectroscopy of clays and PHA-clay

Figs. 3a–3c show FTIR spectra measured for kaolinite (dotted lines) and PHA-kaolinite complexes (solid lines).

Absorbance values, in Fig. 3a at 3693, 3668, 3652 and 3620 cm^{-1} for both kaolinite and PHA-kaolinite complexes have been assigned to stretching and vibrational modes of kaolinite [10,12,51]. The band observed at 3693 cm^{-1} has been previously shown to represent the Al···O—H stretching vibration mode of "inner surface hydroxyls" located at the surface of octahedral sheets opposite to tetrahedral oxygens of the adjacent kaolinite layer [10,12,51]. The band at 3620 cm^{-1}, in Fig. 3a, coincides with that of "inner hydroxyls" located on the plane, common to octahedral and tetrahedral sheets, as described previously. Bands recorded at 3668 and 3652 cm^{-1} are suggested to emerge from the vibration

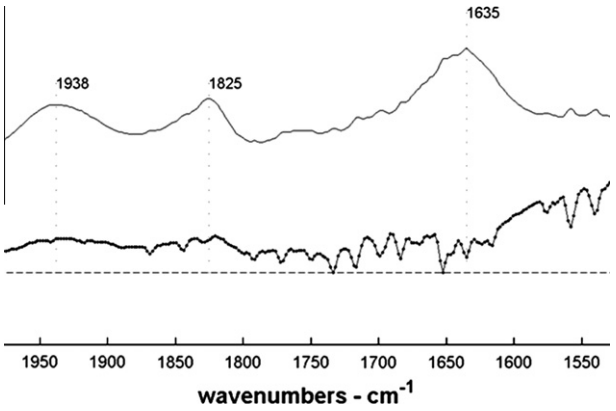

Fig. 3c. Dotted and solid lines represent Fourier transform infrared (FTIR) spectra of kaolinite and PHA-kaolinite respectively depicting absorbance values ranging from 2000 to 1500 cm^{-1}. These weak absorbance peaks, present only in PHA-kaolinite systems, should correspond to amine ($—NH_2$) or carbonyl (>C=O) vibrations.

Table 6
Main IR Absorption bands from the normalized difference spectrum from PHA-kaolinite and kaolinite spectra.[a]

Frequency (cm^{-1})	Assignment[b]
3440	O—H stretching, trace N—H stretching
2930	Aliphatic C—H stretching
2361	Bands at 2361 and 2335 cm^{-1}: OH stretching from COOH
2335	
1652	C=O stretching of COOH and trace ketones
1646	C=O stretching of amide groups (amide I band) and/or
1635	quinone C=O

[a] Spectra for the mineral phases (kaolinite and illite) were normalized to those of PHA-kaolinite and PHA-illite spectra.
[b] Frequency bands in Tables 4 and 5 were assigned according to those described in reference [1,51,52].

of "outer hydroxyls" located at the surface and along broken edges of kaolinite monocrystals [10,12,51]. In Fig. 3b absorption bands at 1113 and 1101 cm^{-1} are associated with Si—O stretching vibrations, while those at 1031 and 1009 cm^{-1} are characteristic of Si—O—Si and Si—O—Al lattice vibrations [10,12,51,52]. Further bands at 937 and 914 cm^{-1} in Fig. 3b can be attributed to "inner surface hydroxyls" and "inner hydroxyls" respectively mainly caused by Al—OH groups. Fig. 3b represents the bands at lower frequency wavenumbers (ranging from 1200 to 400 cm^{-1}). These absorbance values confirm the presence of a Si-translation (791 cm^{-1}), a Si—O stretch (754 and 696 cm^{-1}), an Al—O stretch (645 cm^{-1}). Bending vibrations of Si—O and Si—O—Al were found at 540, and 470 cm^{-1}, as reported earlier for kaolinite [10,12,51]. The absorbance value at 430 cm^{-1} corresponds to the OTO (O—Al—O) bend in the kaolinite [10,12,51,52].

The solid lines in Figs. 3a–3c correspond to the FTIR vibrational frequencies of PHA-coated kaolinite. All absorption bands previously described for kaolinite are present in the PHA-kaolinite spectrum (in Figs. 3a–3c). However, in addition, weak absorption bands characteristic of PHA sorbed to kaolinite (Fig. 3c), were observed at 1938, 1825 and 1635 cm^{-1}. The absorption band at 1938 cm^{-1} suggests the presence of amino acids or amine groups, while the band at 1825 cm^{-1} suggests the presence of C—H vibrations or an anhydrous carbonyl (C=O) stretch. The absorption frequency observed at 1635 cm^{-1} indicates an H—O—H stretch suggesting water sorption to the mineral surface [1,53,54]. Further indication of PHA kaolinite surface interaction arises from the calculated difference spectrum frequencies in Table 6. In order to substract the PHA-kaolinite form the kaolinite mineral spectrum, data from the PHA

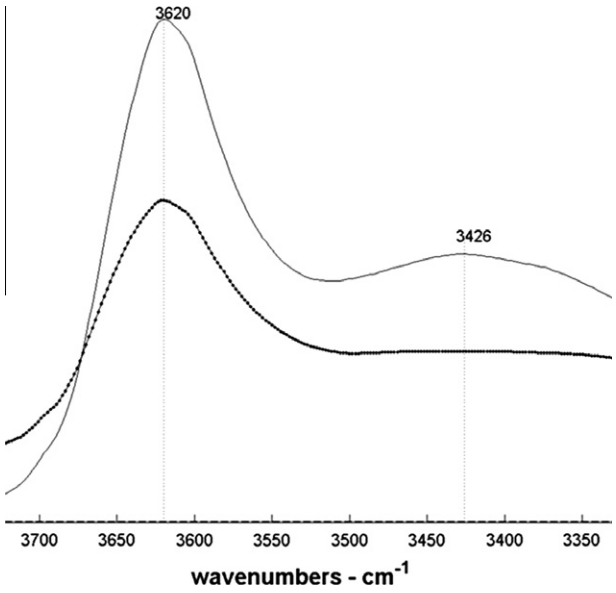

Fig. 4a. Dotted and solid lines represent Fourier transform infrared (FTIR) spectra of kaolinite and PHA-illite respectively depicting absorbance values ranging from 4000 to 3300 cm^{-1}. These peaks are characteristic of illite as described previously.

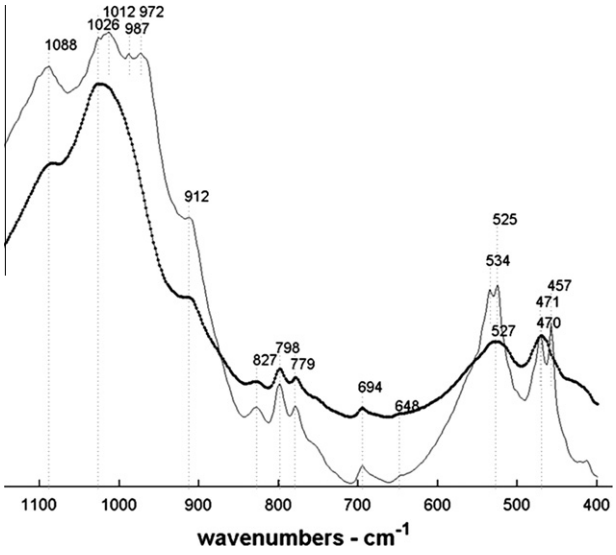

Fig. 4b. Dotted and solid lines represent Fourier transform infrared (FTIR) spectra of illite and PHA-illite respectively depicting absorbance values ranging from 1200 to 400 cm^{-1}. These peaks are characteristic of illite as describe previously.

containing spectrum was normalized to the highest absorbance value in the kaolinite spectrum and the data multiplied by the ratio obtained for the same peak at a particular wavenumber value. These procedure generated absorption bands for the PHA-kaolinite system. Main absorption bands indicating the presence of PHA appear at vibrational frequencies of —CH_2— and —CH_3— structures in humic substances (2920 and 2950 cm^{-1} respectively), and most importantly from —COOH at 2966 cm^{-1} (Table 4) [1,55].

FTIR spectra for illite (dotted lines) and PHA-illite (solid lines) are shown in Figs. 4a–4c.

The main features of the illite spectral data, in Fig. 4a, ranging from 4000 to 3300 cm^{-1}, indicate main vibrational frequencies at 3620 and 3426 cm^{-1} corresponding to Al···O—H stretch vibrations and H—O—H respectively, for bound water and Al_2OH on illite. Fig. 4b shows absorbance bands for illite and PHA-illite in the

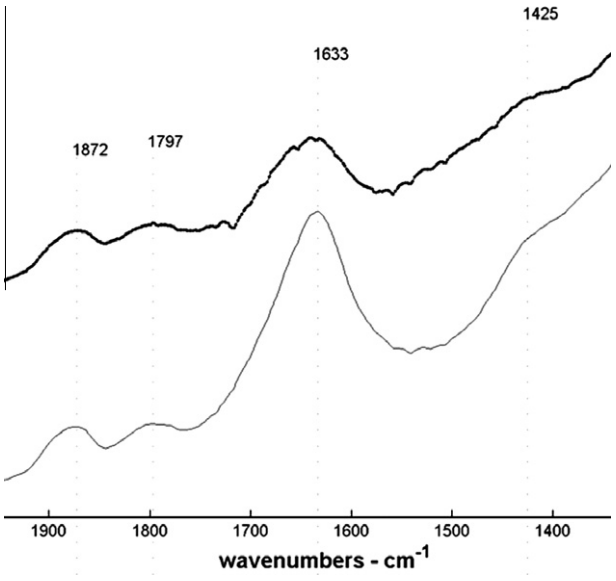

Fig. 4c. Dotted and solid lines represent Fourier transform infrared (FTIR) spectra of illite and PHA-illite respectively depicting absorbance values ranging from 2000 to 1500 cm^{-1}. These weak absorbance peaks shown, may correspond to amine (—NH_2) or carbonyl (>C=O) vibrations, as well as that of water at 1635 cm^{-1}. These peaks could indicate the presence of PHA on the illite surface, as explained in text.

Table 7
Main IR Absorption bands from the normalized difference spectrum from PHA-illite and illite spectra.[a]

Frequency (cm^{-1})	Assignment[b]
3427	O—H stretching, trace N—H stretching
2931	Aliphatic C—H stretching
2856	Bands at 2361 and 2335 cm^{-1}: OH stretching from
2362	COOH
2338	
1716	C=O stretching of COOH and trace ketones
1635	C=O stretching of amide groups (amide I band) and/or quinone C=O
1363	OH deformation and C—O stretching of phenolic OH C—H deformation of CH_2 and CH_3 groups COO^- antisymmetric stretching

[a] Spectra for the mineral phases (kaolinite and illite) were normalized to those of PHA-kaolinite and PHA-illite spectra.
[b] Frequency bands in Tables 4 and 5 were assigned according to those described in reference [1,51,52].

range of 1200–400 cm^{-1}. Wavenumbers extending from 1088 to 972 cm^{-1} correspond to separate Si—O absorptions. The value of 912 cm^{-1}, has been previously reported as characteristic of the presence of illite, as an Al_2OH in-plane vibration band [10,52,56,57]. Wavenumbers in the range of 850–400 cm^{-1}, show an absorption band at 470 cm^{-1} which can be attributed to a Si—O stretch, while that at 527 cm^{-1} results from an Si—O bending mode vibration, in combination with vibrational frequency values of 827, 798, 779 and 694 cm^{-1}. The absorption band at 648 cm^{-1} suggests the presence of iron rich chlorites [10,52,56,57].

The solid line spectra in Figs. 4a–4c, represent those of PHA-coated illite. In addition to the vibrational frequencies described above for the mineral phase, these spectra may suggest characteristic vibrations expected for peat humic acids. These were obtained from the analysis of vibrational frequencies in Fig. 4c and the difference spectrum calculated from the subtraction of illite and normalized PHA-illite spectra (Table 7). Spectra were normalized as

described previously for kaolinite. Absorbance values at 1872, 1797 and 1425 cm^{-1} may arise from sorption of PHA to illite. The absorbance band at 1425 cm^{-1} suggests, for example, bending vibrations of aliphatic C—H. This is unclear, however, as these absorbances are present in both the illite and the PHA-illite spectra (Fig. 4c). The absorbance band at 1633 cm^{-1} (Fig. 4c) represents water adsorption on the mineral surface. From the calculated difference spectra in Table 7, the PHA-illite mineral phase interactions may be inferred from the presence of weak absorption bands, characteristic of organic matter, ranging from 3427 to 1363 cm^{-1} [1,53,54].

4. Conclusions

The use of dissolved organic carbon measurements, acid–base titrations, flexible surface complexation models, zeta potential and infrared spectroscopic data demonstrated PHA adsorption to the clay mineral surface and an increase in the number and concentration of surface sites available for deprotonation and potential sorption of toxic metal cations. The increase in the number of surface functional groups and the increase in surface site concentration, suggest an additive character, rather than a masking of clay surface groups by sorbed humics. Zeta potential measurements were able to confirm a more negative surface charge in the presence of organic matter, attributed to the sorption of PHA on the clay surface as a function of increasing pH. The presence of humic substance interaction with the clay mineral surface was strongly suggested from the analysis of FTIR spectroscopic data.

Acknowledgments

This work was supported by an Alexander von Humboldt Foundation Experienced Researcher Fellowship to REM, an IPSWaT Doctoral Fellowship awarded to PS, and BMBF support to AK. The authors thank Johannes Ofner from the Forschungsstelle Atmosphärische Chemie, Universität Bayreuth, Germany for FTIR measurement of clay samples, Dr. Oleg S. Pokrovsky of the CNRS-OMP-LMTG in Toulouse, France, for the time made available to use the zeta potential instrument in his laboratory. In addition Dr. Martin Obst, Dr. Christian Schröder, and Florian Hegler are thanked for their helpful comments during the preparation of this manuscript.

References

[1] F.J. Stevenson, Humus Chemistry: Genesis, Composition, Reactions, John Wiley & Sons, New York, 1994.
[2] J.R. Kramer, P. Collins, P. Brassard, Mar. Chem. 36 (1991) 1.
[3] I. Sondi, V. Pravdić, Croat. Chem. Acta 71 (1998) 1061.
[4] E. Tombácz, Z. Libor, E. Illés, A. Majzik, E. Klumpp, Org. Geochem. 35 (2004) 257.
[5] R. Kretzschmar, D. Hesterberg, H. Sticher, Soil Sci. Soc. Am. J. 61 (1997) 101.
[6] G. Sposito, N.T. Skipper, R. Sutton, S. Park, A.K. Soper, J.A. Greathouse, Proc. Natl. Acad. Sci. U. S. A. 96 (1999) 3358.
[7] U. Neubauer, B. Nowack, G. Furrer, R. Schulin, Environ. Sci. Technol. 34 (2000) 2749.
[8] S.M.I. Sajidu, I. Persson, W.R.L. Masamba, E.M.T. Henry, J. Hazard. Mater. 158 (2008) 401.
[9] G.C. Gupta, F.L. Harrison, Water Air Soil Pollut 17 (1982) 357.
[10] D. Bougeard, K.S. Smirnov, E. Geidel, J. Phys. Chem. B 104 (2000) 9210.
[11] K.L. Konan, C. Peyratout, J.-P. Bonnet, A. Smith, A. Jacquet, P. Magnoux, P. Ayrault, J. Colloid Interface Sci. 307 (2007) 101.
[12] J. Kristóf, R.L. Frost, A. Felinger, J. Mink, J. Mol. Struct. 410–411 (1997) 119.
[13] J.E. Thomas, M.J. Kelley, J. Colloid Interface Sci. 322 (2008) 516.
[14] J.C. Miranda-Trevino, C.A. Coles, Appl. Clay Sci. 23 (2003) 133.
[15] C. Ma, R.A. Eggleton, Clays Clay Miner. 47 (1999) 174.
[16] W. Liu, Water Res. 35 (2001) 4111.
[17] Q. Du, Z. Sun, W. Forsling, H. Tang, J. Colloid Interface Sci. 187 (1997) 221.
[18] S. Ferrari, A.F. Gualtieri, G.H. Grathoff, M. Leoni, Z. Kristallogr. (Suppl. 23) (2006) 493.
[19] C. Tao, W. HeJing, Sci. China Ser. D – Earth Sci. 50 (2007) 1452.
[20] J.C. Westall, FITEQL: A Computer Program for Determination of Chemical Equilibrium Constants from Experimental Data, Report 82-01. Department of Chemistry, Oregon State University, Corvallis, OR, 1982.
[21] P. Leroy, A. Revil, J. Colloid Interface Sci. 270 (2004) 371.
[22] B.K. Schroth, G. Sposito, Clays Clay Miner. 45 (1997) 85.
[23] E.M. Murphy, J.M. Zachara, Geoderma 67 (1995) 103.
[24] M. Rebhun, R. Kalabo, L. Grossman, J. Manka, Ch. Rav-Acha, Water Res. 26 (1992) 79.
[25] M. Meier, K. Namjesnik-Dejanovic, P.A. Maurice, Y.-P. Chin, G.R. Aiken, Chem. Geol. 157 (1999) 275.
[26] A. Saada, H. Gaboriau, S. Cornu, F. Bardot, F. Villiéras, J.P. Croué, Clay Miner. 38 (2003) 433.
[27] G.U. Balcke, N.A. Kulikova, S. Hesse, F.-D. Kopinke, I.V. Perminova, F.H. Frimmel, Soil Sci. Soc. Am. J. 66 (2002) 1805.
[28] M.B. Hay, S.C.B. Myneni, Geochim. Cosmochim. Acta 71 (2007) 3518.
[29] L. Li, W. Huang, P. Peng, G. Sheng, J. Fu, Soil Sci. Soc. Am. J. 67 (2003) 740.
[30] W. Stumm, J.J. Morgan, Aquatic Chemistry: Chemical Equilibria and Rates in Natural Waters, John Wiley & Sons, New York, 1996.
[31] G.H. Bolt, B.P. Warkentin, Kolloid-Zeitschrift 156 (1957) 41.
[32] S. Nir, Soil Sci. Soc. Am. J. 50 (1986) 52.
[33] T. Polubesova, S. Nir, Clays Clay Miner. 47 (1999) 366.
[34] B.L. Sawhney, Clays Clay Miner. 20 (1972) 93.
[35] O.L. Gaskova, M.B. Bukaty, Phys. Chem. Earth 33 (2008) 1050.
[36] S.A. Hussain, Ş. Demirci, G. Özbayoğlu, J. Colloid Interface Sci. 184 (1996) 535.
[37] M. Tschapek, L. Tcheichvili, C. Wasowski, Clay Miner. 10 (1974) 219.
[38] E. Tertre, S. Castet, G. Berger, M. Loubet, E. Giffaut, Geochim. Cosmochim. Acta 70 (2006) 4579.
[39] D.S. Smith, F.G. Ferris, Methods Enzymol. 337 (2001) 225.
[40] R.E. Martinez, F.G. Ferris, J. Colloid Interface Sci. 243 (2001) 73.
[41] R.E. Martinez, D.S. Smith, E. Kulczycki, F.G. Ferris, J. Colloid Interface Sci. 253 (2002) 130.
[42] R.E. Martinez, K. Pedersen, F.G. Ferris, Interface Sci. 275 (2004) 82.
[43] J.S. Cox, D.S. Smith, L.A. Warren, F.G. Ferris, Environ. Sci. Technol. 33 (1999) 4514.
[44] P. Brassard, J.R. Kramer, P.V. Collins, Environ. Sci. Technol. 24 (1990) 195.
[45] B. Wehrli, E. Wieland, G. Furrer, Aquat. Sci. 52 (1990) 1.
[46] X. Gu, L.J. Evans, Geochim. Cosmochim. Acta 72 (2008) 267.
[47] A.W.P. Vermeer, J.K. McCulloch, W.H. Van Riemsdijk, L.K. Koopal, Environ. Sci. Technol. 33 (1999) 3892.
[48] R.E. Martinez, D.S. Smith, K. Pedersen, F.G. Ferris, Environ. Sci. Technol. 37 (2003) 5671.
[49] E. Ghabbour, G. Davies, M.E. Goodwillie, K. O'Donaughy, T.L. Smith, Environ. Sci. Technol. 38 (2004) 3338.
[50] S. Kang, B. Xing, Langmuir 23 (2007) 7024.
[51] M. Hoch, A. Bandara, Colloids Surf., A: Physicochem. Eng. Aspects 253 (2005) 117.
[52] K. Oinuma, H. Hayashi, Am. Mineral. 50 (1965) 1213.
[53] G. Jalovszky, S. Holly, M. Hollósi, J. Mol. Struct. 348 (1995) 329.
[54] L.O.B. Benetoli, C.M.D. de Souza, K.L. da Silva, I.G. de Souza Jr., H. de Santana, A. Paesano Jr., A.C.S. da Costa, C.T.B.V. Zaia, D.A.M. Zaia, Origins Life Evol. Biosph. 37 (2007) 479.
[55] M. Tatzber, M. Stemmer, H. Spiegel, C. Katzlberger, G. Haberhauer, A. Mentler, M.H. Gerzabek, J. Plant Nutr. Soil Sci. 170 (2007) 522.
[56] J. Pironon, M. Pelletier, P. de Donato, R. Mosser-Ruck, Clay Miner. 38 (2003) 201.
[57] J.L. Post, L. Borer, Appl. Clay Sci. 22 (2002) 77.

6

Effect of dissolved phosphate and silicate on desorption of arsenic from clay and humic acid-coated clay

Prasesh Sharma and Andreas Kappler

Geomicrobiology, Center for Applied Geosciences, University of Tuebingen, Germany

In preparation for Journal of Contaminant Hydrology

Abstract

Arsenic (As) contaminated aquifers contain iron minerals and clays that strongly bind As at their surfaces. Also, it was suggested that As mobilization is driven by natural organic matter (such as fulvic acids (FA) and humic acids (HA)) present in the aquifers either via reductive dissolution of Fe(III) (hydr)oxides or via competitive desorption of As from the mineral surfaces. In the present study we quantified sorption of As(III) and As(V) to Illite (IL) and Kaolinite (Kao) as well as to HA-coated clays, i.e., Illite-HA (IL-HA) and Kaolinite-HA (Kao-HA) at neutral pH. Clay-HA complexes sorbed higher amounts of As than clay only systems by 28-50% upon addition of 100 µM As(III) or As(V). When comparing As(III) vs As(V), sorption of As(V) was higher by 15-32% than As(III). We also followed desorption of As from Kao, Kao-HA, IL and IL-HA by 100 and 500 µM phosphate or silicate both at high (0.41-0.77 µmol As/g clay), and low (0.04 to 0.05 µmol As/g clay) As loadings. Phosphate removed As more effectively than silicate regardless of the amount of As loaded to clay minerals. At high loadings of As, the desorption of both redox species of As from clay-HA complexes ranged from 32-72% compared to 2-54% in clay only systems. No distinct trends were found for desorption by phosphate/silicate when comparing As(III) vs. As(V) or kaolinite vs illite systems (i.e. IL vs Kao and IL-HA vs Kao-HA). At low As loading, up to 80% of As was desorbed, but no noticeable trends were seen between different As species, different types of clay, clay vs clay-HA or the type of desorbant. The results of the study show that HA sorption to clay minerals can increase As binding to the clay although the As sorbed by clay-HA is also released to a greater extent by competing ions such as phosphate and silicate. Desorption of As depended on the initial loadings of As onto the clay/clay-HA. Based on our results, the effect of humic substances on sorption of As, and desorption of As by phosphate and silicate have to be considered in order to fully understand and evaluate the environmental behavior of As in natural environments.

1. Introduction

Arsenic (As) is a toxic element of great concern because of its large scale contamination in many areas of the world (e.g. the Bengal delta or China). Tens of millions of people in countries such as Bangladesh, Vietnam and India suffer from Arsenicosis (As poisoning) by consuming As-contaminated groundwater (Smedley and Kinniburgh, 2002). The concentrations of As in many cases is significantly higher than 10 µg/L which is stipulated by the WHO as safety limit of As in drinking water (Smedley and Kinniburgh, 2002).

Two inorganic species of As, As(III) (arsenite) and As(V) (arsenate), are mainly found in soil and groundwater with As(III) being present under reducing conditions and As(V) in more oxidizing environments (Smedley and Kinniburgh, 2002; Warwick et al., 2005). At neutral pH, As(III) exists as H_3AsO_3 with pK_a values of 9.2, 11.3 and 13.4 whereas As(V) exists mostly as $H_2AsO_4^-$ and $HAsO_4^{2-}$ with pK_a values of 2.3, 6.8 and 11.6 respectively (Warwick et al., 2005). As(III) is considered to be more toxic and more mobile than As(V) at neutral pH. However, both species co-exist in solution and the speciation depends upon the presence of microbes, reactive minerals, redox conditions, radicals and organic matter (Saltikov and Olson, 2002; Redman et al., 2002; Jiang et al., 2009; Amstaetter et al., 2010).

The mobility of As is controlled by sorption to surfaces of clay and Fe(III) oxy(hydr)oxide minerals and depends on the presence of compounds that compete for sorption sites such as natural organic matter (NOM), phosphate and silicate. Interactions of As with natural minerals, such as Fe(III) oxy(hydr)oxides, have been studied previously in the presence and absence of NOM. These experiments demonstrated that NOM can desorb As but also prevent As from sorbing to mineral surfaces in batch and column systems (Redman et al., 2002; Warwick et al., 2005; Ko et al., 2006; Weng et al., 2009). Phosphate has an analogous chemical structure to that of arsenate and therefore competes strongly with

arsenate leading to arsenate desorption from mineral surfaces (Smith et al., 2002; Violante and Pigna, 2002). Silica is environmentally relevant due to its presence in groundwater and its high affinity for mineral surfaces and therefore represents also a potential competitive ligand for As (Swedlund et al., 1999; Davis et al., 2001; Luxton et al., 2006). Compared to phosphate, silica has been shown to be less effective in competing with As (Meng et al., 1999; Stollenwerk et al., 2007). However, while studies on the aforementioned interactions of As with Fe oxides in the presence of NOM have been of great interest, research on As-clay-NOM interactions have not received wide attention.

In countries such as Bangladesh and Cambodia, As-contaminated aquifers contain a significant amount of both clay minerals and NOM (Hossain, 2006). Clay minerals such as kaolinite and illite are found as a result of active weathering of silicates deposited from riverine load. NOM can stem either from organic carbon present in the aquifers e.g. from underlying peat deposits or being transported into the aquifers from surface waters due to intense irrigation leading to large groundwater withdrawal (Smedley and Kinniburgh, 2002; Hossain, 2006; Burgess et al., 2010). Clay minerals are hydrous phyllosilicates containing alternating layers of octahedral and tetrahedral sheets. Clays are divided into 1:1 or 2:1 layer groups, two common clay mineral types found in the environment. Kaolinite (1:1 layer type) has the general formula $Al_2Si_2O_5(OH)_4$ and contains two alternating basal cleavage faces, the tetrahedral siloxane on one side and the octahedral alumina on the other, exposing the Al-OH and Si-OH. Illite (2:1 layer type) has the general formula $K_{0.88}Al_2(Si_{3.12}Al_{0.88})O_{10}(OH)_2$ with one alumina layer in between two tetrahedral siloxane layers (Sposito, 1989). NOM sorbs readily to these clay minerals and competes with As for same sorption sites **(**Wang and Xing, 2005; Martinez et al., 2010 (submitted)). Additionally, NOM sorbed to clay can also modify surface properties of clay minerals (in particular its charge) and potentially enhances binding of As by increasing the number surface binding sites (Martinez et al., 2010 (submitted)). As adsorption to kaolinite-OM aggregates was quantified by (Saada et al., 2003). They

found increased As adsorption to clay-humic acid (clay-HA) aggregates compared to clay only systems. However, this study was limited to only one type of clay (kaolinite), one As redox species (As(V)), did not test various As loadings onto clay/clay-HA, and also only studied adsorption (and not desorption) of As.

While As sorption to clay minerals in the absence of organic matter has been thoroughly studied, there is a lack of knowledge regarding the interactions of arsenite and arsenate with clay minerals that are coated with organic matter as typically the case in the environment. Additionally, while it is known that phosphate and to some extent silica can desorb As from clay minerals, desorption of As sorbed to humics-coated clays by silicate and phosphate has not been carried out so far. Therefore, in the present study we used batch experiments to determine whether and to which extent HA sorbed to clay affect As sorption and As desorption by silicate and phosphate. The specific objectives of this research were: 1) to determine the effect of HA on sorption of As(III) and As(V) to kaolinite and illite by quantification of As(III)/As(V) sorption to clay only (kaolinite and illite) and clay-HA complexes (kaolinite-HA and illite-HA) and 2) to determine desorption of As from kaolinite and illite only, and kaolinite-HA and illite-HA systems by environmentally relevant concentrations of silicate and phosphate anions, at low and high As loadings onto clay/clay-HA.

2. Materials and methods

2.1. Reagents

Stock solutions of 100 mM arsenate and arsenite (Na_2HAsO_4 and $NaHAsO_2$), 2 mM stock solutions of phosphate (KH_2PO_4) and silicate ($NaSiO_2 \cdot 9H_2O$) (all from Fluka, Germany) were prepared in deionized water. For As(III) experiments, arsenite, phosphate and silicate solutions were purged with N_2 for 5 min

(repeated three times for each solution with 30 seconds of vacuum applied in between) before adding the respective components into the clay/clay-HA complexes. Pahokee peat humic acid (PPHA) and $CaCl_2$ were purchased from the International Humic Substances Society (IHSS) and Fluka (Germany), respectively. PPHA solution (0.1 mg/mL equivalent to ~50 mg C/L) was prepared by dissolving dry PPHA in 10 mM $CaCl_2$ under vigorous stirring. No precipitation of PPHA by Ca^{2+} was observed. The pH of the solution was readjusted to pH 7 using 1 M NaOH and stirred for 1 h before filtering with a 0.45 µm mixed cellulose ester (MCE, Millipore) filter. Clay minerals (kaolinite (KGa-1b) and illite (Imt-1)) were obtained from the Clay Mineral Society (University of Missouri, USA).

2.2. Preparation of homoionized clay

25 g of clay was shaken at 150 RPM in a rotable shaker with 1 L of 1 M $CaCl_2$ (solid:liquid ratio of 1:40 w/v) to obtain Ca^{2+}-homoionised kaolinite and illite. This process was repeated three times with 2 h of shaking in between. Excess chloride ion was removed after the last homoionization step by washing with deionised water until $AgNO_3$ addition to the washing water indicated absence of Cl^-.

2.3. Synthesis of complexes of clay and PPHA ('clay-HA' complexes)

To quantify sorption of As to clay-HA complexes compared to clay only systems, clay-HA complexes were first prepared by adding the Ca^{2+}-homoionized clay to the 50 mg C/L PPHA solutions at a ratio of 1:40 (w/v, 25 g clay and 1 L of 0.1 mg/mL HA solution). The clay-HA suspensions were incubated for 48 h at 150 RPM in an overhead shaker. After 48 h, the suspension was centrifuged at 5000 RPM for 15 min. The supernatant was sampled for dissolved organic carbon (DOC) measurements to quantify the non-sorbed PPHA. To remove loosely bound humics from the clay-HA, the pellet containing the clay-

HA aggregates was resuspended and gently shaken by hand with 10 mM $CaCl_2$. The suspension was then again centrifuged for at 5000 RPM for 15 min and the supernatant sampled for further DOC measurements. In all clay-HA systems more than 95% of PPHA added was adsorbed which gives a value of about 0.2 % [~ 2 mg C per g clay] in the clay-HA complexes (data not shown). The synthesis of clay-HA complexes represents a slight modification of the protocol from (Saada et al., 2003). From this point on, for simplicity, illite and kaolinite only systems will be referred as IL and Kao, whereas, illite-HA and kaolinite-HA complexes will be referred IL-HA and Kao-HA complexes or systems, respectively.

2.4. Sorption experiments

Sorption isotherms for As were determined by equilibrating ~500 mg wet clay or clay-HA with 25 mL As(III) and As(V) solutions of concentrations between 1-100 µM (all solutions prepared in 10 mM $CaCl_2$) in 60 mL serum bottles with O_2 tight butyl rubber stoppers. The concentrations of As were chosen to represent environmentally relevant low and some relatively high concentrations of As found in soil solutions of As-contaminated aquifers (Smedley and Kinniburgh, 2002; Hossain, 2006). We did not use concentrations higher than 100 µM As in the sorption isotherms for several reasons: (1) higher As concentrations would exceed the maximum (average) environmental As concentrations found in As contaminated aquifers; (2) the values of As sorbed per g clay obtained upon addition of 100 µM As to the clay and clay-HA systems represent values of As found in clay phases in As contaminated aquifers (Chakraborti et al., 2001) and (3) the goal of the sorption experiments was to determine whether humic substances sorbed to clay enhances As sorption and we found a significant difference in sorption of As to clay vs clay-HA systems upon addition of 100 µM As.

For As(III) experiments, clay and clay-HA suspensions were deoxygenated first by bubbling the suspension with N_2 once for 10 min and then again 5 min before adding anoxic As(III) solution in an anoxic glovebox. After equilibrating the mixtures for 72 h (at 150 RPM) on a horizontal shaker, samples were taken filtered with a 0.45 µm MCE filter and prepared for As total measurements (see analytical section). Sampling from As(III) sorption experiments was conducted in an anoxic glovebox.

2.5. Desorption of As from clay and clay-HA by phosphate and silicate

To quantify desorption of As from clay and clay-HA complexes by phosphate and silicate, setups were chosen from sorption experiments where either 1 or 25 µM As was initially added to the clay and clay-HA complexes (see description of experimental setup in Fig. 1). These amounts of As loaded to clay/clay-HA represent average low and high amounts of As in solid phases (0.1-3.0 µmol As per g clay) in As-rich aquifers reported by several authors (Ullah, 1998; Chakraborti et al., 2001; Mandal and Suzuki, 2002). We would like to note that concentrations of 25 µM As were chosen being representative for 'high As loadings' for the desorption experiments based on recent studies describing clay phases with high (average) As loadings (Ullah 1998; Chakraborti et a., 2001). Therefore, whereas 100 µM As was chosen as the maximum concentration of As added to clay/clay-HA in the sorption experiments (described in section 2.4), for desorption experiments 25 µM As was chosen for obtaining 'high' loadings. 100 µM and 500 µM phosphate and silicate were separately added to each setup. 96 h of desorption time was allowed for all setups before samples were taken and analyzed for total dissolved As (see analytical section).

2.6. Analytical methods

To quantify the amount of As in solution, 400 µL aliquots were taken from each experimental setup, centrifuged for 3 min (at 14,000 RPM), and the supernatant was acidified with 1 M HNO_3. The supernatant was analyzed for total As by ICP-MS. Selected samples were analyzed for As speciation by LC-ICP-MS (sample preparation protocol from Daus et al. (2005). In all systems, there was less than 5% As oxidation or reduction in As(III) and As(V) systems respectively (data not shown), and therefore potential effects on sorption due to As redox changes can be neglected. DOC was quantified from filtered solutions (0.45 µm MCE filter) by a TOC analyser (highTOC II, Elementar Analysensysteme GmbH, Hanau, Germany). The absorbance was measured in a plate reader (FlashScan 550, Jena Analytik, Germany). Surface areas of clay minerals were measured with the BET method (Malvern, Germany).

3. Results and discussion

3.1. Sorption of As to clays in clay and clay-HA systems

In As-contaminated aquifers, both clay minerals and natural organic matter (humic substances) were shown to be present (Hossain, 2006) and therefore As-clay interactions occur either in the presence of dissolved OM or with clay minerals coated with OM. To determine the effect of humic acids on As sorption to clays, we first quantified sorption of As to clay-HA (Kao-HA and IL-HA) complexes in comparison to clay only systems (Kao and IL) (Table 1, Fig. 3A to 3D).

3.1.1. Comparison of sorption of As to clay vs clay-HA complexes

HA adsorbed to clay affected As sorption considerably. After addition of 100 µM of As, As sorption was significantly lower in clay only systems compared to clay-HA systems (Table 1, Fig. 3A to 3D).

The amount of As(III) sorbed increased by 50% in Kao-HA and 28% in IL-HA systems compared to Kao and IL (HA-free) systems. Similar to As(III), also sorption of As(V) increased by 41 and 35% in the presence of HA compared to Kao and IL only systems, respectively. The increased sorption of As by clay-HA complexes compared to clay only is possibly due to sorption of the humic acids to the clay surface that modifies the clay surface properties in a way that enhances the binding of As. Possible mechanisms of As sorption onto the clay minerals and clay-HA complexes are illustrated in Fig. 2. Arsenic can either sorb directly to the clay mineral surface as an inner-sphere complex or as an outer-sphere ternary surface complex using Ca^{2+} as a cation bridge (Fig. 2 - mechanisms '1' and '2'). Complexation of As with OM in the presence of a cation bridge such as Fe has been shown previously in literature (Wang and Mulligan, 2007; Sharma et al., 2010) and it is possible that the negatively charged clay particles and As can be bound via Ca^{2+}as a cation bridge in our systems. In addition to cation bridges, As can also form ternary complexes with HA molecules that are bound to clay minerals provided that there are positively charged functional groups such as amines (Fig. 2 - mechanisms '3' and '4') (Saada et al., 2003) or phenolate groups (Buschmann et al., 2005) which can bind As. In particular, Saada et al., (2003) found enhanced sorption of As onto clay-HA complexes with increasing nitrogen content. However, dialysis and ultracentrifugation experiments of As-HA colloids and dissolved complexes **(**Sharma et al., 2010**)** revealed that, at neutral pH, direct binding of As to HA (in the absence of bridging metal cations) was negligible even when high concentrations of As(V) and HA (100 µM As(V) and 50 mg C/L HA) were incubated together for 5 days. With regard to the potentially involved N-containing As binding sites, this is remarkable since the Pahokee peat HA used in the present study as well as in the study by Sharma et al. (2010) have a relatively high nitrogen content of 3.7% compared to the nitrogen content of 2.1% in the peat humic acids used by Saada et al., (2003). Therefore, although amino groups are possible binding sites for As, binding sites via cation bridges or metal cations in the HA itself are probably more important for As sorption. In our systems, the clay

minerals were homoionized with Ca^{2+}, which is also present in the background solution during the incubation of the clay with the HA and As. It is known that HA bind strongly to the clay mineral surface via cation bridges such as Ca^{2+} (Tipping and Higgins, 1982; Jekel, 1986). In addition, aggregation of HA by Ca^{2+} on the clay mineral surface is possible leading to extended Ca^{2+}-HA structures comprising of multiple Ca^{2+} ions and HA molecules. Both single or multiple HA molecules bound to the clay surface via Ca^{2+} bridges could increase the number of binding sites for As possibly explaining the higher extent of sorption of As to clay-HA systems compared to clay only systems (Fig. 2, mechanism '4').

3.1.2 Comparison of sorption of As(III) vs As(V) to clay/clay-HA.

Not only the presence of HA plus potentially bridging cations influenced As sorption to the clays, also the As redox speciation influenced As sorption behavior (Table 1). As(III) and As(V) were previously shown to sorb to different extents to different mineral phases such as ferrihydrite and goethite (Goldberg, 2002) and therefore, a difference in binding was also expected upon sorption to clay and clay-HA aggregates. We found that at neutral pH and after addition of 100 µM As(III) and As(V), respectively, As(V) sorbed to the clays to a greater extent (15, 20, 25 and 32%, respectively) than As(III) in IL, IL-HA, Kao and Kao-HA systems, respectively (Table 1). This sorption behavior of arsenite and arsenate is different compared to their sorption to iron minerals such as ferrihydrite or goethite at neutral pH where arsenite usually sorbs to a higher extent than arsenate (Raven et al., 1998; Dixit and Hering, 2003; Herbel and Fendorf, 2006; Sharma et al., 2010 (submitted)). The greater adsorption of As(V) to the clays compared to As(III) in our systems can be explained by the electrostatic interactions between positively charged clay mineral surfaces (that was homoionized with 1M Ca^{2+}) and the negative charge of the deprotonated As(III) and As(V) species at pH 7. The first two pKa values of As acid (H_3AsO_4) are 2.2 (pKa_1) and 6.9 (pKa_2) while the first pKa value for arsenous

acid (H_3AsO_3) is 9.2 (pKa_1). Therefore, at a circumneutral pH the positively charged clay surface would preferentially bind the negatively charged arsenate species compared to $H_3AsO^0_3$. This was also demonstrated in a separate study carried out by Smith et al., (2002), where they found that As(V) binds more to clay-rich soils in presence of Ca^{2+} in comparision to As(III).

3.1.3 Comparison of sorption of As to different clay/clay-HA types (i.e. IL vs Kao and IL-HA vs Kao-HA)

In addition to the two different As redox species, also the two tested clay minerals, kaolinite and illite, showed noticeable differences with regard to As sorption (Table 1). For As(III), we found that sorption to IL and IL-HA systems was higher by 29.2 and 11.4% compared to Kao and Kao-HA systems, respectively. For As(V), the sorption maxima on IL and IL-HA were 11.9 and 7.1% higher than in Kao and Kao-HA systems. The sorption of As onto clay mineral surfaces depends on the structure and the surface area of the clay minerals (Lin and Puls, 2000). Aluminol binding sites of phyllosilicates were reported to be more reactive to sorption of organic compounds, anions and trace metals due to significant fractions of free oxygen atoms as compared to silanol sites (Benyahya and Garnier, 1999; Sposito, 1984)). Kaolinite is a 1:1 clay mineral with alternating octahedral and tetrahedral sheet with Si/Al ratio of 1 where as illite is a 2:1 clay mineral with the alumina layer in between the two silica layers with a Si/Al ratio of 2. This means that in kaolinite the more reactive Al-OH octahedral sheet is exposed whereas in illite the Al-OH sheet is masked between two less reactive SiO_4 sheets and therefore, more As is expected to sorb to kaolinite (Manning and Goldberg, 1997; Lin and Puls, 2000). However, in our systems we see the opposite, i.e. higher sorption of As in IL and IL-HA systems. This can probably be explained by the fact that the specific surface area of illite (26.8 m^2/g) is 3.7 times more than that of kaolinite (7.3 m^2/g). A previous study by Lin and Puls (2000) also described more As

binding to illite compared to kaolinite and they also worked with illite and kaolinite clay minerals where the illite had a higher surface area than kaolinite.

3.1.4 Sorption of As to clay/clay-HA at low (1 µM) and high (25 µM) initial As concentrations

After having determined sorption isotherms with As concentrations from 1-100 µM, in a second step (as preparation for the desorption experiments) we loaded the clay/clay-HA complexes with two different concentrations of As. The concentrations of As added (i.e. 1 and 25 µM) were selected in order to yield an environmentally relevant low and high amount of As loading (0.01–3 µmol As/g clay) as observed by previous authors **(**Ullah, 1998; Chakraborti et al., 2001; Mandal and Suzuki, 2002; Smedley and Kinniburgh, 2002; Hossain, 2006). We found that the loading of both As(III) and As(V) onto clay/clay-HA depends not only on the initial concentrations of As added but also on clay type and As species (Table 2).

3.1.4.1 As sorption at low As loadings (addition of 1 µM As to clay/clay-HA)

At low As loading (addition of 1 µM As), no difference was found for the amount of As sorbed when comparing As(III) and As(V), clay vs clay-HA or Kao vs IL systems (Table 2). The values of As ranged from 0.04 to 0.05 µmol As/g clay for both species of As which means almost all As that was added sorbed to clay/clay-HA complexes.

3.1.4.2 As sorption at high As loadings (addition of 25 µM As to clay/clay-HA)

Compared to the low As loading, at high As loading (addition of 25 µM As), there were differences between HA-loaded and HA-free clays, between kaolinite and illite, and between As(III) and As(V) systems following the trends that were already observed when 100 µM As was added (Section 3.1).

Final As(III) loadings were 0.56, 0.71, 0.41 and 0.57 µmol As(III)/g clay and As(V) loadings were 0.77, 0.87, 0.73 and 0.93 µmol As(V)/g clay in IL, IL-HA, Kao and Kao-HA systems, respectively (Table 2).

3.2. Desorption of As from clay and clay-HA by phosphate and silicate.

Many of the As contaminated regions in South Asia include extensive irrigation areas where crops are grown perennially. In these agricultural fields, phosphate is not only naturally present in minerals, as sorbed phases or as dissolved species but also can be present due to a widespread usage of phosphate fertilizers which could enter the groundwater systems (Acharyya, 2000). On the other hand, high concentrations (1-1000 µM) of groundwater silica were found in soils and As contaminated aquifers due to active weathering of silicate minerals (Iler, 1979; Meng et al., 1999). Anions such as phosphate which has an analogous structure to that of arsenate; and silicate, which can effectively sorb to with mineral phases were shown to desorb both arsenate and arsenite from minerals in soils (Meng et al., 1999; Stollenwerk et al., 2007). The concentrations of phosphate and silicate chosen in this experiment to desorb As represent average and high concentrations of the respective anions in solution found in some As contaminated aquifers and natural systems (Violante et al., 2002, Stollenwerk et al., 2007). To quantify desorption of As(III)/As(V) by phosphate and silicate from both clay and clay-HA complexes, we first loaded high and low amounts of As (addition of 25 and 1 µM As, respectively) of either As(III) or As(V) to clay and clay-HA and then desorbed the bound As by 100 and 500 µM phosphate and silicate (see description of experimental setup in Fig. 1).

3.2.1 Desorption of As by phosphate and silicate at high As loading

In our experiments, we found that not only sorption of As, but also desorption of As by phosphate and silicate depended upon the amount of As initially loaded to clay and clay-HA systems.

3.2.1.1 Desorption of As by phosphate and silicate in clay vs clay-HA systems

At high As loading, the differences in desorption in clay only and clay-HA systems were obvious in all systems (Fig. 4). 100 µM phosphate desorbed between 13-36% of As(V) and 25-31% of As(III) and 500 µM phosphate desorbed between 27-34% of As(V) and between 42-48% of As(III) in clay only systems. In clay-HA systems, the amount of As desorbed by 100 µM phosphate increased to between 36-45% for As(V) and 39-48% for As(III) (Fig. 4). When 500 µM phosphate added, 27-60% of As(V) and 48-72% of As(III) was desorbed. Desorption of As by silicate at high As loadings showed a similar trend as observed for the phosphate. In clay only systems, desorption by 100 and 500 µM silicate ions ranged from 2-10 and 8-19% respectively. In clay-HA complexes, the amount of As desorbed ranged between 14-32 and 20-39% by 100 and 500 µM silicate. The results from As desorption experiments compared to the initial amount of As loaded shows that although more As can bind to clay-HA complexes than to clay only (without preloaded HA), the As is also desorbed to a greater extent from HA-treated clays in comparison to clay only systems. This can possibly be explained by the types of sorption sites on the clay mineral surface for these two systems. Inner-sphere complexes of As-clay or As-Ca^{2+}-clay are expected to be stronger than As-Ca^{2+}-HA-clay or As bound to aggregated Ca^{2+}-HA-clay structures (Fig. 2). This means that As bound to clay via Ca^{2+}-HA-clay will possibly be desorbed more easily than that is bound directly to clay mineral surface.

3.2.1.2 Desorption of As by phosphate vs silicate

When comparing desorption of As by phosphate to desorption by silicate, we found that phosphate is more effective in desorbing As compared to silicate in the systems with high As loadings (Fig. 4) corroborating findings from literature (Stollenwerk et al., 2007). For both clay types and with/without HA, phosphate desorbed between 38-72% of the presorbed As whereas with silicate only between 23-50% of As was desorbed in all systems.

Increasing the phosphate concentration from 100 to 500 µM increased the amount of As desorbed in all experimental setups. In contrast, increasing the silicate concentrations from 100 to 500 µM generally did not increase the amount of As desorbed.

3.2.1.3 Desorption of As in IL vs Kao and IL-HA vs Kao-HA

When comparing desorption of As for the two clays tested in this study, i.e. IL vs Kao, at high As loading in the absence of HA, desorption of As(III) and As(V) by phosphate or silicate showed no significant differences between the two clays (Fig. 4). This is in contrast to the sorption experiments with 100 µM As where both forms of As sorbed more to IL compared to Kao. With the HA-pretreated clays, i.e. IL-HA vs Kao-HA, however, some differences in desorption was observed. In As(V) systems, desorption by 100 and 500 µM silicate was significantly higher in Kao-HA systems compared to IL-HA where as in As(III) systems, desorption by 100 and 500 µM phosphate was distinctly higher for Kao-HA compared to IL-HA. The reason for this desorption behavior is not clear.

3.2.1.4 Desorption of As(V) vs As(III) in clay/clay-HA systems

When comparing As(V) to As(III), we found that the relative amounts of As(III) or As(V) desorbed do not follow a specific trend. In clay only systems, more As(III) is desorbed by phosphate in comparison to As(V), whereas, when silicate was added, no definite trends exist. In clay-HA systems, in setups where phosphate was added, the differences were not significant. However, in clay-HA setups where silicate was added, relatively more As(V) was desorbed compared to As(III). The reason behind these desorption patterns are also unclear.

3.2.2 Desorption at low As loadings.

In addition to quantification of As desorption from clays at high As loading, we also quantified As desorption from clay and clay-HA at low As loading (Fig. 4). Significant differences were found when phosphate containing systems were compared to (100 µM and 500 µM) in all systems compared to silicate in clay as well as in clay-HA systems. While comparing desorption by increasing concentrations of phosphate and silicate (i.e. 100 and 500 µM phosphate and silicate) also some trends were observed. Generally, desorption of As by 500 µM phosphate was higher than As desorption by 100 µM phosphate. Between 100 and 500 µM silicate, however, there was no evident difference in amount of As desorbed in any system. This shows that an increase in concentrations of phosphate could desorb more As from clay/clay-HA into groundwater but increasing silicate concentrations from does not necessarily desorb more As from clay or clay-HA complexes also at low As loadings.

Besides the effect of increasing phosphate and silicate concentrations on As deorption, at low As loading, we did not find significant differences when we compared As desorption in clay vs clay-HA, IL vs Kao or As(III) vs As(V) setups. The reason for this could be due to the sorption mechanism of As at low loadings. At low As loadings, almost all As is sorbed to clay/clay-HA systems. However, there is still a large number of binding sites that the desorbing agents can bind to. Therefore, during desorption, phosphate and silicate can sorb to these ‘free’ binding sites without actually desorbing more As. Even if they do desorb As, the amount of As desorbed is too low to make a significant difference when comparing the various systems.

4. Conclusions

In the present study, we quantified sorption and desorption of As in clay (illite and kaolinite) and clay-HA at neutral pH. The results demonstrated that HA sorbed to clay increased sorption of both As(III) and As(V) at neutral pH. Compared to As(III), higher amounts of As(V) sorbed to both clay and clay-HA. Illite and illite-HA generally sorbed more As than kaolinite and kaolinite-HA in the presence of high As concentrations. In desorption experiments, we demonstrated that higher relative amounts of As can be desorbed from clay-HA complexes by phosphate and silicate compared to clay only systems, particularly at high As loading. Phosphate was more effective than silicate in desorbing As confirming findings from literature (Stollenwerk et al., 2007). At low As loading, sorption of HA to clay did not significantly impact the amount As sorption and desorption.

The results of our study imply that in As contaminated aquifer systems with high amounts of NOM and clay, formation of clay-NOM complexes can lead to significantly higher sorption of As to clay. However, depending on the concentration of phosphate and silicate ions present in the soil solutions, As is expected to be effectively mobilized again from clay/clay-NOM. This process is especially relevant in As-contaminated aquifers such as that of South Asia where high amounts of As, NOM, clay, phosphate and silicate are present. However, the stability of As sorbed to clay-HA complexes, possible sorption mechanisms and desorption mechanisms by phosphate and silicate in these systems, are not fully understood yet. Thus, more research on As-clay-NOM interactions in presence of phosphate and silicate is required to gain a holistic understanding of the sorption and desorption processes in As contaminated environments.

Acknowledgements

This work was supported by an IPSWaT fellowship from the German Federal Ministry for Science and Education (BMBF) to PS and by funding from the German Research Foundation (DFG) and the BMBF to AK. We would like to thank J. Breuer, P. Kühn, E.Struve and F. Baumann for their help with ICP-MS.

References

Acharyya, S.K., Chakraborty, P., Lahiri. S., Raymahashay B.C.,Guha, S., Bhowmik, A., 1999. Arsenic poisoning in the Ganges delta. *Nature,* 401, 545.

Amstaetter, K., Borch, T., Larese-Casanova, P., Kappler, A., 2010. Transformation of arsenic by Fe(II)-activated goethite (α-FeOOH). *Environmental Science & Technology,* 44, 102–108.

Burgess, W.G., Hoque, M.A., Michael, H.A., Voss, C.J., Breit, G.N., Ahmed, K.M, 2010. Vulnerability of deep groundwater in the Bengal aquifer system to contamination by arsenic. *Nature Geoscience,* 3, 83-87.

Chakraborti, D., Basu, G.K., Biswas, B.K., Chowdhury, U.K., Rahman, M. M., Paul, K., 2001. Characterization of arsenic bearing sediments in Gangetic delta of West Bengal-India. In: Arsenic exposure and health effects (Chappell WR, Abernathy CO, Calderon RL, eds). New York:Elsevier Science, 27-52.

Daus, B, Mattusch, J, Wennrich, R., Weiss, H., 2002. Investigation on stability and preservation of arsenic species in iron rich water samples. *Talanta,* 58, 57-65.

Davis, C.C., Knocke, W.R., Edwards, M., 2001. Implications of aqueous silica sorption to iron hydroxide: mobilization of iron colloids and interference with sorption of arsenate and humic substances. *Environmental Science and Technology,* 35, 3158-3162.

Dixit, S., Hering, J. G., 2003. Comparison of arsenic(V) and arsenic(III) sorption onto iron oxide minerals: implications for arsenic mobility. *Environmental Science & Technology,* 37, 4182-4189.

Fanning, K.A., Pilson, M.E.Q.,1973. On the spectrophotometric determination of dissolved silica in natural water. *Analytical Chemistry,* 45, 136–140.

Goldberg, S., Johnston, C. T., 2001. Mechanisms of arsenic adsorption on amorphous oxides evaluated using macroscopic measurements, vibrational spectroscopy and surface complexation modeling. *Journal of Colloid and Interface Science,* 234, 204–216.

Herbel, M., Fendorf, S., 2006. Biogeochemical processes controlling the speciation and transport of arsenic within iron coated sands. *Chemical Geology*, 228, 16–32.

Hossain, M. F., 2006. Arsenic contamination in Bangladesh – an overview. *Agriculture, Ecosystems and Environment*, 113, 1-16.

Jekel, M.R., 1986.The stabilization of dispersed mineral particles by adsorption of humic substances. *Water Research*, 20, 1543-1554.

Jiang, J., Bauer, I., Paul, A., Kappler, A., 2009. Arsenic redox changes by microbially and chemically formed semiquinone radicals and hydroquinones in a humic substance model quinone. *Environmental Science & Technology*, 43, 3639-3645.

Iler, R.K. 1979. The chemistry of Silica. Wiley-Interscience, New York.

Ilwon, K., Ju-Yong, K., Kyoung-Woong, K. 2004. Arsenic speciation and sorption kinetics in the As–hematite–humic acid system. *Colloids and Surfaces A:Physicochemical and Engineering Aspects*, 234, 43-50.

Ilwon, K., Davis, A. P., Ju-Yong, K., Kyoung-Woong, K., 2006. Effect of contact order on the adsorption of inorganic arsenic species onto hematite in the presence of humic acid. *Journal of . Hazardous Materials*, 141, 53-60.

Lin, Z., Puls, R.W., 2000. Adsorption, desorption and oxidation of arsenic affected by clay minerals and aging process. *Environmental Geology*, 39, 753-759.

Luxton, T.P., Tadanier, C.J., Eick, M.J., 2006. Mobilization of arsenite by competitive interaction with silicic acid. *Soil Science Society of America Journal*, 70, 204-214.

Mandal, B. K., Suzuki, K. T., 2002. Arsenic round the world: a review. *Talanta*, 58, 201–235.

Manning, B.A., Goldberg, S., 1997. Arsenic(III) and arsenic(V) adsorption on three California Soils. *Soil Chemistry*, 162, 886-895.

Martinez, R.M., Sharma, P., Kappler, A., 2010. Surface binding site analysis of Ca^{2+}-homoionized clay-HA complexes. Submitted to *Journal of Colloid and Interface Science.*

Meng, X., Bang, S., Korfiatis, G.P., 2000. Effects of silicate, sulfate, and carbonate on arsenic removal by ferric chloride. *Water Research*, 34, 1255-1261.

Raven, K.P., Jain, A., Loeppert, R.H., 1998. Arsenite and Arsenate adsorption on ferrihydrite: Kinetics, equililibrium, and adsorption envelopes. *Environmental Science and Technology*, 32, 344-349.

Redman, A. D., Macalady, D. L., Ahmann, D., 2002. Natural organic matter affects arsenic speciation and sorption onto hematite. *Environmental Science & Technology*, 36, 2889-2896.

Saltikov, C.W. and Olson, B.H. , 2002. Homology of E. coli R773 arsA, arsB, and arsC in arsenic resistant bacteria isolated from raw sewage and arsenic enriched creek waters. *Applied and Environmental Microbiology*, 68, 280-288. (abstract/paper).

Saada, A., Breeze, D., Crouze, C., Cornu, S., Baranger, P., 2003. Adsorption of arsenic(V) on kaolinite and on kaolinite-humic acid complexes – Role of humic acid nitrogen groups. *Chemosphere*, 51, 757-763.

Sharma, P., Ofner, J., Kappler, A.,2010. Formation of binary and ternary colloids and dissolved complexes of organic matter, Fe and As. *Environmental Science & Technology*, 44, 4479-4485.

Sharma, P., Rolle, M., Kocar, B., Grathwohl, P., Fendorf, S., Kappler, A. 2010. Influence of organic matter on As transport and retention. Submitted to *Environmental Science and Technology.*

Smedley, P. L., Kinniburgh, D. G., 2000. A review of the source, behaviour and distribution of arsenic in natural waters. *Applied Geochemistry*, 17, 517-568.

Smith, E., Naidu, R., Alston, A.M., 2002. Chemistry of inorganic arsenic in soils. II. Effect of phosphorus, sodium, and calcium on arsenic absorption. *Journal of Environmental Quality*, 31, 557-563.

Sposito, G. 1994. The chemistry of soils. Oxford Univ. Press, New York.

Stollenwerk, K.G., Breit, G.N., Welch, A.H., Yount, J.C., Whitney, J.W., Foster, A.L., Uddin, M.N., Majumder, R.K., Ahmed, N., 2007. Arsenic attenuation by oxidized aquifer sediments in Bangladesh. *Science of the Total Environment*, 379, 133-150.

Swedlund, P.J., Webster, J.G., 1999. Adsorption and polymerization of silicic acid on ferrihydrite, and its effect on arsenic adsorption. *Water Research*, 33, 3413-3422.

Tipping, E., Higgins, D.C., 1982. The effect of adsorbed humic substances on the colloid stability of haematite particles, *Colloid and Surfaces*, 5, 85–92.

Ullah, S.M., 1998. Arsenic contamination of groundwater and irrigated soil of Bangladesh. In: International Conferences on As pollution of groundwater in Bangladesh: Causes effects and remedies, Dhaka Community Hospital, Dhaka, Bangladesh, 8–12 February.

Violante, P., Pigna, M., 2002. Competitive sorption of arsenate and phosphate on different clay minerals and soils. *Soil Science Society of America Journal*, 66, 1788–1796.

Waltham, C.A., Eick, M.J., 2002. Kinetics of arsenic adsorption on goethite in the presence of sorbed silicic acid. *Soil Science Society of America Journal*, 70, 204-214

Wang, K., Xing, B., 2005. Structural and sorption characteristics of adsorbed humic acid on clay minerals. *Journal of Environmental Quality*, 34, 342-349.

Wang, S., Mulligan, C. N., 2006. Effect of natural organic matter on arsenic release from soils and sediments into groundwater. *Environmental Geochemistry and Health*, 28, 197-214.

Warwick, P., Inam, E., Evans, N., 2005. Arsenic's interaction with humic acid. *Environmental Chemistry*, 2, 119-124.

Weng, L., Riemsdijk, W.H.V., Hiemstra, T., 2009. Effects of fulvic and humic acids on arsenate adsorption to goethite: Experiments and modeling. *Environmental Science & Technology*, 43, 7198–7204.

Figures and Tables

Figure 1. Illustration of the experimental setup for desorption experiments: (1) Sorption of As(III)/As(V) to clay only (kaolinite and illite only) and clay-HA (kaolinite-HA and illite-HA complexes) was carried out either at low (1 µM As) or at high (25 µM As) As concentration, (2) Desorption of As(III) and As(V) from clay only and clay-HA complexes was carried out by addition of either 100 and 500 µM phosphate or 100 and 500 µM silicate, (3) Analysis of dissolved As after 96 h of incubation. It has to be noted that all As(III) related experiments including addition of desorbing agents and sampling were carried out in an anoxic glovebox.

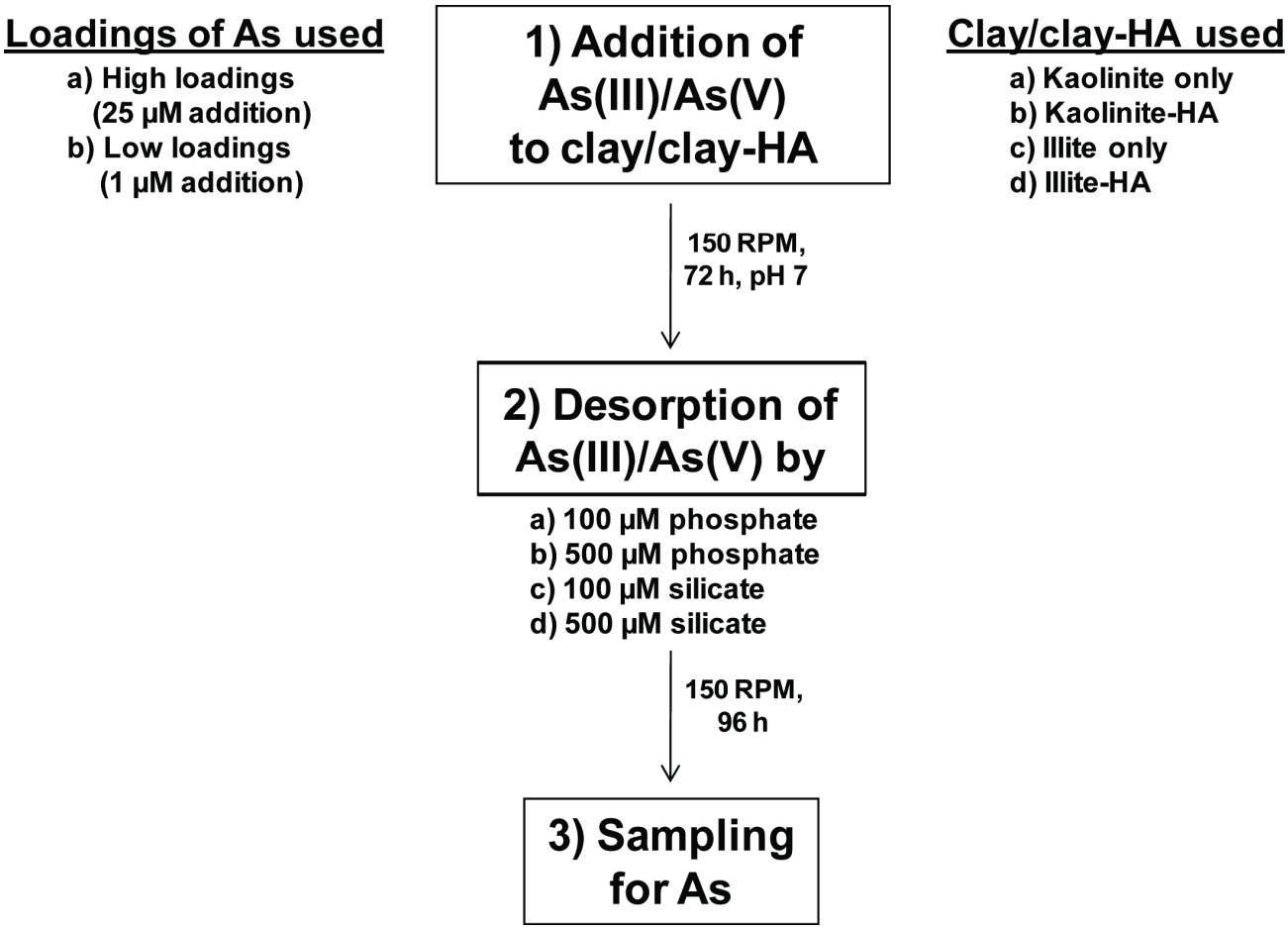

Figure 2. Possible interactions between As(III)/As(V), clay minerals and humic acids (HA): (1) sorption of As(III) or As(V) directly to the clay mineral surface via an inner-sphere complex, (2) binding of As(III) or As(V) to the clay mineral surface via ternary complex formation with Ca^{2+} functioning as cation bridge (outer sphere complex), (3) interactions of As with single, isolated Ca^{2+}-HA or amine groups from humic molecules sorbed to clay surface, and (4) aggregated structure of Ca^{2+}-HA on the clay mineral surface where As(III)/As(V) could bind to form As-Ca^{2+}-HA-clay structures.

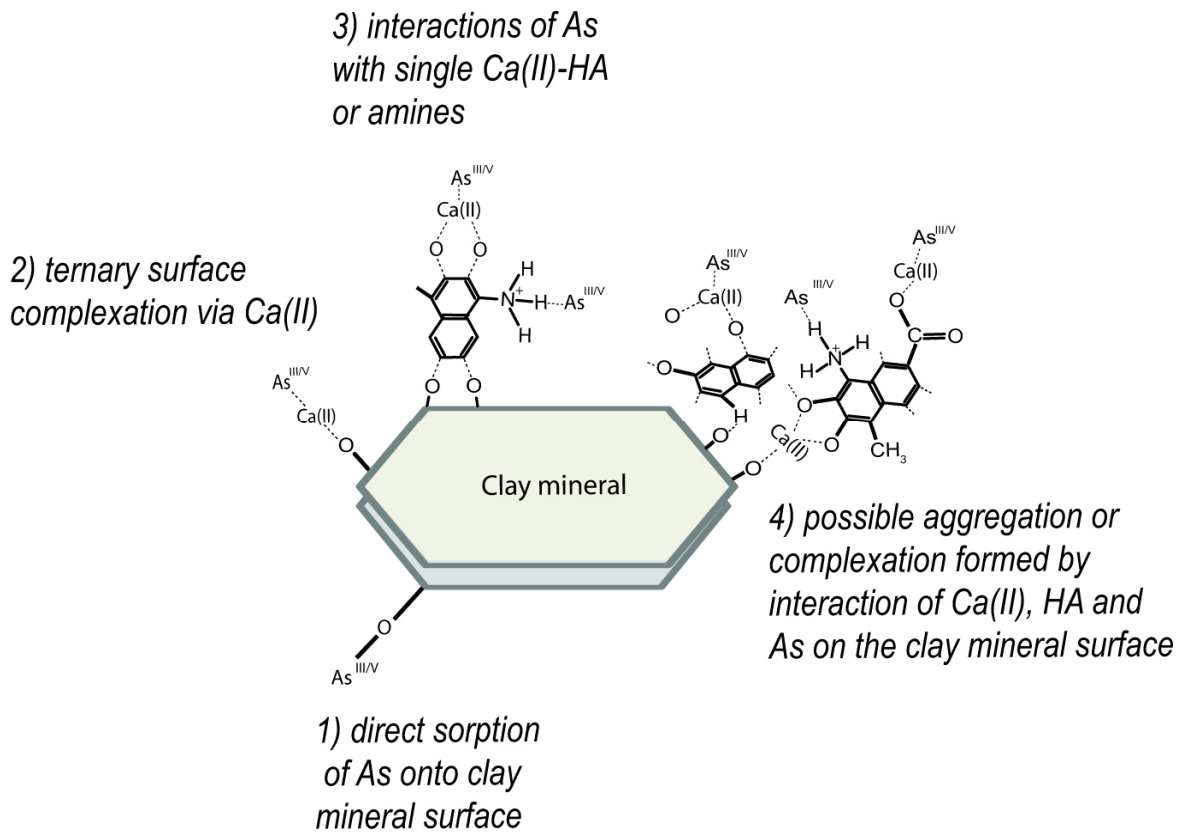

Figure 3. Sorption isotherms of As(III) and As(V) to Kaolinite (Kao – panel A), Illite (IL – panel C), Kaolinite-HA (Kao-HA – panel B) and Illite-HA (IL-HA – panel D). The plots show the As concentration in solution after equilibrium has been reached (after 72 hours) vs the amount of As sorbed to the clay mineral surface in µmol per g of clay mineral present. Error bars represent standard deviation calculated from three parallel samples.

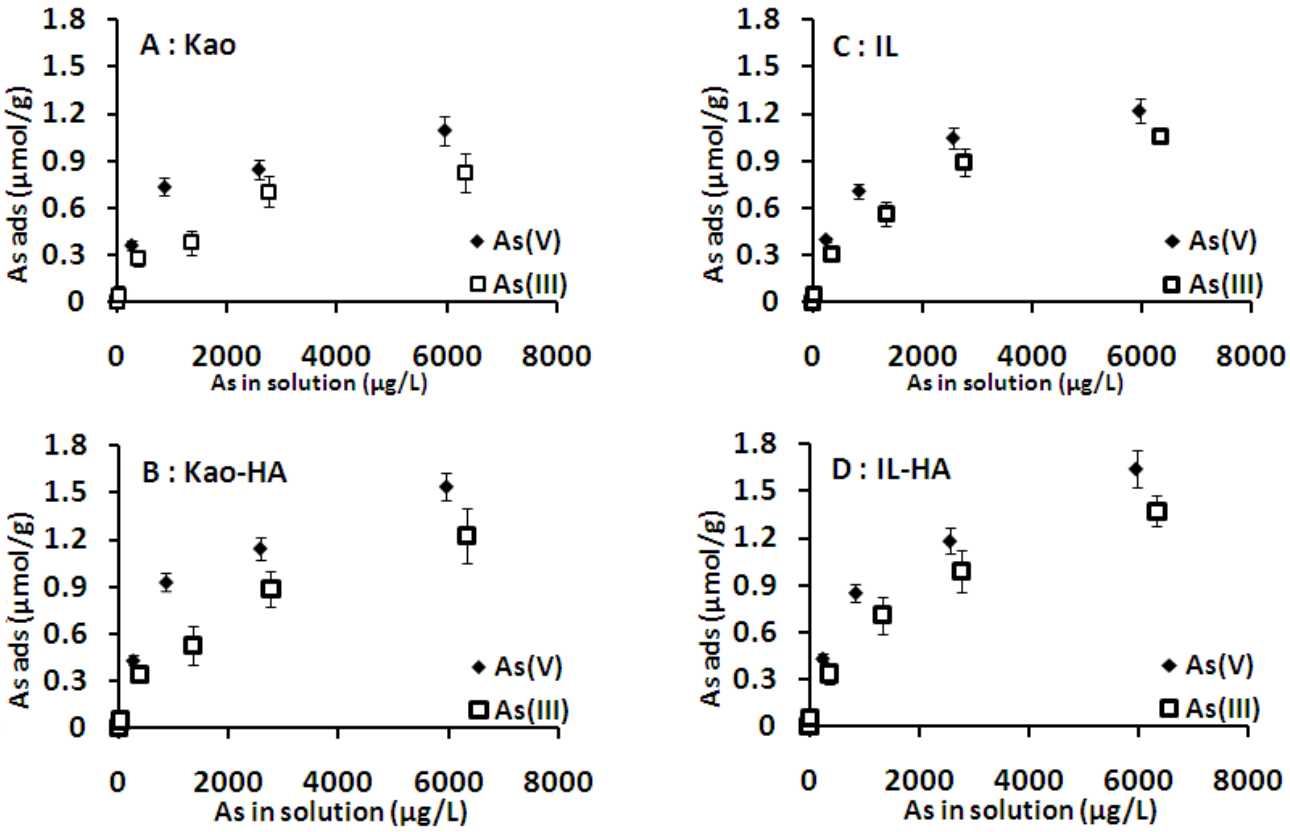

Figure 4. Desorption of As(III) and As(V) from IL, IL-HA, Kao and Kao-HA by 100 or 500 µM phosphate, and by 100 or 500 µM silicate with white bars showing the amount of As sorbed in the absence of phosphate and Si. Panels A-D denote experiments for As desorption with initially added (A) 1 µM As(V), (B) 1 µM As(III), (C) 25 µM As(V) and (D) 25 µM As(III). Error bars represent standard deviation calculated from two parallel samples.

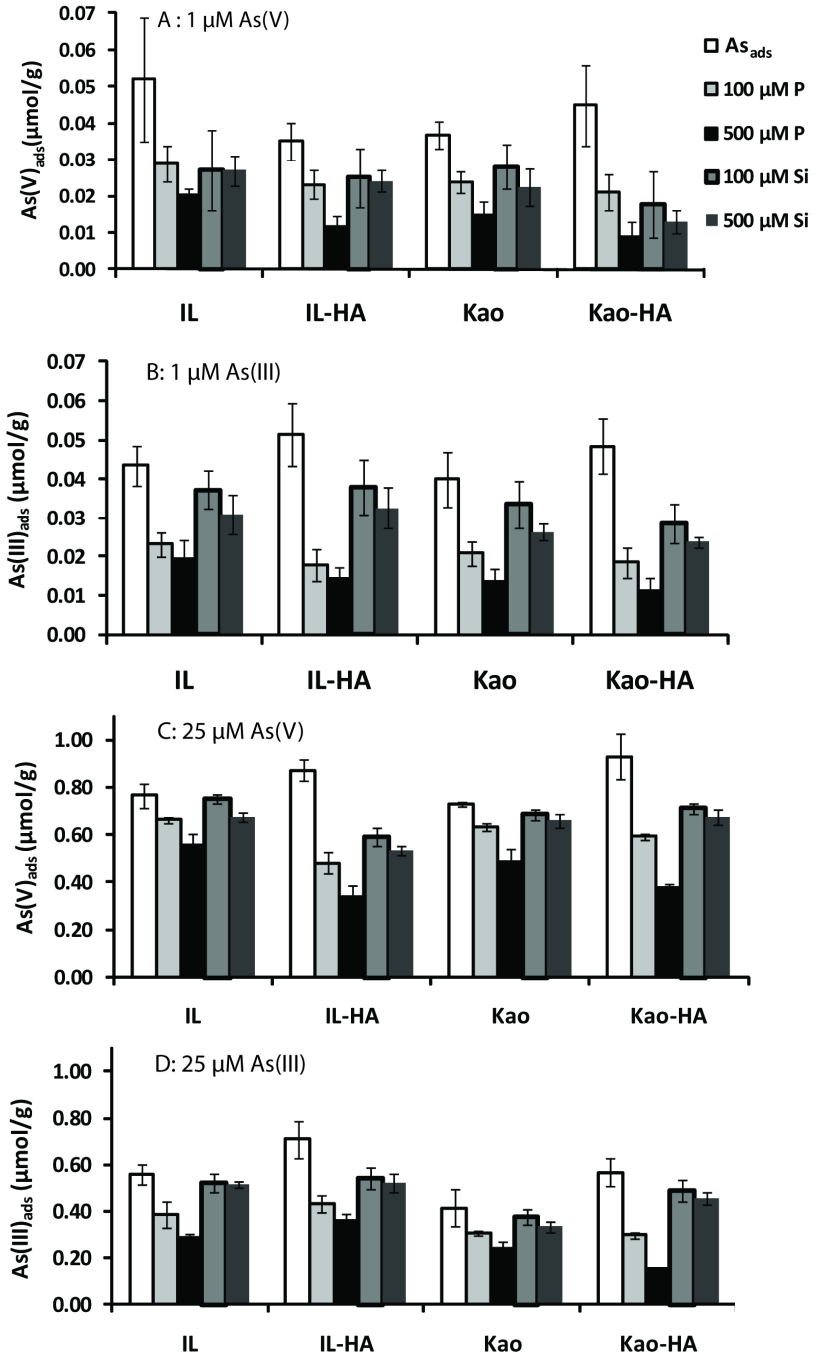

Table 1
Amount of As(III) and As(V) sorbed (µmol As/g clay) upon addition of 100 µM As(III) and As(V) in kaolinite and illite only, and kaolinite-HA and illite-HA complexes.

setups	As(III) µmol/g	As(V) µmol/g
Illite only	1.22 (0.08)	1.06 (0.03)
Kaolinite only	1.09 (0.10)	0.82 (0.12)
Illite-HA	1.65 (0.12)	1.37 (0.10)
Kaolinite-HA	1.54 (0.09)	1.23 (0.18)

The solid: solution ratio was 1: 50 (m/v) 0.5 g clay/clay-HA to 25 ml of 10 mM $CaCl_2$. Background solution in all experiments was 10 mM $CaCl_2$. As was equilibrated with clay/clay-HA for 72 h at 150 RPM. All experiments were carried out in duplicates. Number in parentheses show standard deviations from duplicate measurements.

Table 2
Amount of As(III) and As(V) sorbed (µmol As/g clay) upon addition of 1 µM As(III)/As(V) [low As loadings] and 25 µM As(III))/As(V) [high As loadings] in kaolinite and illite only, and kaolinite-HA and illite-HA complexes.

setups	Low As loadings		High As loadings	
	As(III) µmol/g	As(V) µmol/g	As(III) µmol/g	As(V) µmol/g
Illite only	0.04(0.02)	0.05(0.02)	0.56(0.05)	0.77(0.08)
Kaolinite only	0.04(0.01)	0.04(0.01)	0.41(0.06)	0.73(0.08)
Illite-HA	0.05(0.02)	0.04(0.02)	0.71(0.03)	0.87(0.11)
Kaolinite-HA	0.05(0.02)	0.04(0.02)	0.57(0.04)	0.93(0.09)

The solid: solution ratio was 1: 50 (m/v) 0.5 g clay/clay-HA to 25 ml of 10 mM $CaCl_2$. Background solution in all experiments was 10 mM $CaCl_2$. As was equilibrated with clay/clay-HA for 72 h at 150 RPM. All experiments were carried out in duplicates. Number in parentheses show standard deviations from duplicate measurements.

7

Conclusions and Outlook

NOM is ubiquitous in groundwater/aquifers, and can affect As biogeochemistry on several levels. In this research, we conducted studies under environmentally relevant conditions (neutral pH, relevant concentrations of As, NOM, phosphate and silicate; and relevant minerals such as ferrihydrite, kaolinite and illite, etc) and showed that NOM is intrinsically involved in processes like complexation, sorption, desorption and transport of As.

Formation of ternary colloids and complexes of OM, As and Fe

NOM can leach Fe from Fe(III) minerals to form Fe-NOM colloids or complexes (Liang et al., 1992; Sharma et al., 2010). These complexes can further interact with free As in soil solution to form ternary As-Fe-NOM colloids and complexes (Sharma et al., 2010). For the first time, we systematically demonstrated the mechanism of formation of Fe-NOM and As-Fe-NOM colloids/complexes at environmentally relevant conditions (pH 7, ferrihydrite and relevant concentrations of NOM and As) (Chapter 2). Interestingly, when we incubated just As with NOM, there was no As present in the colloidal or the dissolved fraction. Previously, it was supposed that As can use metals or positively charged functional groups (such as amines) at neutral pH in humic molecules as binding agents to

complex with NOM (Saada et al., 2003; Ritter et al., 2005). It was also suggested that As can bind directly to NOM (Buschmann et al., 2006). From our research it is clear that As can only bind to NOM in presence of a cation bridge such as Fe(III). Although Fe(III) was used as a cation source in our systems, in nature, other divalent and trivalent cations (i.e. Ca^{2+}, $Mn^{2+/4+}$, Mg^{2+}, and Al^{3+}) are present as well and have to be considered for future studies. These different cations offer a vast possibility for the formation of ternary As-metal-NOM colloids/complexes. The inability of As to bind directly to NOM (without metal bridges) denotes that As binding to FH-NOM colloids and Fe-NOM colloids/complexes are most probably the most common mechanisms of association of As with NOM in the environment. The rate of transport of these complexes, their toxicity and their possible uptake by microbes (or even humans) compared to free As is however, not known but this probably depends upon the size, charge and bioavailability of the NOM fraction in which As is bound to. In addition, we demonstrated the existence of Fe-NOM using Mössbauer spectroscopy and As-Fe-NOM complexes/colloids using ATR-FTIR spectroscopy. This method provides an original approach to identify metal-NOM associations in nature as well as in laboratory studies. However, further research using synchrotron-based FTIR measurements in combination with EXAFS (for bonding environment), scanning transmission x-ray microscope (STXM), and STXM in combination with fluorescence yield detection, and/or analytical transmission electron microscopy (TEM) (for localization of As, Fe and NOM in As-Fe-NOM colloids) could enable higher resolution measurements to understand binding mechanisms in Fe-NOM and As-Fe-NOM colloids/complexes. Improvement in cyclic voltammetric resolution (or detection limit) could also allow an alternative method of identification of As-metal-NOM complexes.

This research study leaves as well many open questions. Although the presented experiments mainly focused on As(V)-Fe-NOM, the investigation of As(III)-Fe-NOM complexes with similar methodologies would be of great interest as As(III) is considered to be even more mobile and toxic

compared to As(V). In order to understand the stability of such complexes in the environment, the long term fate of As-Fe-NOM colloids/complexes should be further evaluated. This could be followed at different pH and ionic strength with titration experiments. The experimental setup could as well be broadened towards the use of other organic material such as fulvic acids or even solid-phase humics, both of which are environmentally relevant fractions of NOM found in soils/aquifers. To understand the forementioned processes in an environmentally relevant scenario in laboratory studies, the experiments could be carried out with soil organic matter (SOM) extracted from As-contaminated soils. By means of this approach i) pre-existing As-metal-SOM colloids/complexes can be identified in natural systems or ii) formation of As-metal-SOM complexes can be determined using methods presented in this particular study.

Influence of organic matter on As retention and transport

Apart from complexation of As, NOM also actively affects sorption, transport and mobilization of As (Redman et al., 2002; Ko et al., 2004, 2006). In chapter 3, we demonstrated the effect of different fractions of NOM (humic acids (HA) vs fulvic acids (FA)) on As sorption and desorption in ferrihydrite-coated sand. All fractions and concentrations of NOM used caused (i) lower amount of As sorption onto ferrihydrite-coated sand, (ii) faster transport of As in breakthrough experiments, and (iii) higher extent of As desorption in desorption experiments compared to NOM-free systems. Increasing concentrations of NOM and decreasing molecular weight (i.e. FA has a lower molecular weight than HA) had a pronounced effect on the desorption and transport of As. A major outcome of the present study was the strong effect of SOM on sorption and (im)mobilization of As in ferrihydrite-coated sand systems in batch and column experiments. SOM was extracted from a forest soil by shaking with DI

water. This method is comparable to the process of solubilization and leaching of NOM from soil/sediments by infiltrating groundwater/rainwater. The concentration of SOM used was 11.5 mg C/L which is five times lower than the highest concentration (50 mg C/L) of FA and HA used in our other column studies carried out in parallel (chapter 2). Additionally, the extracted SOM lacked competing agents such as phosphate and silicate which can effectively desorb As or compete with As bound to minerals. In both As(III) and As(V) containing systems, SOM transported As equally fast as FA, and desorbed As to a similar extent as FA. This shows that fresh NOM infiltrating from surface waters during rainfall can lead to rapid As mobilization. Drinking water problems with respect to As, often occur in monsoon influenced environments such as South East Asia. Therefore, this process (i.e. leaching and infiltration of NOM into the subsurface layers) is of high relevance in such systems. This study also suggests that results solely based on experiments obtained with purified NOM would possibly underestimate the role of NOM in the As-contaminated aquifers. Conclusions from other As-NOM interaction studies are mostly based on experiments with purified HA and FA (Redman et al., 2002; Ritter et al., 2005; Ko et al., 2007). Furthermore, we also showed for the first time, the formation of ternary As-Fe-NOM complex/colloids in flow-through systems. We quantified colloids/complex fraction from eluates of the column (breakthrough) experiments in NOM-free vs. NOM containing systems using dialysis and centrifugal filtration methods described in chapter 2. We found appreciable amounts of As and Fe in the dissolved fraction in columns with NOM signifying the possibility of ternary colloids/complex formation. In NOM-free columns, no As or Fe was present in the dissolved fraction suggesting that a cation bridge such as Fe could be essential for the interaction between As and NOM also in flow- through systems. The formation of these complexes/colloids should be tested in column systems where SOM extracted from As-contaminated aquifers to fully understand how important these complexes/colloids are in environmentally relevant systems.

Although these results improved the knowledge of NOM-Fe mineral-As geochemistry, further work is necessary to gain more understanding of effect of NOM on As (im)mobilization in natural systems. As-contaminated aquifers are complex mixtures of different minerals including Fe oxides/Fe oxides-NOM, and clay/clay-NOM complexes. Column experiments with these relevant minerals/mineral-NOM phases, mixed in different ratios, might provide a more realistic view of As transport in natural systems (i.e. aquifers). Besides, the SOM from forest soil represented a good model to gain a first hand understanding of As transport by natural organic matter. However, such studies should be also conducted with SOM extracted from As-contaminated aquifers to give an accurate representation of As sorption and transport in the environment. Moreover, the behavior of NOM depends on the cation type and concentration that is present in soil solution. Background solutions of different concentrations and cation type can be prepared for column experiments and their effect on As transport can be quantified. As(III) and As(V) co-exist in many geochemical systems and thus desorption/breakthrough experiments of As(III)/As(V) in the same system would give a comparative understanding of the two species in column systems. Flow interruption or changes in flow rates which represent inhomogenous conditions in groundwater (i.e. events such as high rainfall and flooding followed by periods of dryness which can change groundwater infiltration rates) can be applied to columns to evaluate how As transport/mobilization is affected by such parameters. To improve on the column set-ups, a tank experiment could be conducted with sediments from As-contaminated aquifers. Such a setup will give even a better representation of flow-through systems in the environment. Conducting column/tank experiments with aquifer materials and SOM extracted from different As-contaminated regions could give a comparative understanding of As mobilization in different aquifers. In addition, redox reactions are important components of NOM-Fe mineral-As interactions. Specially, wet-dry cycles (high rainfall followed by a period of dryness) in soils could switch redox conditions (oxic while dry and sub-oxic/anoxic while wet) causing changes in dissolved organic carbon content in soils (Fierer and

Schimel, 2002) which could in turn alter sequestration or mobilization of As. Therefore, column studies to understand how interactions of reduced humics with Fe minerals in presence of As in flow-through systems will affect As (im)mobilization should be studied. This could give an indication of how NOM from reduced zones (or in reduced conditions) will interact with iron minerals and As upon changes in groundwater conditions.

Effect of NOM sorption on clay minerals in (im)mobilizing As

In our studies, NOM not only affected As-Fe mineral interactions but also interactions of As with clay minerals. We found that NOM sorption to clay minerals increases the number of binding sites available for contaminants such As to bind to (Chapter 5). This was quantified by conducting titration experiments and surface complexation modeling of clay and clay-NOM complexes. Although it was already known that NOM enhances the binding site density of clay minerals, there was only one study that showed increased As sorption to clay-NOM complexes (Saada et al., 2003). By following As sorption to clay/clay-NOM complexes, we found that the binding of both As species to clay-NOM complexes was higher than in clay only systems (Chapter 6). However, the desorption of As by the addition of phosphate and silica at environmentally relevant levels was relatively higher in clay-NOM complexes than in clay only systems, particularly at high As loadings. These results clearly show that NOM can enhance As uptake, but the release is equally higher, suggesting that the binding between As to clay-NOM complexes might be slightly weaker than As binding directly to clay surface (particularly at high As loadings). Also, phosphate and silica were found to desorb more than 50% As from clay/clay-NOM surfaces. This outcome raises strong environmental concerns since many paddy fields lie in South and South East Asia lie in As-contaminated areas which contains large amounts of clay,

NOM, silica and phosphate. Effective desorption of As by phosphate and silica in these systems means that As could potentially end up in the crops that are cultivated in the region or in groundwater.

The studies on the interactions of As with clay vs clay-NOM also raised a number of ideas for further research. As we showed in the chapter 2 and 3, NOM can leach metal ions from mineral surfaces which can form ternary colloids/complexes with As. NOM interactions with clay surfaces can similarly leach out cations such as Al^{3+} which could promote the formation of As-Al(III)-NOM colloids/complexes. With regards to the binding/desorption mechanism of As to clay-NOM, prevailing uncertainties (i.e. does As bind to clay via a cation bridge such as Ca^{2+}, or does it prefer binding to single/aggregated molecules of Ca^{2+}-NOM bound to clay) require further research. Titration experiments and XAFS measurements of As-clay and As-NOM-clay could give a better understanding of the stability and binding mechanisms of As-clay and As-NOM-clay systems respectively. To date, the transport of As through clay/clay-NOM systems remains unclear although clay and clay-NOM associations are equally important in natural systems as Fe minerals. Following As breakthrough in columns or tank filled with synthetic or natural clay/clay-NOM mixtures will allow to understand the transport of As in aquifers. Possible redox reactions that could occur during clay-NOM and As-NOM-clay interactions have also not been studied widely so far. It is possible that clay rich in redox sensitive elements such as Fe (e.g. nontronite contains >30% Fe) or Mn could undergo redox reactions with NOM and consequently affect (im)mobilization of As.

Overall, the presented study improved the knowledge on interactions of NOM with respect to As sorption, transport and desorption in minerals. NOM plays an important role in contaminant transport in general. Thus, some of the novel ideas and techniques used in this study can be extended to study other major contaminants such as heavy metals or nitroaromatic compounds present in soils and aquifers.

Arsenic in drinking water is a major environmental problem in the world. Groundwater contamination of As is intricately connected by geochemical interactions to minerals and NOM. From this research we learned that the processes related to As sorption and release in the subsurface can be more complex than thought as it is affected by a multitude of geochemical factors (pH, mineral type, ionic strength, presence of competing ions, type and concentration of NOM, loading capacities to minerals etc). In the environment, seasonal variations (i.e. periods of dryness followed by torrential monsoonal rainfall) could potentially affect NOM-mineral-As interactions by leaching NOM or by changing redox patterns in soils. Similarly, climatic effects (global warming which can cause erratic weather such as increased intensity of monsoonal rainfall), and agricultural practices (irrigation, use of fertilizers) could strongly impact the As-mineral-NOM geochemistry in these contaminated areas. All these factors need to be considered to understand and counter As contamination and therefore, ongoing research on As contamination is clearly necessary.

References

Buschmann, J., Kappeler, A., Indauer, U., Kistler, D., Berg, M., Sigg, L. Arsenite and Arsenate Binding to Dissolved Humic Acids: Influence of pH, Type of Humic Acid, and Aluminum. *Environmental Science & Technology*, **2006**, *40*, 6015-6020.

Fierer, N., Schimel, J.P. Effects of drying–rewetting frequency on soil carbon and nitrogen transformations. Soil Biology and Biochemistry, **2002,** *34*, 777–787.

Ilwon, K., Ju-Yong, K., Kyoung-Woong, K. Arsenic speciation and sorption kinetics in the As–hematite–humic acid system. *Colloids and Surfaces A:Physicochemical and Engineering Aspects*, **2004**, *234*, 43-50.

Ilwon, K., Davis, A. P., Ju-Yong, K., Kyoung-Woong, K. Effect of contact order on the adsorption of inorganic arsenic species onto hematite in the presence of humic acid. *Journal of Hazardous Materials*, **2006**,*141*, 53-60.

Liang, L., McCarthy, J. F., Jolley, L. W., McNabb, J. A., Mehlhorn, T. L. Iron dynamics: transformation of Fe(II)/Fe(III) during injection of natural organic matter in a sandy aquifer. *Geochimica Et Cosmochimica Acta*, **1992**, *57*, 1987-1999.

Redman, A. D., Macalady, D. L., Ahmann, D. Natural organic matter affects arsenic speciation and sorption onto hematite. *Environmental Science & Technology*, **2002**, *36*, 2889-2896.

Ritter, K., Aiken, G. R., Ranville, J. F., Bauer, M., Macalady, D. L. Evidence for the aquatic binding of arsenate by natural organic matter-suspended Fe(III). *Environmental Science & Technology*, **2006**, *40*, 5380-5387.

Saada, A., Breeze, D., Crouze, C., Cornu, S., Baranger, P. Adsorption of arsenic(V) on kaolinite and on kaolinite-humic acid complexes – Role of humic acid nitrogen groups. *Chemosphere*, **2003**, *51*, 757-763.

Sharma, P., Ofner, J., Kappler, A. Formation of binary and ternary colloids and dissolved complexes of organic matter, Fe and As. *Environ. Sci. and Technol.* **2010**, *44*, 4479-4485.

8

Summary

The biogeochemistry of As is largely affected by interactions with natural organic matter (NOM) and various minerals in the environment. NOM, or humic substances, are ubiquitous in the environment, both in aquatic or terrestrial systems. Although a lot of research has been focused on the influence of NOM on As biogeochemistry, our present knowledge is still very limited. Therefore, the overall goal of this study was to investigate different aspects of As-NOM interactions, particularly the role of NOM in As complexation and the effect of NOM on As sorption and transport in Fe minerals and clays. Formation of Fe-NOM and As-Fe-NOM colloids/complexes as well as sorption of NOM and As to ferrihydrite-coated sand and clay minerals were studied in batch systems. Using flow-through systems, the effect of different concentrations and types of NOM on As transport/desorption systems. In these systems, the formation of binary/ternary colloids and complexes of As and NOM vs. As, Fe and NOM was also studied.

The mechanisms of As transport in groundwater are still debated in literature; i.e. in which form is As transported – colloidal, complexed, or as a free anion? In previous studies it has been shown that As complexes with NOM via metal bridges such as Al^{3+}, $Mn^{2+/4+}$, Mg^{2+}, Ca^{2+} etc. Estimation on the particular importance of Fe(III) as a cation bridge was previously investigated but had never experimentally demonstrated. In this thesis (chapter 2), we investigated whether Fe(III) indeed plays a significant role in complexing As to organic matter. For this purpose, ferrihydrite (a naturally relevant

iron mineral) was incubated with peat humic acid (a model NOM) in order to produce Fe-NOM colloids/complexes. This step was followed by addition of As to form As-Fe-NOM colloids/complexes. Finally the As-Fe-NOM colloids/complexes were dialysed to separate free As from colloidal/complexed As. The As-Fe-NOM colloids/complexes remaining inside the dialysis bags were again subjected to centrifugal filtration (to separate colloids from complexes) to quantify the amount of dissolved (complexed) As, Fe and NOM compared to the colloidal part. The results showed that a small but significant part of the added As was present in complexed form (i.e. associated with Fe-NOM complexes). For comparison, As was incubated with NOM only (without Fe) and then dialysed in the same manner. These experiments showed that As did not bind to NOM in the absence of Fe(III). The inability of As to bind directly to NOM (without metal bridges) means that formation of As-Fe(III)-NOM complexes are possibly the most common mechanisms of As association with NOM in the environment and can play an important role in transporting As in As-contaminated aquifers rich in NOM and Fe(III) minerals.

To determine the effect of NOM on transport of As under conditions more relevant to the environment, additional experiments were performed in flow-through set-ups (chapter 3). In these experiments, the transport and desorption of As (breakthrough) through columns filled with ferrihydrite-coated sand was carried out. As was quantified in the effluent and compared to either the amount of arsenic in the influent (as in breakthrough experiments) or to the amount of As pre-sorbed to ferrihydrite-coated sand (in case of desorption experiments). The breakthrough and desorption experiments were also carried out with soil organic matter (SOM) extracted from a nearby forest soil in order to compare the influence of SOM on As transport as compared to purified organic matter (humic acids (HA) and fulvic acids (FA)). The results showed that the smaller molecular weight fraction (FA) transported As faster than HA through ferrihydrite-coated sand. FA also desorbed As to a greater extent than HA in desorption

experiments. Due to the smaller molecular size of FA, there is lower steric hindrance upon interaction with mineral surfaces and therefore, FA can better interact with the surface sites of minerals. In addition, it can also desorb As from binding sites that are otherwise inaccessible to HA thereby increasing the desorption/transport of As. Between the two As species, As(III) was transported faster in breakthrough experiments compared to As(V) and desorbed twice as much than As(V) in desorption experiments, both in presence and absence of NOM. Most importantly, SOM transported As equally fast and desorbed As to a similar extent as 50 mg C/L of FA although the concentration of SOM (~11.5 mg C/L) used was about five folds lower than the highest concentration of FA used (50 mg C/L). SOM also contained very low concentrations of phosphate and silica, which can compete with or desorb arsenic in the environment. SOM is the fraction that is mobilized by rainfall or groundwater flow (leaching and solubilising organic carbon from mineral phases) and is thus relevant to environment. In contrast to SOM, HA and FA that were used for the experiments were extracted by repeated addition of acids and bases and therefore, are significantly less representative of what we find in soil/aquifers. Compared to HA and FA, the environmentally relevant remains of polar groups in SOM may strongly affect the mobilization of As. These findings might indicate that the effect of SOM on contaminant transport in nature is underestimated. Besides, it also signifies the fact that studying contaminant-mineral interactions in the presence of purified HA and FA only, provides limitations on studying the biogeochemistry of contaminants. Additional experiments were carried out to investigate whether ionic strength affects the transport/desorption of As (chapter 4). The change in ionic strength by one order of magnitude (from 5 mM to 100 mM NaCl background) showed slight but significant decrease in As desorption in presence of NOM. In absence of NOM, there were no changes in the amount of As desorbed upon changing ionic strength. However, this probably depends on the kind of ion present (divalent or trivalent ions) in the system. Additionally, an extreme increase in ionic strength (i.e. from 100 mM to 1 M) might severely affect the geochemistry of the system.

By following methods from chapter 2, we also followed the formation of As-Fe-NOM complexes and colloids in column experiments where NOM and As was injected through ferrihydrite-coated sand (chapter 3). Selected samples from As breakthrough experiments in presence of NOM (fulvic acid (FA), humic acid (HA) and SOM) and NOM-free systems were separated into colloidal and dissolved fraction using dialysis and centrifugal filtration. A small proportion of As was found in the dissolved fraction in systems containing FA, HA and SOM which shows that different forms of NOM are able to complex As.

Apart from ferric minerals/ferrihydrite, clay is another mineral commonly found in soil/aquifers and can play a major role in (im)mobilzation of As. The As contaminated areas in South East Asia are located in regions where rivers deposit a lot of alluvium that is enriched in silicate material. Clays are weathering products of these silicate deposits. The interactions of clay with NOM and As with clay-NOM complexes is poorly understood. Therefore, firstly, we identified and quantified the reactive functional groups on kaolinite and illite surfaces that are responsible for NOM and metal sorption by sorption and titration experiments followed by surface complexation modeling (chapter 5). We found that sorption of HA to clay minerals increases the number and concentration of surface sites for potential sorption of As. We then confirmed this by carrying out sorption experiments where As was added to clay vs clay-HA complexes (chapter 6). Previously, it was shown that NOM can effectively compete with As for sorption sites in clay and Fe oxides. However, we found that this is not always the case. Our experiments showed that in the presence of divalent cation such as Ca^{2+}, which can act as a cation bridge between NOM and clay minerals, as well as between As and NOM, sorption of As to clay increases. Sorption of both As(III) and As(V) were higher for Kaolinite-HA and Illite-HA complexes compared to the respective clay only systems. Between As(III) and As(V), as opposed to iron minerals, As(V) sorbed to a greater extent than As(III) in both clay and clay-HA systems. When As was desorbed by phosphate and silica,

two compounds which can effectively compete with As, we found that phosphate is more effective than silica in desorbing As from all systems confirming findings from literature. Interestingly, in most cases, in our experiments, the relative amount of As desorption is also higher from clay-HA compared to clay only systems. This shows that As is weakly bound to clay-HA complexes, possibly only via outer-sphere ternary complexes with Ca^{2+} as cation bridge. The results show that, in the environment, the sorption of contaminants like As depends upon what kind of ion is present in the background solution, the type of mineral surface, presence of competitive agents and sorption of NOM to mineral surfaces. For desorption, in addition to previously mentioned parameters for sorption; the type and concentration of desorbing agent and the initial loading of As to clay/clay-HA surfaces are important factors which can affect desorption processes.

Overall, the results from the experiments carried out in this thesis showed the multiple roles and effects NOM can have on contaminant transport (i.e. of As). NOM can react with Fe-minerals forming Fe-NOM complexes/colloids and mobilize As as As-Fe-NOM complexes/colloids, can enhance both transport and desorption of As in ferrihydrite flow-through systems and not only compete but also enhance sorption of As by sorbing itself to clay mineral surfaces. The methods, characterization techniques and ideas used in this project can also be extended to study effect of NOM in complexation, sorption and transport of other contaminants such as heavy metals, chlorinated and nitroaromatic compounds etc.

Although we were able to answer key questions regarding the effect of NOM on As geochemistry, there were still some open questions which remain to be answered. The stability and mobility of the binary/ternary complexes could be determined by forming the complexes and colloids at different geochemical conditions (varying pH, ionic strength etc). Whether As(III) or As(V) is more likely to form complexes with Fe-OM can be demonstrated by forming As(III)-Fe-NOM complexes/colloids

following protocols from chapter ‘2’ and comparing it with As(V)-Fe-NOM. With regards to breakthrough and desorption studies in column systems, if (and how) iron minerals coated with NOM will influence As transport compared to NOM-free systems can be studied by injecting As solutions into columns filled with ferrihydrite-NOM-coated sand vs ferrihydrite-coated sand. Moreover, the transport studies can also be extended to determine breakthrough/desorption of As from clay/iron oxide mixtures since both mineral phases are important in nature. Additionally, flow rates can be changed or even flow interruptions can be applied to such column systems since stoppage of flow can affect transport of As and also interactions of NOM with the minerals in the columns.

In case of clay minerals, sorption of As to clay-FA or clay-SOM complexes can be studied to determine how different NOM coatings to clay minerals can affect As sorption. Moreover, the sorption of NOM depends strongly on the type of cation (Ca^{2+}) that has been used to homoionize the clay minerals, therefore, ions such as Na^{+}, Al^{3+}, Fe^{3+} or even mixed ions can be used since these are also environmentally relevant in nature and actively participate in ion exchange with clay mineral surfaces.

Zusammenfassung

Die Arsen-Biogeochemie wird in der Umwelt maßgebend durch die Interaktion mit natürlichem organischen Material (NOM) und mit verschiedenen Mineralen bestimmt. NOM oder Huminstoffe sind allgegenwärtig in der Umwelt, sowohl in aquatischen wie auch in terrestrischen Systemen. Trotz zahlreicher Forschungsarbeiten zum Einfluss von NOM auf die Arsen-Biogeochemie, ist unser gegenwärtiges Wissen noch sehr eingeschränkt. Daher war die Zielsetzung dieser Arbeit, die verschiedenen Aspekte der As-NOM Interaktion besser zu untersuchen und insbesondere die Rolle von NOM bei der Arsenkomplexierung und auf die Arsensorption und den Arsentransport in Gegenwart von Eisenmineralen und Tonmineralen zu bestimmen. Die Bildung von Fe-NOM- und As-Fe-NOM-Kolloiden und Komplexen, sowie die Sorption von NOM und As an Ferrihydrit-beschichteten Sand und an Tonminerale wurden in Batchexperimenten untersucht. In Durchflusssystemen wurde der Effekt verschiedener NOM-Konzentrationen und -Arten auf den Arsentransport und die Arsendesorption bestimmt. Auch die Bildung binärer und ternärer Komplexe von As und NOM bzw. As, Fe und NOM war Gegenstand der Untersuchungen.

Die verschiedenen Mechanismen des Arsentransportes im Grundwasser werden in der Literatur kontrovers diskutiert, unter anderem gehen die Meinungen über die transportierte Form des As, kolloidal, komplexiert oder als freies Anion, auseinander. In früheren Arbeiten konnte gezeigt werden, dass As über Metallbrücken wie z. B. Al^{3+}, $Mn^{2+/4+}$, Mg^{2+}, Ca^{2+} etc. an NOM komplexiert. Die Bedeutung von Fe(III) als Kationenbrücke wurde zwar bereits untersucht, konnte aber bisher nicht experimentell nachgewiesen werden. In der hier vorliegenden Arbeit (Kapitel 2) haben wir untersucht, ob Fe(III) tatsächlich eine signifikante Rolle bei der Komplexierung von organischem Material spielt. Dazu wurde Ferrihydrit, ein umweltrelevantes Eisenmineral, mit Torfhuminsäuren als typisches NOM inkubiert, um Fe-NOM-Kolloide/-Komplexe zu synthetisieren. Anschließend wurde As zugegeben, um

As-Fe-NOM-Kolloide/-Komplexe zu erhalten. Schließlich wurden die As-Fe-NOM-Kolloide/-Komplexe dialysiert, um freies As von den As-Fe-NOM-Kolloiden/-Komplexen zu trennen. Die in den Dialysebeuteln zurückgebliebenen As-Fe-NOM-Kolloide/-Komplexe wurden zentrifugalfiltriert (um Kolloide von Komplexen zu trennen) und die Konzentration an gelöstem (komplexiertem) As, Fe und NOM wurde mit der kolloidalen Phase vergleichen. Es konnte gezeigt werden, dass ein kleiner aber signifikanter Anteil des zugegebenen As in komplexierter Form vorlag, z.B. in Verbindung mit Fe-NOM Komplexen. Zu Vergleichszwecken wurde As nur mit NOM und ohne Fe inkubiert und dann auf gleiche Weise dialysiert. Dieszeigte, dass As in Abwesenheit von Fe(III) nicht an NOM bindet. Da As ohne Metallbrücken nicht direkt an NOM binden kann, ist die Bildung von As-Fe(III)-OM-Komplexen möglicherweise die häufigste Form von As und NOM Verbindungen in der Umwelt. Diese Ternärekomplexe spielen somit eine wichtige Rolle beim Transport von As in arsenkontaminierten NOM- und Eisenmineral-reichen Grundwasserleitern.

Um die Auswirkung von NOM auf den Arsentransport unter umweltrelevanten Bedingungen fest zustellen, wurden weitere Experimente in Durchflusssystemen durchgeführt (Kapitel 3). In diesen Experimenten wurde der Transport von Arsen durch Säulen, die mit Ferrihydrit beschichtetem Sand (Durchbruch) beladen waren, und die Desorption von Arsen von Ferriyhdrit beschichtetem Sand verfolgt. Die Menge an As wurde im Abfluss quantifiziert und mit der Konzentration im Zufluss (bei Durchbruchexperimenten) oder der Menge des an den Ferrihydrit beschichteten Sand vorsorbierten As (bei Desorptionsexperimenten) verglichen. Die Druchbruch- und Desorptionsexperimenten wurden zusätzlich in Gegenwart von organischem Bodenmaterial (soil organic matter, SOM) durchgeführt, welches aus dem Boden eines nahegelegenen Waldes extrahiert worden war. Es wurde der Einfluss von SOM auf den Arsentransport im Vergleich zu aufbereitetem organischen Material (Huminsäuren (HA) und Fulvinsäuren (FA)) untersucht. Die Ergebnisse zeigten, dass die Fraktion mit dem geringeren

Molekulargewicht (FA) As schneller durch den Ferrihydrit beschichteten Sand transportierte als HA. In den Desorptionsexperimenten desorbierte FA As ebenfalls stärker als HA (Kapitel 3). Aufgrund der geringeren Molekülgröße der FA können diese besser mit den funktionellen Gruppen an Mineraloberflächen interagieren, da die sterische Hinderung bei der FA-Mineral-Interaktion geringer ist als bei der HA-Mineral-Interaktion. Dies zeigt, dass die Bindung von As an Mineraloberflächen sehr effektiv durch FA verhindert werden kann. Zusätzlich können FA mit As um Oberflächen bindungsstellen konkurrieren und diese von Mineraloberflächen lösen, die für HA unzugänglich sind. Dies führt zu einer erhöhten Desorption und einem besseren Transport von As. Von den beiden Arsenspezies wurde As(III) in Durchbruchexperimenten schneller transportiert als As(V) und desorbierte doppelt so stark wie As(V) in Desorptionsexperimenten, sowohl in der Gegenwart wie in Abwesenheit von OM. Das bedeutendste Ergebnis aber ist, dass SOM As genauso schnell transportierte und in einem ähnlichen Ausmaß desorbierte wie 50 mg C/L FA, obwohl die benutzte SOM Konzentration (~11.5 mg C/L) ungefähr fünfmal niedriger war als die höchste benutzte FA Konzentration (50 mg C/L). Das extratierte SOM enthielt nur geringe Konzentrationen an Phosphat und Silizium, welche in der Umwelt mit As um die Mineralbindungsstellen konkurrieren und As desorbieren können. Da SOM die Fraktion ist, die durch Regen oder Grundwasserfluss (wobei organischer Kohlenstoff aus der Mineralphase auswaschen und in Lösung gebracht wird) mobilisiert wird, ist sie daher sehr relevant in der Umwelt. Im Gegensatz zu SOM wurden die für das Experiment benutzten HA und FA Fraktionen durch wiederholte Zugabe von Säuren und Basen extrahiert und sind daher bedeutend weniger repräsentativ für das organische Material in natürlichen Böden/Grundwasserleitern. Im Vergleich zu HA und FA könnten die umweltrelevanten Reste von polaren Gruppen in SOM die Arsenmobilisierung stark beeinflussen. Diese Ergebnisse könnten darauf hinweisen, dass die Auswirkung von SOM auf den Schadstofftransport in der Natur bisher unterschätzt wurde. Zusätzlich bedeutet es, dass die Untersuchung von Schadstoff-Mineral-Interaktionen in der Gegenwart von nur

aufbereiteten HA und FA eine Limitierung bei der Erforschung der Biogeochemie von Schadstoffen darstellt.

In weiteren Testreihen wurde untersucht, ob die Ionenstärke einen Einfluss auf den Transport und die Desorption von Arsen hat. Eine Veränderung der Ionenstärke um eine Zehnerpotenz (von 5 mM NaCl auf 100 mM NaCl in der Hintergrundslösung) hatte keine signifikanten Änderungen im Arsentransport und der Arsendesorption in Gegenwart oder Abwesenheit von NOM zur Folge. Allerdings hängt dies wahrscheinlich von der Art der im System anwesenden Ionen ab (zweiwertige oder dreiwertige Ionen). Zusätzlich könnte eine extreme Zunahme der Ionenkonzentration (z.B. von 100 mM auf 1 M) die Geochemie des Systems beeinträchtigen.

Im nächsten Kapitel (3) wurde die Bildung von As-Fe-OM-Komplexen und -Kolloiden ebenfalls in Säulenexperimenten verfolgt, die mit Ferrihydrit beschichtetem Sand gefüllt waren. Ausgewählte Proben der Arsendurchbruchexperimente in Anwesenheit von OM (Fulvinsäuren (FA), Huminsäuren (HA) und SOM) und von OM-freien Systemen wurden unter Verwendung der gleichen Methode wie in Kapitel ‚2' in die kolloidale und gelöste Phase aufgeteilt (Dialyse und Zentrifugalfiltration). In Systemen die FA, HA oder SOM enthielten, fanden sich kleine Mengen As in den gelösten Fraktionen wieder, wodurch gezeigt werden konnte, dass verschiedene Formen von OM in der Lage sind, diese Art von Dreifach-Komplexen zu bilden.

Neben Fe(III)-Mineralen/Ferrihydrit sind zudem Tone häufige Minerale, die man in Böden/Grundwasserleitern findet. Sie können ebenfalls eine wichtige Rolle bei der Sorption und dem Transport von Arsen spielen. Die arsenbelasteten Gegenden in Südostasien liegen in Regionen, in denen Flüsse große Mengen von Alluvium ablagern, das mit silikat-haltigem Material angereichert ist. Tone sind Verwitterungsprodukte dieser silikat-reichen Ablagerungen. Die Wechselwirkungen von Tonen mit

NOM und von As mit Ton-NOM-Komplexen sind noch sehr wenig untersucht. Deshalb haben wir als erstes die reaktiven funktionellen Gruppen an Kaolinit- und Illitoberflächen, die für die Sorption von NOM und Metallen verantwortlich sind, in Sorptions- und Titrationsexperimenten bestimmt und quantifiziert und ein Oberflächenkomplexierungsmodell aufgestellt. Wir konnten feststellen, dass die Sorption von HA an Tonminerale die Anzahl und Konzentration von potenziellen Bindungsstellen für die Arsensorption erhöht. Als nächsten verifizierten wir dies durch Sorptionsexperimente, bei denen As zu Tonen bzw. Ton-HA-Komplexen gegeben wurde. Schon in früheren Veröffentlichungen wurde gezeigt, dass NOM wirkungsvoll mit Arsen um Sorptionsstellen an Tonen und Eisenoxiden konkurrieren kann. Doch wir stellten fest, dass dies nicht immer der Fall ist. Unsere Experimente zeigten, dass die Sorption von As an Tone in Gegenwart von zweiwertigen Kationen wie z.B. Ca^{2+}, das als Kationenbrücke zwischen NOM und Tonmineralen sowie zwischen As und NOM dienen kann, steigt. Die Sorption von sowohl As(III) als auch von As(V) an Kaolinite-HA- und Illit-HA-Komplexe war höher. As(V) sorbierte in stärkerem Maße an Tone als auch an Ton-HA-Systeme verglichen mit As(III), was im Gegensatz zu dem Sorptionsverhalten an Eisenminerale steht. Einhergehend mit der Literatur stellten wir bei den Desorptionsversuchen von As durch Phosphat und Silizium fest, dass Phosphat in allen Systemen As wirkungsvoller desorbiert als Silizium. Interessanterweise war in unseren Experimenten meist die relative Menge an desorbiertem As in Ton-HA-Systemen größer als wenn nur Ton verwendet wurde. Das zeigt, dass As nur locker an Ton-HA-Komplexe gebunden ist; wahrscheinlich über outer-sphere ternäre Komplexe mit Ca^{2+} als Kationenbrücke. Diese Ergebnisse zeigen, dass in der Umwelt die Sorption von Schadstoffen wie As von der Art der Ionen in der Hintergrundlösung, der Art der Mineraloberfläche, der Anwesenheit konkurrierender Stoffe und der Sorption von OM an die Mineraloberflächen abhängt. Für die Desorption sind neben den bereits genannten Parametern der Sorption auch die Art und Konzentration der desorbierenden Stoffe und die

Ausgangsbeladung der Ton-/Ton-HA-Oberfläche mit As wichtige Faktoren, die den Desorptionsprozess beeinflussen.

Insgesamt haben die Experimente im Rahmen dieser Arbeit gezeigt, wie vielseitig die Rolle und der Einfluss von NOM auf den Schadstofftransport (z.B. von As) sein können. NOM kann mit Eisenmineralen interagieren und Fe-OM-Komplexe/-Kolloide bilden und dann As als As-Fe-OM-Komplexe/-Kolloide mobilisieren.Es kann sowohl den Transport als auch die Desorption von As in Ferrihydrit-Durchflusssystemen verstärken und nicht nur mit As um Sorptionsplätze konkurrieren, sondern auch die Sorption von As verstärken, wenn es in Gegenwart von Kationen an Tonmineraloberflächen bindet. Die Methoden, Charakterisierungstechniken und Ideen, die in diesem Projekt benutzt wurden, können auch ausgeweitet werde, um die Komplexierung, den Schadstofftransport und den Effekt von OM in anderen biogeochemischen Systemen zu studieren.

Obwohl wir in der Lage waren einige Fragen im Hinblick auf den Effekt von NOM auf die As-Biogeochemie zu beantworten, gibt es trotzdem noch einige offene Fragen. Die Stabilität und die Mobilität der binären/ternären Komplexe könnten bestimmt werden, indem man die Komplexe und Kolloide unter verschiedenen geochemischen Bedingungen (verschiedene pH-Werte, Ionenstärke etc.) synthetisiert. Ob As(III) oder eher As(V) Komplexe mit Fe-OM bildet, könnte durch die Bildung von As(III)-Fe-OM-Komplexe/-Kolloide (nach den gleichen Protokollen wie in Kapitel ‚2‘ beschrieben) und dem Vergleich mit As(V)-Fe-OM Daten beantwortet werden. In Bezug auf Durchbruch- und Desorptionsexperimente in Säulensystemen, könnte untersucht werden, ob (und wie) Eisenminerale, die mit NOM beschichtet wurden, den Arsentransport beeinflussen und dies mitSystemen ohne NOM vergleichen. Dafür könnte man Arsenlösungen in Säulen mit Ferrihydrit-OM beschichtetem Sand im Vergleich zu Ferrihydrit beschichtetem Sand injizieren. Darüber hinaus können die Transportexperimente auch ausgedehnt werden, um den Durchbruch/ die Desorption von As von Ton-

Eisenoxid-Mischungen zu bestimmen, da beide Mineralphasen in der Natur eine Rolle spielen. Zusätzlich könnte man die Flussraten variiert oder Unterbrechungen in den Säulensystemen eingesetzen, da ein Flussstopp den Transport von Arsen und auch die Interaktion von OM mit den Mineralen in der Säule beeinflussen kann.

Im Fall von Tonmineralen könnte die Sorption von As an Ton-FA- oder Ton-SOM-Komplexe untersucht werden, um zu bestimmen, wie verschiedene OM Beschichtungen auf den Tonmineralen die Arsensorption beeinflussen. Zudem hängt die Sorption von OM stark von der Art der Kationen (Ca^{2+}) ab, die benutzt wurden um die Tonminerale zu homoionisieren. Daher könnten verschiedenen Ionen wie z.B. Na^{+}, Al^{3+}, Fe^{3+} oder sogar Mischungen verschiedener Ionen eingesetzt werden, da diese Ionen alle eine wichtige Rolle in der natürlichen Umwelt spielen und aktiv am Ionenaustausch an Tonmineralen teilnehmen.

PUBLICATIONS

Published

Prasesh Sharma*, Johannes Ofner and Andreas Kappler; Formation of binary and ternary colloids and dissolved complexes of organic matter, iron and arsenic. Published in **Environmental Science and Technology (44, 4479-4485, 2010)**.

Raul Martinez, **Prasesh Sharma** and Andreas Kappler; Surface binding site analysis of Ca2+-homoionized clay–humic acid complexes (**Journal of Colloid and Interface science, Sept 2010 (**doi:10.1016/j.jcis.2010.08.082).

Submitted

Prasesh Sharma*, Massimo Rolle, Benjamin Kocar, Scott Fendorf, and Andreas Kappler; Influence of natural organic matter on Arsenic transport and retention (Submitted to **Environmental Science and Technology, July 2010).**

In preparation

Prasesh Sharma*, and Andreas Kappler; Effect of dissolved phosphate and silicate on desorption of arsenic from clay and humic acid-coated clay (In preparation for **Journal of Contaminant Hydrology, 2010**).

Presentations

September 2007, Napoli, Italy – Natural organic matter summer school (poster)

July 2008, Telluride, USA – Iron Biogeochemistry conference (attendee)

August 2008, Germany – IPSWAT conference (oral)

Dec 2008, San Fransisco, USA – EXAFS conference (poster)

Dec 2008, San Fransisco, USA – American Geophysical Union (poster)

June 2009, Davos, Switzerland - Goldschmidt conference (poster)

August 2009, Stuttgart, Germany – IPSWAT conference (oral)

June 2010, Knoxville, USA – Goldschmidt conference (oral)

Statement of personal contribution

The work described was funded by a BMBF IPSWAT scholarship to Prasesh Sharma (PS) from Feb 2007 – Feb 2010. The conceptual background for the proposal for IPSWAT was designed by me with the help from Prof. Dr. Andreas Kappler (Principal Advisor).

Throughout the thesis, the planning of experiments, analysis, discussion of the results and preparation of manuscripts were carried out either by me or in coordination with Prof. Andreas Kappler.

However, in some cases, scientific help from other researchers were required. These specific contributions from other researchers to my thesis are mentioned below.

In **Chapter 2 (Formation of binary and ternary colloids and complexes of organic matter, Fe and As)**, all experiments were carried out by PS. Measurements, analysis and interpretation of FTIR/ATR-FTIR data and Mössbauer data were carried out in coordination with Johannes Ofner (Bayceer, Bayreuth University) and Urs Dippon (Geomicrobiology, University of Tuebingen) respectively.

In **Chapter 3 (Influence of OM of As transport and retention)**, all experiment were carried out by PS. Initial experiments were conducted in Stanford University supervised by Dr. Benjamin D. Kocar (from Prof. Dr. Scott Fendorf's group, Stanford University, USA). Reaction transport modeling for chapter three was conceptualized and carried out by Dr. Massimo Rolle (Hydrogeology group, Center for applied geosciences (ZAG), Tuebingen). All measurements, analysis and interpretation of data was carried out by PS and Dr. Rolle.

In **Chapter 5 (Surface binding site analysis of Ca^{2+}-homoionized clay-humic acid complexes)**, all experiments were conducted in collaboration with Dr. Raul E. Martinez (Geomicrobiology group, Center for Applied Geosciences (ZAG), Tuebingen). PS did the experimental work and helped RM with titration experiments. Dr. Martinez carried out major parts of the titration experiments and modeling of data. Interpretation of data was carried out by PS and Dr. Martinez.

Acknowledgements

My foremost thank you goes to **Prof. Dr. Andreas Kappler**, who one day decided to show up in Bremen when I was doing my Masters ☺. The next thing I know, I am doing a PhD in Andreas's group in Tuebingen. Thank you Andreas for giving me this amazing opportunity to be a part of your group, for making science fun, for and most importantly, also being a **GREAT MENTOR**. These last years have been a great learning experience for me, academically and personally.

My sincere gratitude to BMBF (Federal Ministry of Education and Research, Germany) for providing me with the IPSWAT scholarship to pursue PhD in Tuebingen.

I would also like to thank Dr. Andreas Voegelin (Eawag, SWI) and Prof. Dr. Stefan Haderlein for taking the time to examine my thesis.

During my PhD, I spent a couple of months at Stanford University (Soil Sci. Dept (PI: Prof. Scott Fendorf)). Thank you **Scott** for accepting me as a visiting scholar in your group. **Dr. Benjamin D. Kocar** and Dr. Yoko Masue-Slowey for helping me setup the column systems. Dr. Guangchao Li, Mike Massey, Adam Jew, Prof. Dr. Ruben Kretzschmar (ETH, Zurich, Switzerland), and Prof. Dr. Thomas Borch for their suggestions and help during my stay.

Geomicrobiology group past members (Dr. Phil Larese-Casanova, Iris, Jie, Katja, Nicole, Katharina) always gave me valuable suggestions when I needed it. Thanks guys !

All present Geomicrobio group members, particularly, Ellen, Dr. Raul Martinez, Annette, Dr. Caroline Schmidt, Emily, Marie, Maren, and Urs are acknowledged for specific help/for sampling/paper revisions/translations. Florian, Inga, Claudia, Merle, Detlef, Meenakshi, Dr. Martin Obst and Dr. Sebastian Behrens – thank you for your help and assistance during my PhD. I am glad to have been a part of this group.

Also thank you to the lab technicians from geomicrobio/hydrgeochem group (ZAG, Tuebingen), Frau Horn/Dr. Jöern Breuer (Soil Sc. Dept, Universität Hohenheim), Dr. Peter Kühn/Frank Baumann (Geography Dept, Uni Tuebingen) and Dr. Birgit Daus (UFZ, Leipzig) for As measurements. Johannes Ofner/Prof. Dr. Zetzsch for help with IR spectroscopy (Atmospheric Chemistry, Bayceer, Bayreuth) and Dr. Simona Regenspurg (previously at EPFL, Lausanne) for dialysis experiments.

Sincere thanks to my friends from the hydrogeochem/geology group – Ilka, Alicia, Chrissy, Dietmar, Massimo, Gabriele, Sebastian and Satoshi for the fun times we had and their help.

I am grateful to all my friends from Tuebingen (Maria, Barbara, Avneesh, Rebecca, Krafft Family and the rest of the gang for making my life a lot of fun), and from Bremen (Robert Eckhoff and family, Steffen, Irene, the Bortmanns and Prof. Andrea Koschinsky) for their good wishes/visits/good times and friendship.

Finally, thanks to my family, particulary to my **mum and dad**, and my sisters **Priyanka and Pranita (+ Family)** for their immense and unconditional love, and for supporting me throughout my 8 years of education in Germany.